GaO-based Thin Films: Deposition, Characterization and Photovoltaic Applications

2011

Supria Chowdhury

GaO-based Thin Films: Deposition, Characterization and Photovoltaic Applications

by

Supria Chowdhury

Thesis for Ph. D. degree in Engineering

Department of Engineering Physics, Electronics and Mechanics

Graduate School of Engineering

Nagoya Institute of Technology

Nagoya, Japan.

April 2011

GaO-based Thin Films: Deposition, Characterization and Photovoltaic Applications

Thesis submitted to
The Department of Engineering Physics, Electronics and Mechanics
Graduate School of Engineering
Nagoya Institute of Technology for the degree of
DOCTOR OF PHILOSOPHY in Engineering

by

Supria Chowdhury

Supervisor

Prof. Masaya Ichimura

Department of Engineering Physics, Electronics and Mechanics
Nagoya Institute of Technology

April 2011

Dedicated To –

My mother- my inspiration, my ultimate shelter

My husband- who fills me up with eternal love and support

My son SWOPARJO - his smiling face makes me the happiest one in this world

Declaration of Originality

I, hereby declare that the research recorded in this thesis and the thesis itself was accomplished and originated entirely by myself in the Department of Engineering Physics, Electronics and Mechanics, Graduate School of Engineering at Nagoya Institute of Technology, Japan.

Supria Chowdhury

Abstract

GaO- based thin films deposition from aqueous solution; characterization and their applications for photovoltaic were included in this doctoral thesis. The n-type GaS_xO_y thin films were electrochemically and photochemically deposited and characterized which are promising candidates as buffer layers for solar cell applications. Beside, the p-type $CuGa_xS_yO_z$ thin films were electrochemically deposited in potentiostatic and galvanostatic process which are considered as a new absorber layer for thin film solar cells. Since GaO-based compounds are toxic free material, low cost, available in earth crust, have higher optical transmission in the visible region of the light spectrum and wider energy band gap, so it attracts much attention for the researchers.

This thesis contains six chapters. In the first chapter, we introduced a brief background on the renewable energy sources, general properties of photovoltaic and literature review, advantages and disadvantages of thin film solar cells. In this chapter, we also discussed the importance of the thin-film-based solar cells and introduced the popular deposition techniques i.e. electrochemical deposition and photochemical deposition in more details, which were used for this work.

In the second chapter, GaS_xO_y thin films were deposited on indium-tin-oxide and fluorine-doped-tin-oxide coated glass substrates by electrochemical deposition from an aqueous solution of $Ga_2(SO_4)_3$ and $Na_2S_2O_3$. The as-deposited films were characterized by Auger electron spectroscopy, scanning electron microscopy and optical transmission spectroscopy etc. We observed the photosensitivity of the films by means of photoelectrochemical measurements. We confirmed that GaS_xO_y films show n-type conduction. The film deposited under the optimum conditions exhibited high transmission and a wide energy band gap of 3.5 eV. Therefore, wide band gap semiconductor GaS_xO_y is suitable as a buffer layer in solar cells.

In the third chapter, we explained details about GaS_xO_y film deposition by photochemical

deposition, which is a technique of film preparation from solutions by UV light illumination. GaS_xO_y thin films were deposited over fluorine-doped-tin-oxide-coated glass substrates from an aqueous solution of $Ga_2(SO_4)_3$ and $Na_2S_2O_3$ at different pH. The electrical and optical characterizations of as-deposited films were carried out by Auger electron spectroscopy, scanning electron microscopy, optical transmission spectroscopy and photo electrochemical measurement etc. O/Ga ratio was close to the stoichiometric ratio, 1.5, and S/Ga ratio is much smaller, less than 0.3 for a film deposited under the optimum condition. The film exhibited a wide energy band gap of 3.5 eV and resistivity of the order of 10^2 Ω–cm.

In the fourth chapter, $CuGa_xS_yO_z$ thin films were fabricated onto fluorine-doped-tin-oxide-coated glass by potentiostatic electrochemical deposition (P-stat ECD) and galvanostatic electrochemical deposition (G-stat ECD) techniques from an aqueous solution. Using P-stat ECD, the films were deposited at six different Cu to Ga ratios in solution bath, i.e., Cu/Ga= 3/2, 1/1, 1/2, 1/4, 1/12 and 1/30. The impact of the Cu/Ga ratio on composition, surface morphology, photosensitivity and optical transmission of the films were investigated. We successfully deposited both the Cu-rich and Ga-rich thin films. The deposited films have bandgap energy of 1.5~2.8 eV depending on the Cu/Ga ratio. Photoelectrochemical measurement confirms that deposited films are mainly p-type semiconductor except that Cu/Ga = 1/30 leads to a nearly intrinsic semiconductor. We succeed to deposit $CuGa_xS_yO_z$ thin films by galvanostatic electrochemical deposition (G-stat ECD). Since in P-stat ECD, $CuGa_xS_yO_z$ films deposited from Cu/Ga = 1/2 ratio have better physical appearance and high photosensitivity then we selected this ratio for G stat-ECD technique. Films deposited by G stat-ECD exhibit p-type conductivity and have bandgap energy of 1.85~2.8 eV depending on deposition current densities. Moreover, under optimum condition, characteristics of $CuGa_xS_yO_z$ thin films deposited by both P stat-ECD and G stat-ECD were compared to understand the best film quality and effect of deposition process on film characteristics. It was found that the optical transmission and bandgap energy, Eg were increased for G stat $CuGa_xS_yO_z$ films may be due to lower film thickness. However, different deposition process had no significant effect on atomic composition and film's colour.

In the fifth chapter, we fabricated GaO-based thin film heterostructucture and then characterize for SnS/ GaS_xO_y , $CuGa_xS_yO_z$ / GaS_xO_y and $CuGa_xS_yO_z$ /ZnO heterojunction solar cells

applications. Some of them showed a rectifying property and photovoltaic response but their conversion efficiencies were very low.

In the sixth chapter, conclusion for this work and suggestions for future work have included.

Acknowlegements

It is a great pleasure to acknowledge many people who made this thesis possible.

At first, I would like to express my heartfelt appreciation and sincere thanks to my Ph.D. supervisor Prof. Masaya Ichimura for his enthusiasm, excellent guidance, numerous ideas, sound advice and continuous support.

My sincere thanks are extended to Prof. Jimbo Takahashi and Associate Prof. Niraula Madan on behalf of devoting their precious time to read and made valuable comments on different parts of the manuscript, which indeed helped to improve of this thesis.

I wish to express my gratitude to Dr. Kato for his useful discussion and valuable suggestions.

I am particularly indebted to my teacher Dr.Jiban Podder, Prof. of Department of Physics, Bangladesh University of Engineering and Technology (BUET), Bangladesh. He introduced me with this exciting field of research and encouraged me to overcome many limitations, for which I am very grateful.

My cordial appreciation is also due to Dr. Ashraf M.A. Haleem Hassan for his contributions of time, scientific discussions, technical support, and encouragement during this work. My special thanks are due to Mr. Moriguchi for his technical assistance during this research work.

I wish to extend my sincere thanks to all the past, present and short term members of thin film group, especially Mr. Akita, Mr.Rifaat, Mr. Nakashima, Mr.Nishimura, Mr. Muhibbullah, Ms.Seki, Ms. Odon, Ms.Soue, Mr.Junie, Mr. Tajimi and Mr.Sakamoto, who together made it possible for me to spend these precious three years in NIT, Japan with research facilities, creative discussions, technical assistance and friendly environment. These help me to learn so much not only about science but also enjoy a very special and memorable period of my life indeed.

It is difficult to overstate my gratitude to Mrs. Kanako Ichimura for her kindness and affection

and extensive contribution to my personal and professional time at Nagoya.

I gratefully acknowledge the funding sources that made my Ph.D. work possible. I was funded by- “Nagoya Institute of Technology I-scholarship”. It is an honor to be the 1st “I-scholar”, which becomes possible only for strong recommendation of my supervisor Prof. M. Ichimura, founder of this scholarship.

I am forever indebted to my family members in Bangladesh for their everlasting sacrifice, support and encouragement. Most importantly, for the presence of my mother at Nagoya for 6 months and her endless patience, strong support and encouragement when it was most required.

Finally, my wholehearted gratitude goes to my husband and my seven months old son “SWOPARJO” - for their patience and mental support to concentrate on completing this dissertation.

Contents

Chapter 2: Electrochemical deposition of GaS_xO_y thin films

Chapter 3: Photochemical deposition of GaS_xO_y thin films

Chapter 4: Potentiostatic and galvanostatic electrochemical deposition of $CuGa_xS_yO_z$ alloy thin films for photovoltaic applications

Chapter 5: Applications of GaO-based thin films on solar cells

Chapter 6: Conclusion and Future Work

Chapter 1
Introduction

1.1. The flaming of fossil fuels

From the beginning of human civilization to till date, in the every sphere of scientific and technological development, we have been using and vastly depending on the natural energy sources; such as- fossil fuels (oil, coal, uranium) etc. Whereas, the limited supply of this energy sources is now seriously facing to the world and we have no choice but to establish an alternative energy sources to meet future energy demands. However, the flaming of fossil fuels in the past has already harmful effects on the delicate balance of nature and now a day about 20×10^{12} kg of carbon dioxide (CO_2) are put into the atmosphere every year, mainly by burning fossil fuel [1-3].

Today's plants are unable to absorb this huge amount of extra CO_2 resulting the greenhouse effect which will increase the global mean surface temperature- depending on future emission scenarios and the actual climate sensitivity - by another 0.6-7.0°C by the year 2100, that will have more despoiling effect for all living being of earth within the next decades [2].Therefore, development of clean energy resources as an alternative to fossil fuels has become one of the most important tasks assigned to modern science and technology in the 21st century. Essentially, this alternative energy sources should be renewable, sustainable, environment friendly and economic.

1.2. Renewable energy sources

We have perfect renewable energy sources -sun, wind and water etc. They are non-polluting, renewable, efficient and neither run out nor have any significant harmful effects on our environment. Among a wide variety of renewable energy projects in progress, photovoltaic (PV) is the most promising one as a future energy technology [4]. Compared to non-renewable

sources such as coal, gas, oil, and nuclear, the advantages are clear: it's totally non-polluting, has no moving parts to break down, and does not require much maintenance.

A very important characteristic of photovoltaic power generation is that it does not require a large scale installation to operate, as different from conventional power generation stations. This electric energy is the most convenient energy form in respect of mass production, transport, and distribution for modern civilization. Photovoltaic production has been increasing faster, making it the world's fastest-growing energy technology [5, 6]. As of October 2010, the largest photovoltaic (PV) power plants in the world are the Sarina photovoltaic Power (Canada, 80 MW). Photovoltaic panels based on crystalline silicon modules are being partially replaced in the market by panels that employ thin film solar cells (CdTe [7] CIGS,[8] amorphous Si, [9] microcrystalline Si), which are rapidly growing and are expected to account for 31 percent of the global installed power by 2013[10].Still, according to the European Photovoltaic Industry Association, solar power could provide energy for more than one billion people by 2020 and 26% percent of global energy needs by 2040[4].

1.2.1. General properties of Photovoltaic

The ultimate source of energy is the sun, hence photovoltaic are best known as a method for generating electric power by using solar cells to convert energy from the sun into electricity. The photovoltaic effect refers to photons of light, knocking electrons into a higher state of energy to create electricity.

In a photovoltaic device, there is two constituent parts-(1) absorber-generator: absorbs the incident sunlight (photon) to generate the charge carriers (electrons and holes) and (2) collector-convertor: collects these charge carriers and converts them into majority carrier (electrons for n-type semiconductor and holes for p-type semiconductors). It is important to consider three main parameters for absorber materials [11], such as –

(i) Band gap: Incident photons of higher energy than band gap are absorbed by material and create an electron-hole pairs. In this process, created charges are collected by the collector electrode without any recombination.

It has noted that semiconductor with a band gap between 0.8 [12, 13] and 2.4 eV could achieve 10% conversion efficiency. In practical, efficiencies cannot be fully attained at 100% due to reflection losses and the other losses.

(ii) Absorption coefficient: The absorption coefficient depends on the material and also on the wavelength of light which is being absorbed. Semiconductor materials have a sharp edge in their absorption coefficient, since light which has energy below the band gap does not have sufficient energy to raise an electron across the band gap. Consequently this light is not absorbed. This parameter is very important in determining the efficiency of solar cell. Cu_2S absorbs 90% of the sunlight with energy greater than its band gap energy within a thickness of only 0.4 μm. Si will absorb about 70% of the useful photons in 10 μm thickness and 90% of the photons in 100 μm layers. Except Si, other materials with an energy band gap between 1.0-1.7 eV absorb 90% of the photons in a 5 μm thick layer.

(iii) Minority carrier diffusion length: The diffusion length of absorb material depends on doping and impurity concentration in a material and also on the structure of a material i.e.; crystalline or noncrystalline (polycrystalline or amorphous). Therefore, the thickness of the absorber layer in a photovoltaic cell is limited by the minority carrier diffusion length.

On the other hand, to select an appropriate collector-convertor, three material properties [11] should be considered-

(i) Electrical conductivity: The collector material and the absorber material must be in opposite conductivity type to each other. Hence, the generated minority carriers in absorber materials are converted to majority carriers in collector materials without any recombination lost.

(ii) Electron affinity: The collector material and the absorber material must have matched electron affinity. Because, electron affinity mismatch influence the photovoltaic efficiency to decrease.

(iii) Lattice constant: The lattice constant of the collector material also must be matched with

the absorber material. Lattice mismatch produces interface states [14] at the junction of the photovoltaic and then act as recombination surface, shorten the photogenerated current collection efficiency. For example: GaAs, AlGaAs and AlAs have almost equal lattice constant making it possible to grow efficient cell structure.

1.3. Thin film solar cell

High price of solar cell module is one of the main barriers for the expansion of large-scale power-source application of photovoltaic systems. One of the solutions to achieve a reduction in this cost is the development of the thin film solar cell technology, which saves both materials and energy in the production of cells and modules [4]. Now a day, thin film solar cells have high worldwide demand to generate an efficient, renewable and clean solar energy.

1.3.1. Literature review

There is a glorious history behind harnessing solar energy to today's famous thin film technology. Roman legends say that at about 298-212 BC, a Roman warrior intensified the sun's heat and caught fire to the enemy's approaching ships. At about 200 BC, the Chinese used curved mirrors to start fires. In 19th century France, experiments with solar powered engines concluded with a 1-horsepower solar steam engine invented by Augustin Mouchot.
At 1839, French scientist Edmond Becquerel discovers the photovoltaic effect while experimenting with an electrolytic cell. He observed that two metal electrodes placed in an electricity-conducting solution increased electricity generation when exposed to light.During 1880s, Charles Fritts described the first solar cells made from selenium wafers. Although selenium solar cells were failed to convert enough sunlight to power electric equipment. In 1954, the first single crystalline silicon (sc-Si) solar cell capable of converting enough solar energy into electric current was silicon solar cell, developed in Bell Laboratories, USA. This silicon solar cell achieved efficiency from 4% to 11%. Following this development, commercial sc-Si PV cells were routinely used on U.S. satellites. Because, in space applications, cost is not a major factor and these cells continue to be used on practically all satellite systems. During the early 1970s, technical success of PV cells in space applications encourages both public and private sectors in terrestrial applications of PV energy generation.

Initial efforts focused on – (1) lowering the cost of sc-Si solar cell modules since the basic technology already was well developed. (2) Polycrystalline Si (pc-Si) solar cell module technology was introduced to further lower manufacturing costs; however, the initial cost advantages of pc-Si technology are approximately offset by its lower efficiency, leaving the generated energy cost practically unchanged[15].

In 1976, D.Carlos and C.Wornski fabricated first amorphous silicon photovoltaic cells. In 1980, the first non-Si thin film solar cell Cu_2S/CdS exceeds 10% efficiency at the University of Delaware. The first real application of silicon cells was in 1958 when solar power was used on the Vanguard 1, which was the second American satellite to orbit earth.

Later on solar cells were developed from different new material such as-solar dyes, solar inks, conductive plastics etc. Now a days in thin film solar cell, amorphous Si, CdTe, GaAs or CIGS (Copper Indium Gallium Diselenide) are widely used, which are much cheaper and easier to manufacture than the traditional standard solar crystalline panels.

1.3.2. Advantages and disadvantages of thin film solar cells

This new and exciting thin film solar-cell technology has different advantages and disadvantages which are listed below-

Advantages-

1. Thin-film solar cells, for instance, require less material than traditional solar cells, and are therefore cheaper, lighter, and flexible.
2. Numerous application options are one of the biggest advantages of thin film solar cell. Such as- flexible panels in a wide variety of surface, integrating into roof tiles and siding, being molded to cars, backpacks, clothing and even windows.
3. Because of simple manufacturing process, thin film solar cell has fewer defects compared to traditional solar panels.
4. Less voltage drop and many thin solar panels have better energy production in low-light and shading situations.

5. Thin film solar cells are not brittle like crystalline Si thus has longer use.

Disadvantages-

1. The formation of grain boundaries is one of the vital disadvantages in polycrystalline thin films. Therefore, carrier recombination, charge trapping and slowing down the carrier movement etc. are existing and affect the cell efficiency and stability. However, now a days, thin film polycrystalline solar cell such as- CdTe, CIS, CIGS, GaAS etc. are the best attraction for researcher due to cost effective, mass production and application with in large device.CIGS based solar cell achieved 19.9% efficiency by the US National Renewable Energy Lab (NREL) [16].This result is closed to the world record for a common solar panel of 24.7%.
2. For same efficiency or same amount of electricity production, thin film solar cells need about more 50% space than traditional solar cell setup.
3. Thin film solar cell are usually applied directly to a surface therefore, preserves more heat than traditional panel.

1.4. Thin film deposition techniques

Thin film deposition process has three main steps [17]: (1) Production of atomic, molecular or ionic species (2) Transportation of those species to the substrate via a medium (3) condensation onto the substrate, directly or via a chemical and/or electrochemical reaction, to form a solid deposition. On the basis of thin film's physical properties, cost and environment issues, deposition techniques can be considered. The electrical, optical, morphological and structural properties of the deposited films are strongly influenced by the deposition technique and by the several experimental parameters. Some deposition techniques allow film thickness to be controlled within a few tens of nanometers and some techniques allow single layers of atoms to be deposited at a time. Deposition techniques are classified in two basic categories, specifically- physical and chemical deposition techniques.

Among various deposition methods as shown in Fig 1.1, in following we have discussed in details about the electrochemical deposition (ECD) and photochemical deposition (PCD) techniques which are used to deposit our above mentioned films in this thesis.

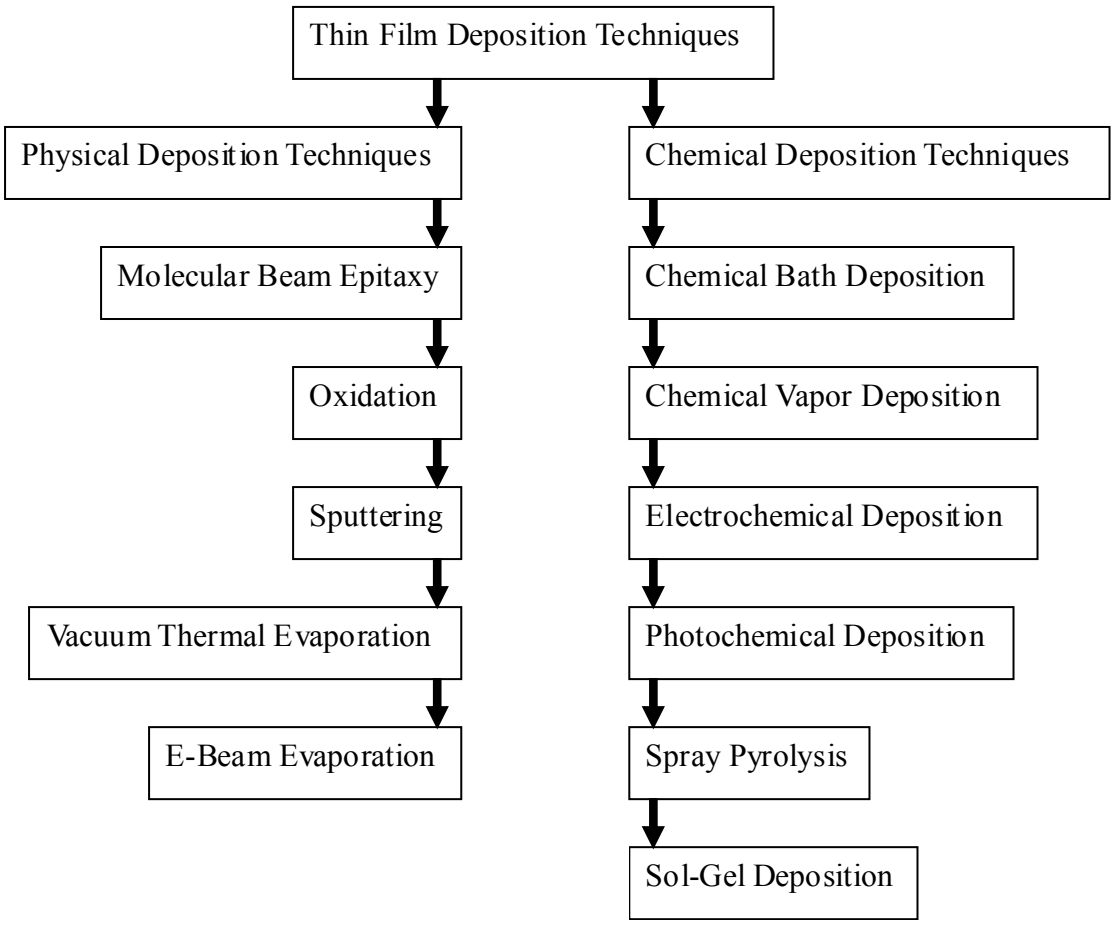

Fig.1.1: Thin film deposition techniques

1.4.1. Electrochemical deposition (ECD)

1.4.1.1. Background

Electrochemical deposition (ECD) is a technique in which a film of solid metal is deposited from a solution of ions onto an electrically conducting surface. Based on applied electric field across the electrolysis cell [18], ECD techniques can be classified in three different categories, i.e. deposition- (1) at a constant potential (potentiostatic) (2) at a constant current densities (galvanostatic) and (3) using periodic pulsed potential (two or three step voltage bias).In case of pulsed deposition, value and duration time of each voltage step plays significant role to control the properties of the deposited films.

In the late 1970s, for the first time ECD was applied for semiconductor materials fabrication

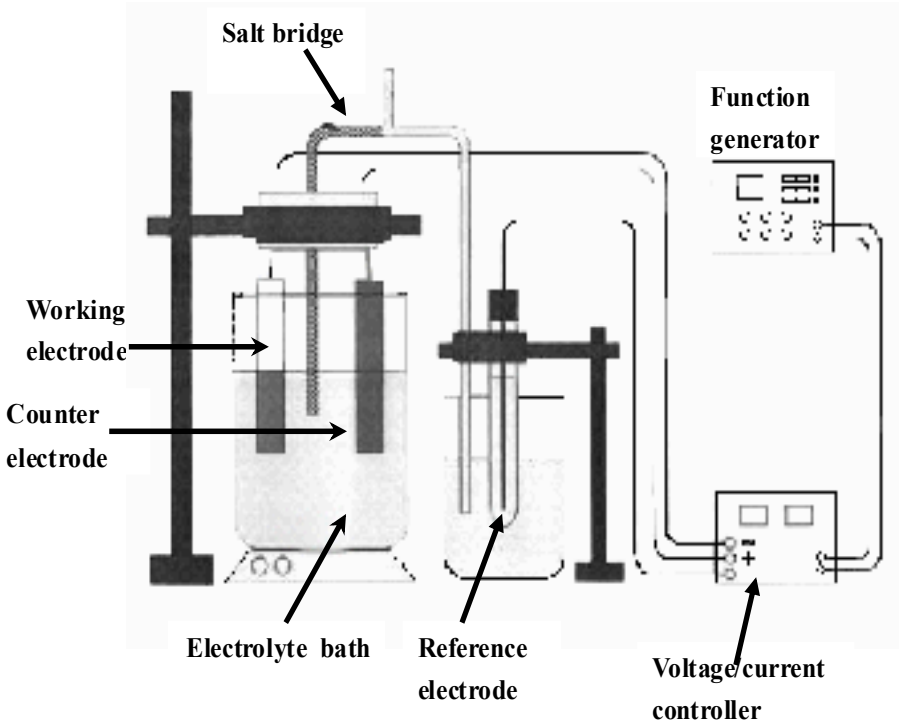

Fig.1.2(a): A schematic diagram of the 3-electrode cell apparatus used for electrochemical deposition of thin films.

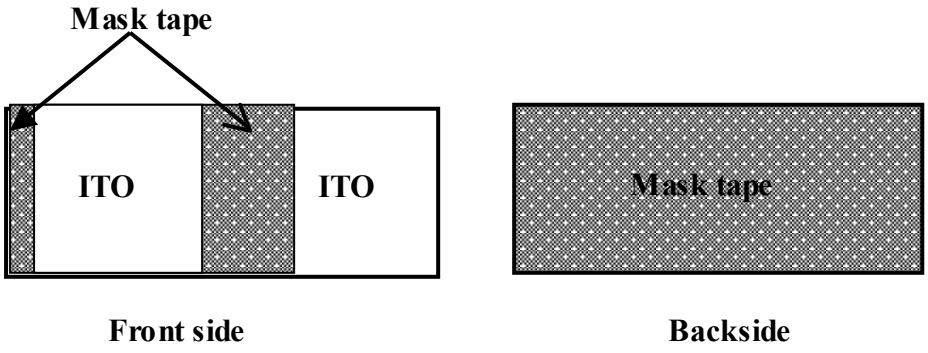

Fig. 1.2(b): The masking form for the substrate to be ready for film deposition.

[19-23]. In the early 1980s, the production of a thin-film solar cell CdS/CdTe based on electrodeposited CdTe layer [24] with efficiency greater than 10% was a notable achievement and attracts worldwide research attention in electrochemical deposition of semiconductors since the past two decades. Now a day, electrochemical deposition is very famous to deposit many materials such as III-V, I-III-VI_2, and other alloy semiconductors. Besides, elemental semiconductors such as silicon [25] and mechanically harder materials such as nitrides [26] are under consideration to grow by ECD.

1.4.1.2. Process of ECD

The ECD of semiconductor materials requires three electrodes with an electrolyte solution containing ions. As shown in Fig. 1.2(a), working electrode was used as cathode, counter electrode as anode and reference electrode was a standard electrode. A fixed potential difference is applied between the working electrode and the reference electrode. This potential drives the electrochemical reaction at the working electrode's surface. The current produced from the electrochemical reaction at the working electrode is balanced by a current flowing in the opposite direction at the counter electrode. The potential applied to the working electrode is measured within the context of a known potential, which is in turn obtained from the reference electrode. The role of the reference electrode is to establish a stable potential. On the other hand, the function of the counter electrode is to convert ionic conduction in the electrolyte to electronic conduction by electrochemical reaction. There are different types of reference electrode such as, silver/silver chloride, mercury/mercurous chloride, hydrogen/palladium, calomel etc. and counter electrodes are such as, graphite plate, NiO, Pt etc. In this work, we used ITO or FTO-coated glass as the working electrode (substrate) and a platinum sheet as the counter electrode with a saturated calomel electrode (SCE) as the reference electrode. As shown in Fig. 1.2 (b), working electrode should be masked and then hanged as working electrode in the electrochemical cell, before the film deposition. In this process, an external dc power is applied across the anode and the cathode, the positive ions from electrolyte solution are attracted to the cathode, discharged, and chemically reacted to form the material layer. Deposited material properties i.e; structural, electrical, and optical properties of film were influence by several parameters, such as- ionic concentrations, stirring rate, temperature, pH, deposition voltage and deposition time. Therefore, it is important to optimize those parameters

to obtain a best quality film.

1.4.1.3. Advantages and disadvantages of ECD technique

ECD is a low-cost, simple technique and suitable for large scale deposition [27-29], and has been found successful in depositing various semiconductor thin films from aqueous solutions. The advantage of ECD method with respect to other solution methods is the possibility to increase the control over film properties and thickness by means of the electrochemical variables, potential and current. Furthermore, by changing the deposition time, deposited film thickness can easily be controlled. ECD is usually carried out in room temperature without requiring a vacuum system. The electrochemical deposition enables self-purification, extrinsic and intrinsic doping. The variation in electrical conduction through p+, p, i, n, and n+ has been recently established for $CuInSe_2$ [30] and $CuInGaSe_2$ [31] based materials. It is also possible to change the conduction type (n-type, intrinsic or p-type) by varying the deposition voltages or ion concentration in the solution [32]. It is also possible to engineer the bandgap of alloy semiconductors such as- bandgap of $CuInSe_2$ (~1.10) can be increased by adding gallium into the layers and changing the growth voltage. Thus, the bandgap of $CuInGaSe_2$ can be obtained ~ 2.20 eV by changing the deposition voltage [33]. ECD also has ability of defect passivation in a wet chemical environment. As for example, CdS/CdTe solar cells enhance efficiency values from ~3 to 5% to ~12 to 14% [26] by $CdCl_2$ treatment. Since, the material layers grown by ECD are usually amorphous, nano- or micro-crystalline; hence this method is a convenient technique for growth of materials for nanotechnology research and applications.

The main drawback of ECD is that, it needs conducting substrates. Another challenge is to get oxygen free film because, water is a common solvent for ECD and there is much possibility to absorb the dissolved oxygen of deposition bath inside the deposited films.

1.4.2. Photochemical deposition (PCD)

1.4.2.1. Background

A novel technique called photochemical deposition (PCD), recently has been developed to deposit compound semiconductor and a variety of metals, metal oxides [34-37], sulfides and

selenides [38-42] thin films from an aqueous solution using UV light and can be carried out at ambient temperature, from simple precursor compounds. PCD is a very advantageous technique for solar cell fabrication [38, 39, 43, 44].

About 1982-1984, PCD was widely used to deposit metal, large area oxide, nitride films and applied to deposit semiconductor materials [43]. Recent advances have included the deposition of InP and the group II-VI compounds such as- HgTe, CdTe and $Cd_xHg_{1-x}Te$.The HgTe growth was the first reported instance of the UV photolytic deposition of a compound semiconductor [43]. Great concerns were devoted to metals and metal oxides deposition by PCD for catalytic purposes. Indeed, the use of semiconductor and metal nanoparticles on semiconductors is particularly appealing for the catalytic photochemical removal of contaminants from waste stream water and the optimization of the water-splitting reaction, which require high photocatalytic activity [43]. Besides this general use of photochemical deposition, specific attention was directed towards laser assisted micropatterning of surfaces focusing mainly on laser chemical vapor deposition [34, 39, 43, 44].

At the same time, some authors developed an alternative method using condensed phase precursors for the photo deposition of conducting materials in the form of films [35] or spots [36]. The technique uses UV or visible light sources to efficiently break molecular bonds, generate a new species, and induce its rapid deposition in the illuminated area [37].On the other hand, controlled localized laser deposition of high resolution metal lines was, for example, used to repair photo masks and form interconnects in integrated circuits. That is why this technique represents now a day a well established approach for direct writing on surfaces without mask-based photolithography [45].

1.4.2.2. Process of PCD

PCD method consists in the direct irradiation of precursor bath with ultraviolet light. In PCD, the energy is absorbed by the precursor species. The absorbed photon may promote electrons to excited states (Fig.1.3 (a)) if UV or visible wavelengths are used, the ground state energy increase by single-or multi-photon absorption process at longer wavelengths. The simplicity of the method allows for the deposition of very thin films depending on the reactions conditions,

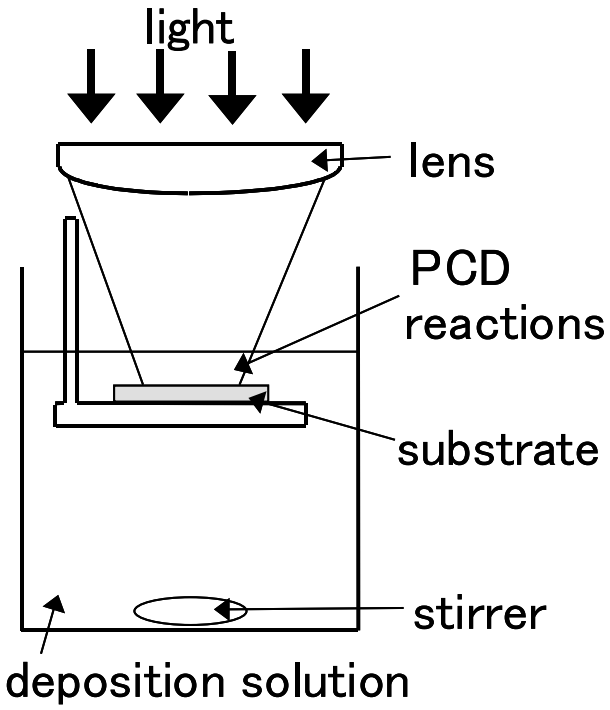

Fig.1.3 (a). Schematic diagram of the PCD method

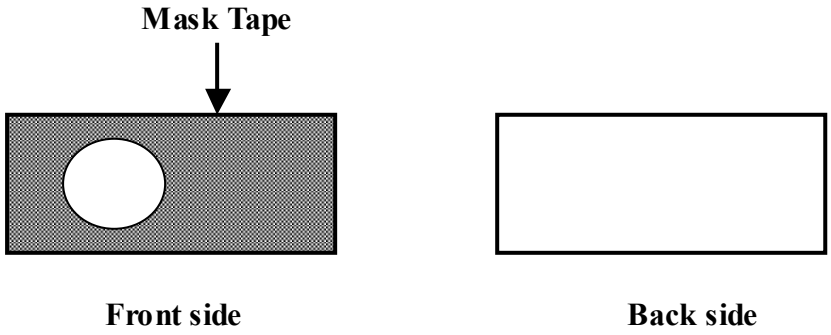

Fig. 1.3 (b): The masking form for the substrate to be ready for film deposition.

on substrates which are not affected by the UV light. For this reason photochemical deposition is attracting increasing attention as a research field.

1.4.2.3. Advantages and disadvantages of PCD technique

The PCD technique is the advantageous because of its simplicity, cheapness, low cost of the starting materials, better controllability and capability of large area deposition [46].PCD offers more several important advantages, including low-temperature selected area deposition, freedom of substrate selection (powders and flat surfaces) [47], and reaction control by optical modulation.

In PCD, films are deposited onto the substrate immersed in the solution. The solution is stable without illumination, and substrates do not need to be conductive. Thus the shortcomings of ECD and CBD are all overcome by PCD [45].

It has also many other advantages: (i) the method can be applied to a very broad range of precursors and (ii) the production is very easy since experiments can be performed in simple homemade tight cells.

Photochemical deposition of nearly all types of materials has various applications such as-catalysis, chemical sensing, magnetic data storage, optoelectronics, spin-dependent electron transport, and solar cells.

The problems associated with PCD is that of low deposition rate[41] and it was observed that the substrate position affects the deposited film thickness and it is difficult to control this position precisely[46].Overall, for low temperature, damage –free deposition, PCD processes is increasingly important.

1.5. Literature review of GaO - based thin films

Fabrication of novel materials with felicitous properties for different applications is the main goal of semiconductor research. Materials containing a chalcogen (O, S, Se or Te) and Group

13 metals (Al, Ga, In or Tl) have been the subject of quite intense study in the last two decades. Nowadays, more attention is focused on the Ga-based binary and ternary chalcogenides semiconductors, which are academically interesting and have industry potential. Compounds $CuInSe_2$ and $CuInS_2$, and related alloys (I-III-VI) are popular for the absorber layer in heterojunction solar cells. InS_x and InS_xO_y also attract attention as a window layer material, which can replace toxic CdS. However, In is a relatively rare material, and its price increases rapidly with increase in its consumption for the display devices. On the other hand, Ga, another group III element, is also nontoxic and much more abundant than In: its amount in the earth crust is larger by about two orders of magnitude than In. Therefore, in this work, we deposit thin films of GaO-based compounds, aiming at application for the solar cells.

Gallium sulfide GaS and Ga_2S_3, gallium oxide Ga_2O_3, and their alloy gallium sulfide oxide GaS_xO_y are n-type wide-gap semiconductors and thus are promising candidates for solar cell application as a buffer layer material. So far, several studies have been performed on gallium sulfide fabrication techniques such as metal-organic chemical vapor deposition [48], a modified Bridgman method [49], a microwave glow discharge method [49], a chemical vapor-transport method [51], and chemical vapor deposition [52], and on gallium oxide fabrication techniques such as spray pyrolysis [53] and molecular-beam epitaxy [54].But fabrication of GaS_xO_y by ECD and PCD method are presented in this work is the first report as our knowledge concern.

We attempt to deposit Ga-based chalcopyrite compounds which are suitable for the absorber layer also. Solar cells based on $CuInSe_2$ (CIS) and Cu $(In,Ga)Se_2$ (CIGS) have reached conversion efficiencies as high as 18.8% and 19.5% [55].

$CuGaS_2$ has a direct band gap of 2.5 eV at 293 K and thus has great potential for optical applications in the green part of the visible spectrum [56]. Many deposition methods have been developed for the preparation of $CuGaS_2$, such as metal-organic chemical vapor deposition [57, 58], modulated flux deposition [59], vacuum evaporation [60, 61], and molecular beam epitaxy [62]. Bhoslea et al. [63] deposit conducting and transparent Ga-doped ZnO films on glass substrates by PLD.

Ishikawa et al. [64] deposit amorphous Ga_2O_3 and $Cu_xGa_{1-x}O$ thin films were prepared on glass substrates by ultrahigh-vacuum radio frequency magnetron sputtering at room temperature. Using hydrothermal process and ethylene glycol as a reducing agent, Srinivasan et al. [65] synthesized nano-layered particles of delafossite $CuGaO_2$. Other techniques to fabricate GaO-based thin films are - Spray pyrolysis [66], Atomic layer deposition [67], Electrodeposition [68] etc.

Currently, a great deal of effort is being expended to develop low-cost technologies for fabricating CIGS thin films [69–79].Long et al. [80] fabricate CIS (CIGS) thin films by One-step electrodeposition in alcohol solution. Several methods for preparation CIS (CIGS) absorber films have been reported, such as co-evaporation [81], sputtering and selenization [82], and electrodeposition [83]. Until now, co-evaporation is the most successful technique for the preparation of CIS (CIGS), which achieved the highest efficiency CIGS-based solar cells, but it seems difficult to scale up now a days. Among these methods, electrodeposition technique is potentially suitable to obtaining good-quality, large-area CIGS precursor films.

Depending on our knowledge, fabrication of $CuGa_xS_yO_z$ thin film by both P-stat ECD and G-stat ECD, are the first report of this alloy system.

1.6. Objectives of this work

The main objective of this thesis is to fabricate and characterize GaO-based thin films by cost effective and environment friendly manner, with the purpose of photovoltaic applications.

1.7. Outline of the thesis

Chapter 2 is aimed to explain details about the electrochemical deposition (ECD) of gallium – sulfide - oxide thin films (GaS_xO_y) on to indium - tin – oxide (ITO) coated glass substrate and fluorine – tin – oxide (FTO) coated glass substrate from aqueous solution. Deposited GaS_xO_y films are n-type semiconductor with high transmission and wide energy band gap of 3.5 eV. Thus, GaS_xO_y is suitable as a buffer layer in solar cells.

Chapter 3 presents with particulars about GaS_xO_y thin films deposition by novel photochemical deposition (PCD).Films were deposited over FTO from aqueous solution at an unadjusted pH and high pH. At an unadjusted pH, film growth rate of about 0.2-0.3 μm/h but the rate is very slow at high pH of 9, where relatively smooth films were obtained by adding lactic acid in growth solution. The films deposited under the optimized condition at an unadjusted pH have a wide band gap of about 3.5 eV and a resistivity of 6.6 x 10^2 Ω-cm.

Chapter 4 deals with electrochemical deposition of copper gallium sulfide oxide ($CuGa_xS_yO_z$) thin films onto FTO-coated glass using potentiostatic electrochemical deposition (P-stat ECD) and galvanostatic electrochemical deposition (G-stat ECD) process. For P- stat ECD, the films were deposited at different Cu/Ga ion ratios in the solution bath; namely Cu/Ga = 3/2, 1/1, 1/2, 1/4, 1/12 and 1/30 in order to study the impact of Cu/Ga concentration on film properties. Both the Cu-rich and Ga-rich thin films were successfully deposited with bandgap energy values of 1.5–2.8 eV depending on the Cu/Ga ratio. It was confirmed that deposited films are mainly p-type except for the film deposited at Cu/Ga = 1/30, which behaved as a nearly intrinsic semiconductor. On the other hand, in G-stat ECD, $CuGa_xS_yO_z$ thin films were deposited for Cu/Ga ion ratio = 1/2 in solution bath. Deposited films exhibit p-type conductivity with wide band gap energy of 1.85-2.8 eV. A comparative study between the P-stat ECD $CuGa_xS_yO_z$ films and G-stat ECD $CuGa_xS_yO_z$ films were studied to understand the best film quality and effect of deposition process on film characteristics. It was found that at optimum condition, G-stat ECD $CuGa_xS_yO_z$ films show higher transmission and band gap energy, though no significant effect of different deposition process were noted on atomic composition and film colour.

Chapter 5 explains details on fabrication and characterization of and GaO-based heterostructucture for SnS/ GaS_xO_y , $CuGa_xS_yO_z$ / GaS_xO_y and $CuGa_xS_yO_z$ /ZnO heterojunction solar cells applications. Rectification and photovoltaic response were observed for some of the cells but their conversion efficiencies are very low.

Chapter 6 focuses on a conclusion for this work and suggestions for future work.

References:

[1] P. Benett, "Earth: The Incredible Recycling Machine", Wayland (Publishers) Ltd, East Sussex (1993).

[2] Intergovernmental Panel on Climate Change (IPCC) "Second Assessment Report - Climate Change 1995", (1995).

[3] United Nations Environment Programme (UNEP) "Global Environment Outlook (GEO)-2000", Earth- scan Publications Ltd., London (2000).

[4] Y. Hamakawa, "Thin-film solar cells: next generation photovoltaics and its applications", Springer-Verlag Berlin Heidelberg (2004).

[5] www.socialfunds.com

[6] http://vitalsigns.worldwatch.org

[7] http://firstsolar.com

[8] http://www.wuerth-solar.de

[9] http://www. uni-solar.com

[10] www. renewableenergyworld.com. "Thin film's share of solar panel market to double by 2013", Retrieved July 7(2010).

[11] A.M.A.hallem Hassan, PhD thesis- "Electrochemical Deposition of InS-based Thin Films for Photovoltaic Applications", (2010).

[12] M. Prince, J. Appl. Phys. 26 (1955) 534.

[13] J. J. Loferski, J. Appl. Phys. 27 (1956) 777.

[14] J. A. Bragagnolo, A. M. Barnett, J. E. Phillips, R. B. Hall, A. Rothwarf and J. D. Meakins, IEEE Trans. Electron Devices, 27 (1980) 645.

[15] R. W. Birkmire and E. Eser, Annu. Rev. Mater. Sci. 27(1997) 625-53.

[16] I.Repins, M.A.Contreras, B.Egaas, C.DeHart, J.Scharf, C.L.Perkins, B.To, R. Noufi, Prog. Photovolt:Res. Appl.16 (2008) 235.

[17] Willium Andrew, Inc. NY.

[18] R.K.Pndey, S.N.Sahu, S.Chandra, "Handbook of Semiconductor Electrodeposition", Marcel. Dekker, Inc, USA (1996).

[19] W. J. Danaher and L. E. Lyons, Nature, 271 (1978) 139.

[20] F. A. Kröger, J. Electrochem. Soc. 125 (1978) 2082.

[21] M. P. R. Panicker, M. Knaster, and F. A. Kröger, J. Electrochem. Soc. 125 (1978) 566.

[22] G. F. Fulop and R. M. Taylor, Annu. Rev. Mater. Sci. 15 (1985) 197.

[23] J. Ortega and J. Herrero, J. Electrochem. Soc. 136 (1989) 3388.

[24] B. M. Basol, J. Appl. Phys. 55 (1984) 601.

[25] T. Nohira, K. Yasuda, Y. Ito, Nat. Mater. 2 (2003) 397.

[26] L. E. Griffiths, M. R. Lee, A. R. Mount, H. Kondoh, T. Ohta, and C. R. Pulham, Chem. Commun. 579-580 (2001) 579.

[27] NEDO report on plating technology for $CuInS_2$ thin film solar cells, (2002) 5.

[28] J. F. Guillemoles, O. Roussel, O. Ramdani, M. Benosman, C. Hubert, J. P. Fauvarque, A. Chomont, N. Bodereau, P. Panheleux, P. Fanouillere, J. Kurdi, N. Naghavi, P. P. Grand, L. Parissi, M. Ben-Farah, J. Connolly, S. Taunier, P. Mogensen, D. Lincot, and O. Kerrec, Proc. of the 19th European Photovoltaics Conference, Paris, France, June 7-11(2004) 1669.

[29] R. N. Bhattacharya, W. Batchelor, H. Wiesner, F. Hasoon, J. E. Granata, K. Ramanathan, J. Alleman, J. Keane, A. Mason, R. J. Matson, and R. N. Noufi, J. Electrochem. Soc. 145 (1998) 3435.

[30] N. B. Chaure, J. Young, A. P. Samantilleke, and I. M. Dharmadasa, Sol. Energy Mater. Sol. Cells, 81 (2004) 125.

[31] N. B. Chaure, A. P. Samantilleke, R. P. Burton, J. Young, and I. M. Dharmadasa, Thin Solid Films, 472 (2005) 212.

[32].S.Chowdhury, M.Ichimura, Mater.Science and Semiconductor Processing (Accepted on October 2010)

[33] I.M. Dharmadasa, N.B. Chaure, G.J. Tolan, and A.P. Samantilleke, Journal Electrochem. Soc. 154 (2007) H466.

[34] G.E. Buono-Core, M. Tejos, G. Cabello, N. Guzman, R.H. Hill, Mater. Chem. Phys. 96 (2006) 98.

[35] G.E. Buono-Core, M. Tejos, G. Alveal, J. Mater. Sci. 35 (2000) 4873.

[36] G.E. Buono-Core, G. Cabello, J.L. Cayon, M. Tejos, R.H. Hill, J. Chil. Chem. Soc. 50 (2005) 541.

[37] G.E. Buono-Core, G. Cabello,H.Espinoza,A.H.Klahn, M. Tejos,R.H.Hill, J. Chil. Chem. Soc., 51, N°.3 (2006) 950-956.

[38] F. Goto, M. Ichimura and E. Arai. Jpn. J. Appl. Phys. 36 (1997) L1146.

[39] M. Ichimura, F. Goto, Y. Ono and E. Arai. J. Cryst. Growth, 198-199 (1999) 308.

[40] M. Ichimura, A. Nakamura, K. Takeuchi, E. Arai, Thin Solid Films, 384 (2001) 157.

[41] J. Podder, R. Kobayashi, M. Ichimura, Thin Solid Films, 472(2005) 71.

[42] R. Kumaresan, M. Ichimura, E Arai, Thin Solid Films, 414, 25 (2002).

[43] A.W. Vere, Crystal Growth Principles and Progress. , Plenum, New York (1987).

[44] M.Gunasekaran, R.Gopalkrishnan, P.Ramasamy.Materials Letters, 58, Issues 1-2(2004) 67-70.

[45] R. Kobayashi*, N. Sato, M. Ichimura, E. Arai, Journal of Optoelectronics and Advanced Materials, 5(2003) 893 – 898.

[46] S. Chowdhury and M. Ichimura, Jpn.J.Appl. Phys. 49 (2010)062302.

[47] E. Hugonnot, M. Delville, J.Delville1, Physical Review E 75(2007)061602.

[48] A. Keys, S. G. Bott, A. R. Barron, Chem. Mater. 11 (1999) 3578.

[49] N. M. Gasanly, A. Aydinli, H. Ozkan, C. Kocabas, Solid State Commun. 116 (2000) 147.

[50] X. Chen, X. Hou, X. Cao, X. Ding, L. Chen, G. Zhao, X. Wang, J. Cryst. Growth, 173 (1997) 51.

[51] C. H. Ho, Y. S. Huang, P. C. Liao, K. K. Tiong, J. Phys. Chem. Solids, 60 (1999) 1797.

[52] S. Suh, D. M. Hoffman, Chem. Mater. 12 (2000) 2794.

[53] Z. Ji, J. Du, J. Fan, W. Wang, Opt.Mater. 28 (2006) 415.

[54] T. Oshima, T. Okuno, S. Fujita, Jpn. J. Appl. Phys. 46 (2007) 7217.

[55] Contreras, M. A. Romero, M. J. Noufi, R. Thin Solid Films. 480(2005) 2.

[56] S .Shirakata, K .Saiki, S.Isomura, J. Appl. Phys. 68 (1990)1.

[57] S .Chichibu, S .Shirakata, M .Uchida, Y .Harada, T .Wakiyama, S .Matsumoto, H .Higuchi, S.Isomura, J. Appl. Phys. 34(1995)3991.

[58] MS .Branch, PR. Berndt, WL. Leitch, J. Weber, JR.Botha, Thin Solid Films, 480-481(2005)188.

[59] C, Guillen, J. Herrero, Phys Stat Sol. (a) 203(2006) 2438.

[60] WJ. Jeung, GC. Park, Sol Energy Mater Sol Cells, 75(2003)93.

[61] SK .Kim, JP .Park, MK .Kim, KM .Ok, IW. Shim, Sol. Energy Mater. Sol. Cells, 92(2008) 1311.

[62] H .Metzner, Th. Hahn, J. Cieslak, U.Grossner, U. Reislohner, W. Witthuhn, R.Goldhahm, J. Eberhardt, G..Gobsch, J.Krau Blich, Appl. Phys. Lett.81 (2002)156.

[63] V. Bhoslea,J. T. Prater,Fan Yang and D. Burk,S. R. Forrest,J. Narayan, J. Appl. Physics, 102 (2007) 023501.

[64] H.Ishikawa, N.Takeuchi, N.Okuda, T.Takeuchi and Y.Horikoshi, Jpn. J. Appl. Phys. 46

(2007) 2527-2529.

[65] R. Srinivasan, B. Chavillon, C. Doussier-Brochard, L.Cario, M. Paris, E. Gautron, P.Deniard, F. Odobel and S. Jobic, J. Mater. Chem. 18(2008), 5647–5653.

[66] R.B.V. Chalapathy and K.T. Ramakrishna Reddy, ADV. Mat. Sci. and Tech, 1(1998), N°2, 01 – 05.

[67] C. Platzer-Björkman, J. Lu, J. Kessler and L. Stolt, Thin Solid Films, 431-432(2003) 321 –325.

[68] M.E. Calixto, P.J. Sebastian, R.N. Bhattacharya and R. Noufi, Solar Energy Materials and Solar Cells, 59(1999), N°1-2, 75 – 84.

[69]**.** R. N. Bhattacharya, A. M. Fernandez1, Solar Energy Materials & Solar Cells, 76 (2003) 331–337.

[70] R.N. Bhattacharya, W. Batchelor, J.F. Hiltner, J.R. Sites, Appl. Phys. Lett. 75 (1999) 1431.

[71] R.N. Bhattacharya, H. Wiesner, T.A. Berns, R.J. Matson, J. Keane, K. Ramanathan, A. Swartzlander, A. Mason, R.N. Noufi, J. Electrochem. Soc. 144 (1997) 1376.

[72] K. Kushiya, M. Tachiyuki, T. Kase, I. Sugiyama, Y. Nagoya, D. Okumura, M. Satoh, I. Sugiyama, O. Yamase, H. Takeshita, Sol. Energy Mater. Sol. Cells, 49 (1997) 277.

[73] R.N. Bhattacharya, W. Batchelor, H. Wiesner, F. Hasoon, J.E. Granata, K. Ramanathan, J. Alleman, J. Keane, A. Mason, R.J. Matson, R.N. Noufi, J. Electrochem. Soc. 145 (1998) 3435.

[74] V.K. Kapur, B.M. Basol, E.S. Tseng, Sol. Cells, 21 (1987) 65.

[75] L. Thouin, J. Vedel, J. Electrochem. Soc. 142 (1995) 2996.

[76] C. Guillen, J. Herrero, J. Electrochem. Soc. 142 (1995) 1834.

[77] R.N. Bhattacharya, W. Batchelor, R.N. Noufi, Electrochem. Solid-State Lett. 2 (1999) 222.

[78] A.M.A. Haleem, M. Ichimura, Materials Science and Engineering: B, 164 (2009) 180.

[79] S .Chowdhury, M. Ichimura, J. Appl. Phys. 48(2009)061101.

[80] F. Long, W. Wang, J. Du, Z.Zou, Journal of Physics: Conference Series, 152 (2009) 012074.

[81] A H Moharram, M M Hafiz, A.Salem, Applied Surface Science, 172 (2001)61.

[82] J .Muler, J .Nowoczin, H.. Schmitt, Thin Solid Films, 496 (2006) 364.

[83] M E Calixto, P J Sebastian, R N Bhattacharya, R. Noufi, Solar Energy Materials and Solar Cells, 59(1999) 75.

Chapter-2
Electrochemical deposition of GaS_xO_y thin films

2.1. Introduction

Gallium sulfide GaS and Ga_2S_3, gallium oxide Ga_2O_3, and their alloy gallium sulfide oxide GaS_xO_y are n-type wide-gap semiconductors and thus are promising candidates for solar cell application as a buffer layer material. The aim of this research is to deposit GaS_xO_y thin films by the electrochemical deposition (ECD) method. So far, several works have been done on gallium sulfide fabrication techniques such as metal-organic chemical vapor deposition [1], modified Bridgman method [2], microwave glow discharge method [3], chemical-vapor transport method [4], chemical vapor deposition [5], and on gallium oxide fabrication techniques such as spray pyrolysis [6] and molecular-beam epitaxy [7]. However, there is no single report on GaS_xO_y fabrication by ECD or any other chemical methods. Thus, this is the first report on the fabrication of GaS_xO_y by ECD to the best of our knowledge. In this chapter, gallium sulfide oxide thin films are deposited by cathodic ECD from an aqueous bath containing $Na_2S_2O_3$ (sulfur source) and $Ga_2(SO_4)_3$ (gallium source) using DC biasing.

2.2. Experimental details

A three-electrode cell was used for ECD with a saturated calomel electrode (SCE) as the reference electrode. Indium-tin-oxide (ITO)-coated glass and fluorine-doped-tin-oxide (FTO)-coated glass were used as the working electrode (substrate) and a platinum sheet was used as the counter electrode. In the following, all the potential values are vs SCE. Both the ITO substrate and the platinum sheet were washed ultrasonically in alkyl benzene and dried in nitrogen before the experiment. The deposition area was about 1x1 cm^2. An aqueous bath containing $Na_2S_2O_3$ with a concentration range of 0-200 mM and $Ga_2(SO_4)_3$ with a concentration range of 2-30 mM was used for the deposition, which was performed at room temperature (22-25^oC). The pH of the solution was varied from 1 to 3 by adding a few drops of H_2SO_4 and NaOH, but the solution was stable. After the experiment, the deposited films were

carefully washed in pure water and naturally dried in air.

Gallium sulfide is expected to be formed by the following mechanism, as reported for other sulfides [8]. Elemental sulfur is released from $S_2O_3^{2-}$ by the reaction

$$S_2O_3^{2-} + 2H^+ \longrightarrow S + H_2SO_3 . \qquad (1)$$

Ga_2S_3, for example, is expected to be formed at the cathode by the reaction

$$2Ga^{3+} + 3S + 6e^- \longrightarrow Ga_2S_3 . \qquad (2)$$

We confirmed that pure Ga_2S_3 is vigorously dissolved in water. Thus Ga_2S_3 once formed will react with water, and Ga_2O_3 and $Ga(OH)_3$ will be formed. The oxide may also be formed by the following reaction with dissolved oxygen:

$$3O_2 + 4Ga^{3+} + 12e^- \longrightarrow 2Ga_2O_3 . \qquad (3)$$

We may assume that the reaction rate is very slow for elemental S release and since above mentioned reactions are in continuous process hence we could not get pure Ga_2O_3 but a GaS_xO_y alloy only.

Compositional analysis was carried out by Auger electron spectroscopy (AES) using a JEOL JAMP 7800 Auger microprobe at a probe voltage of 10 kV and a current of $2x10^{-8}$ A. Argon ion etching with an acceleration voltage of 3 kV and a current of 20 mA was used to sputter the film surface. The S/Ga and O/Ga atomic ratios were calculated using standard Ga_2S_3 and Ga_2O_3 compounds, respectively. The X-ray diffraction (XRD) measurement was carried out by the RIGAKU RINT-2000 diffractometer using Cu $K\alpha_1$ radiation at 40 kV/30 mA.The thickness of the films was measured by an Accretech Surfcom-1400D profile meter. The optical transmission measurement was performed using a JASCO U-570 UV/VIS/NIR spectrometer with the substrate as the reference. The surface morphology of the film was analyzed using a Hitachi S-2000S scanning electron microscope (SEM) at a constant acceleration voltage of 10 kV and a magnification of 2000. Furthermore, to determine the type of conduction and to estimate the photosensitivity of the deposited films, photoelectrochemical (PEC) measurements were carried out.

2.3. Results and discussion

We investigate GaS_xO_y thin film deposition by ECD from three different view points: (1) $Na_2S_2O_3$ dependence, (2) pH dependence, and (3) $Ga_2(SO_4)_3$ dependence.

Figure 2.1 shows the cyclic voltammogram obtained using the ITO substrate for solutions containing $Na_2S_2O_3$ = 0, 50, 100, and 200 mM with $Ga_2(SO_4)_3$ =10 mM at an unadjusted pH. From these graphs we study the current response of the electrochemical system under the application of a triangular voltage sweep. The current response for the FTO substrate was essentially the same as that shown in Fig. 2.1. The cathodic scan is from 0 to -1.5 V and the anodic scan is from -1.5 to +0.5 V with a scan rate of 20 mV/s. For the solutions containing $Na_2S_2O_3$, the deposition is associated with a cathodic current of below -1.0 V. In the negative scan, negative current peaks were observed between -1.1 and -1.3 V, and the peak shifted to a less negative voltage with increasing $Na_2S_2O_3$. Also, there are well-defined reoxidation anodic peaks around -0.8 V in the case of solutions containing $Na_2S_2O_3$. In case of the solution containing $Ga_2(SO_4)_3$ only, two reoxidation peaks appeared around –0.76 V and –0.25 V, and in the negative scan, the current increased monotonically. We found that without adding $Na_2S_2O_3$ there is no deposition of a GaS_xO_y film, even at -1.2 V. For the $Na_2S_2O_3$ added solutions, the deposition potential was set at the potential of the first cathodic peak observed in cyclic voltammetry.

Table 2.1 shows the compositional ratio and thickness of films deposited on the ITO substrate at an unadjusted pH and different $Na_2S_2O_3$ concentrations for a deposition time of 2 min. The AES spectra were recorded after sputtering the surfaces for 5 to 10 s. Figure 2.2 shows an example of an AES spectrum for the film deposited with a $Na_2S_2O_3$ concentration of 100 mM. As shown in Table 2.1, the S/Ga and O/Ga ratios of the deposited films are very close for different $Na_2S_2O_3$ concentrations, i.e., an increase in the amount of $Na_2S_2O_3$ did not lead to an increase in the sulfur content of the films. This can be explained as follows; for high $Na_2S_2O_3$ concentrations (>100 mM), white sulfur colloids are quickly formed, thus, the amount of atomic sulfur in the solution does not increase with $Na_2S_2O_3$ concentration. In the following, the amount of $Na_2S_2O_3$ is fixed at 100 mM.

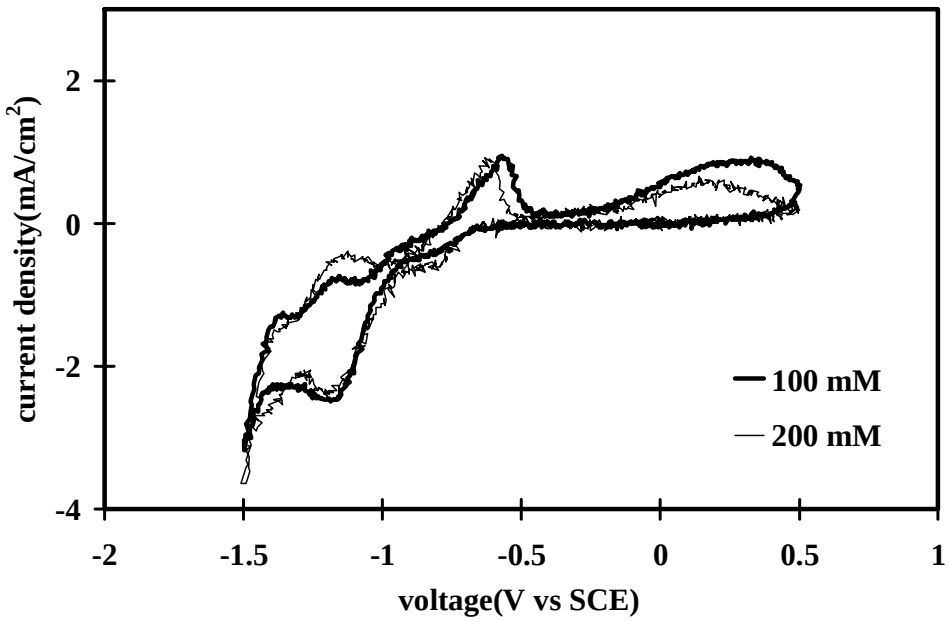

(a)

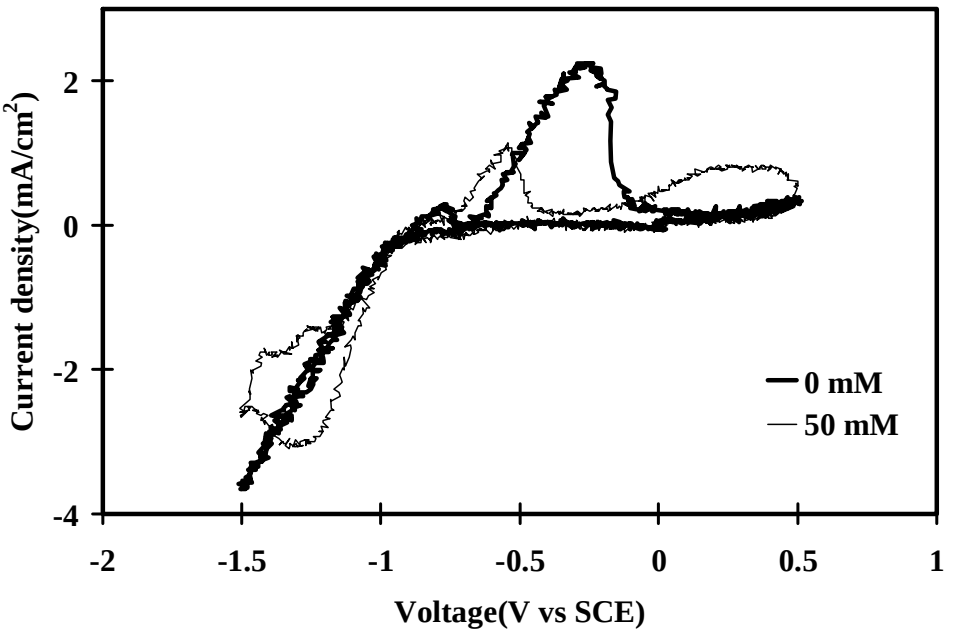

(b)

Fig.2.1. Cyclic voltammograms of the deposition solutions for different $Na_2S_2O_3$ concentrations at a scan speed of 20 mV/s: (a) $Na_2S_2O_3$ = 200 and 100 mM and (b) $Na_2S_2O_3$ = 50 and 0 mM.

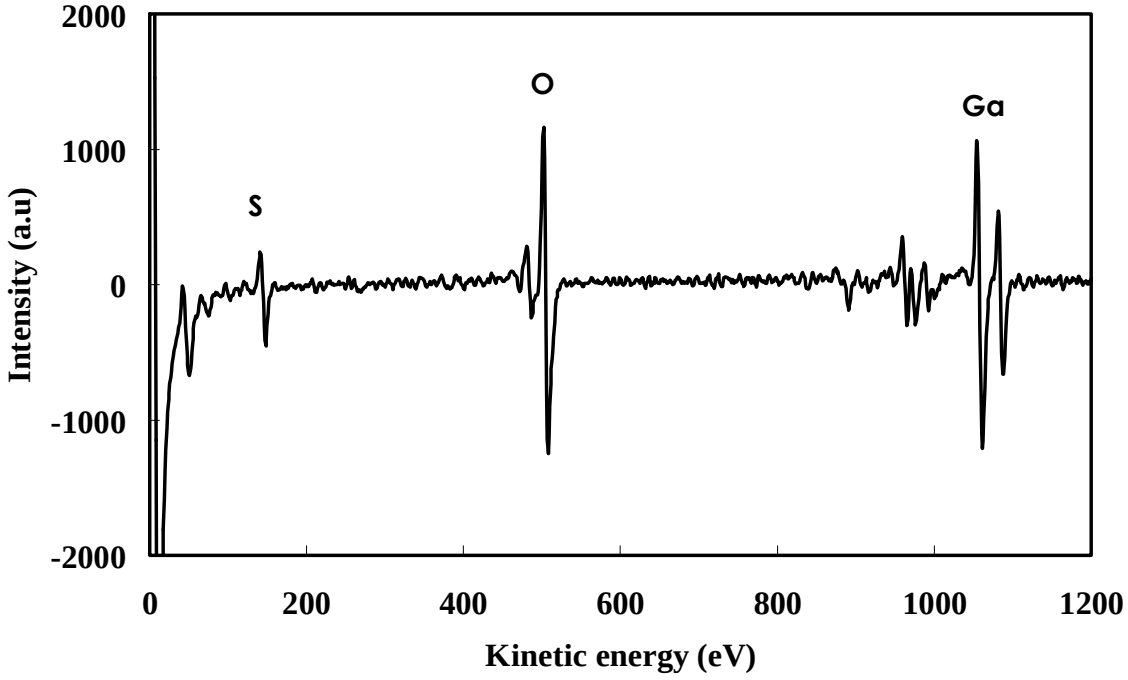

Fig.2.2. AES spectrum for GaS_xO_y thin film deposited at $Ga_2(SO_4)_3$ = 10 mM and $Na_2S_2O_3$ = 100 mM, unadjusted pH

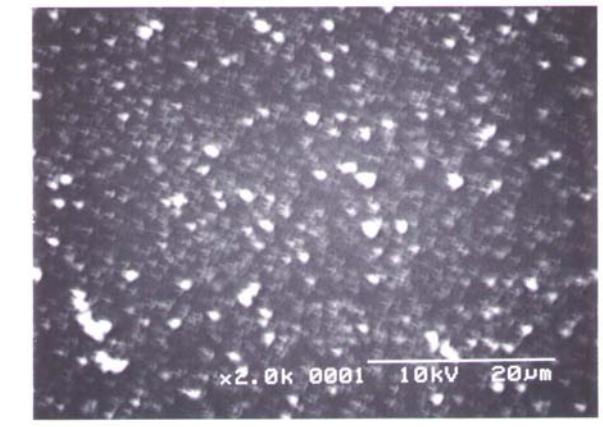

Fig.2.3. SEM image of the film deposited at $Na_2S_2O_3$ =100 mM and $Ga_2(SO_4)_3$ = 20 mM, unadjusted pH

Table - 2.1: Atomic composition and characteristics of the GaS_xO_y films deposited on ITO at different $Na_2S_2O_3$ concentrations

$Na_2S_2O_3$ (mM)	$Ga_2(SO_4)_3$ (mM)	Deposition voltage (V)	pH	Thickness (m)	S/Ga	O/Ga
0	10	-1 to -1.2	2.0	No film		
50	10	-1.3	2.1	0.25	0.18	1.65
100	10	-1.15	2.6	0.2	0.14	1.54
200	10	-1.15	2.6	0.3	0.16	1.48

Table - 2.2: Atomic composition and characteristics of the GaS_xO_y films deposited on ITO at different pH values

$Na_2S_2O_3$ (mM)	$Ga_2(SO_4)_3$ (mM)	Deposition voltage(V)	pH	Thickness (m)	S/Ga	O/Ga
100	10	-1.3	1	No film	-	-
100	10	-1.15	2	0.1	0.18	2.11
100	10	-1.15	2.6(N)	0.2	0.14	1.54
100	10	-1.3	3	0.025(too thin)	-	-

Table -2.3: Atomic composition and characteristics of the GaS_xO_y films deposited on ITO at different $Ga_2(SO_4)_3$ concentrations

$Na_2S_2O_3$ (mM)	$Ga_2(SO_4)_3$ (mM)	Deposition voltage (V)	pH	Thickness (m)	S/Ga	O/Ga
100	2	-1.06	3	No film	-	-
100	5	-1.13	3.0	0.1	0.10	1.63
100	10	-1.15	2.6	0.2	0.14	1.54
100	20	-1.15	2.5	0.25	0.14	1.51
100	30	-1.15	2.4	0.3	0.12	1.58

As shown above, the composition is oxygen-rich (x<y) even for a high $Na_2S_2O_3$ concentration (~200 mM), whereas deposition does not occur without $Na_2S_2O_3$ in the solution. Thus, we did not succeed in depositing pure gallium sulfide or oxide but only the alloy.

In order to obtain the most suitable pH value for the deposition bath, GaS_xO_y thin films were deposited at different pH values. The results of deposition on ITO substrates are summarized in Table 2.2. The films were deposited at pH = 1 and 2 (adjusted by H_2SO_4), pH=2.6 (unadjusted) and pH=3 (adjusted by NaOH) for a deposition time of 2 min. The unadjusted pH value varied slightly (by ±0.2) from deposition to deposition. We observed that there is no deposition at pH =1, even at -1.3 V. Also a high pH (pH=3) is not suitable because a very thin and nonuniform film is deposited. On the other hand, the pH value did not have a significant effect on the compositional ratios S/Ga and O/Ga in the pH values of 2 and 2.6. Among the four pH values examined, we conclude that the unadjusted pH of 2.6 is optimum.

In order to optimize the $Ga_2(SO_4)_3$ concentration, the experiment was carried out using different concentrations of $Ga_2(SO_4)_3$. Table 2.3, shows the compositional ratio and thickness of films deposited on ITO at different $Ga_2(SO_4)_3$ concentrations with a deposition time of 2 min. $Ga_2(SO_4)_3$ concentration does not have a significant effect on the composition. Films were also deposited on FTO under the conditions given in Table 2.3, and we found that there is no significant difference between the films on ITO and FTO. Figure 2.3 shows the surface morphology of the film deposited on ITO in the case of the solution containing 100 mM $Na_2S_2O_3$ and 20 mM $Ga_2(SO_4)_3$ at the unadjusted pH. The substrate surface was covered with a continuous layer, and grains were observed on the layer.

We performed XRD measurements for the deposited films on the ITO and FTO substrates for $Ga_2(SO_4)_3$ =20 mM with $Na_2S_2O_3$ =100 mM at the unadjusted pH, but we observed only peaks due to substrate(ITO or FTO). Hence, our deposited films are amorphous in nature. Figure 2.4 shows the optical transmission of the films deposited on the ITO and FTO substrates at the unadjusted pH. It is observed that the film deposited on FTO has higher transmission at short wavelengths with a gradual absorption edge near 350 nm, whereas the film on ITO exhibits two absorption edges near 450 and 350 nm. Since the AES analysis did not confirm any significant difference in compositional ratio for the films on ITO and FTO, the absorption edge near 450

nm for the films on ITO are considered to be due to an interfacial layer at the film/ITO interface formed by the electrolyte-ITO interaction [9]. The optical band gap energy was calculated from the classical relation for direct-band optical absorption, $=k(h -Eg)^{1/2}/h$, where k is a constant, Eg is the band gap and h is the photon energy. Fig. 2.5 shows that Eg is about 3.5 eV for both the substrates. For the film on ITO, another lower band gap appears at about 2.9 eV, and this can be attributed to the interfacial layer as noted above. The estimated value of Eg (3.5 eV) is reasonably close to the reported values for GaS, 2.53 eV(indirect)[10], 2.59 eV(indirect) and3.04 eV(direct)[11], 3.05 eV(direct)[12], and that reported for Ga_2S_3, 3.42 eV(direct)[12], whereas it is considerably lower than those reported for gallium oxide, 5.16 eV[6] and 4.94 eV[13], even though the composition is oxygen-rich. The lower value of Eg may be due to the effects of the random atom arrangement (i.e., the amorphous nature) and band-gap bowing in the gallium sulfide oxide alloy. On the other hand, theoretically, for amorphous semiconductors, the lack of crystal structure, removes the possibility of phonon momentum; thus for direct transition, $=k(h -Eg)^2/h$ .Considering this point, the plot of $(h)^{1/2}$ versus h , shown inset of Fig.2.5 exhibits the lower value of Eg. Further studies are needed to explain this behavior which will be considered in future.

The PEC measurements were performed using the same three-electrode cell with the light incident from a xenon lamp toward the backside of the sample (working electrode) as shown in Fig.2.6 (a). The incident light was turned off and on mechanically every 5 s by inserting and removing a barrier between the lamp and the sample, respectively (i.e., a 200 mHz periodic pulse of light). This light chopping was performed under the application of a ramp voltage between the working and reference electrodes. This measurement was accomplished through two different voltage range; first in the anodic bias range (from 0 to +1 V) and then in the cathodic bias range (from 0 to -1 V).Before measurement, the deposited film sample was prepared as shown in Fig.2.6 (b) and then hanged as a working electrode in the electrochemical cell (film facing the counter electrode, Pt sheet). Figure 2.7 shows the PEC measurements for the films deposited using the solution with 100 mM $Na_2S_2O_3$ and 20 mM $Ga_2(SO_4)_3$. It is clear that the current was changed as a result of the light chopping. Under illumination, some carriers were excited in the illuminated region of the GaS_xO_y thin film. The excited minority carriers then diffused to the surface during their lifetime to participate in the electrochemical reaction at

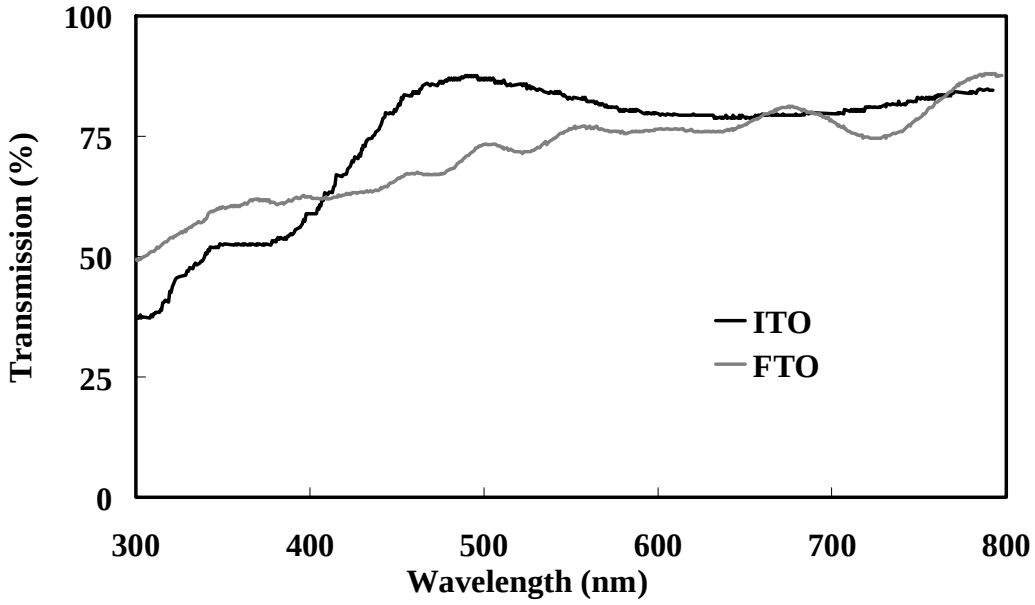

Fig.2.4. Optical transmission of the films deposited at $Na_2S_2O_3$ =100 mM, $Ga_2(SO_4)_3$ = 20 mM, and unadjusted pH on the ITO and FTO substrates

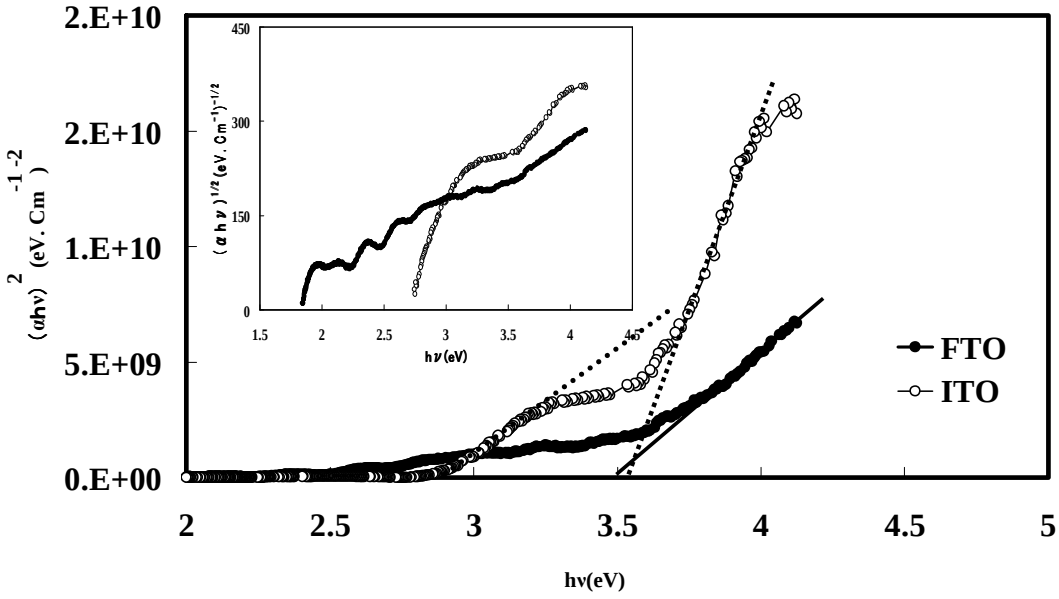

Fig.2.5. Estimated band gap for the films deposited with $Na_2S_2O_3$ =100 mM and $Ga_2(SO_4)_3$ = 20 mM at unadjusted pH on the ITO and FTO substrates.

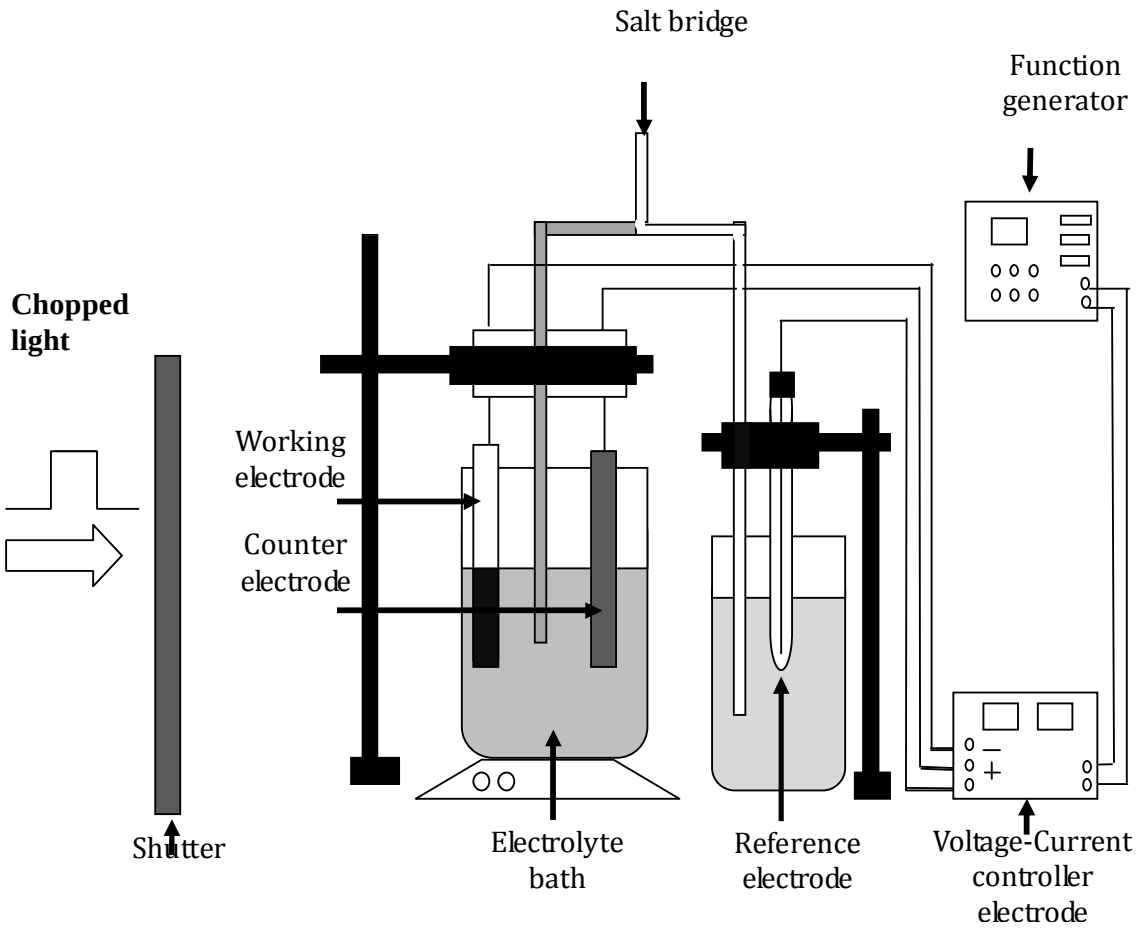

Fig.2.6 (a): A schematic diagram of the 3-electrode cell apparatus used for photoelectrochemical (PEC) study of the deposited films

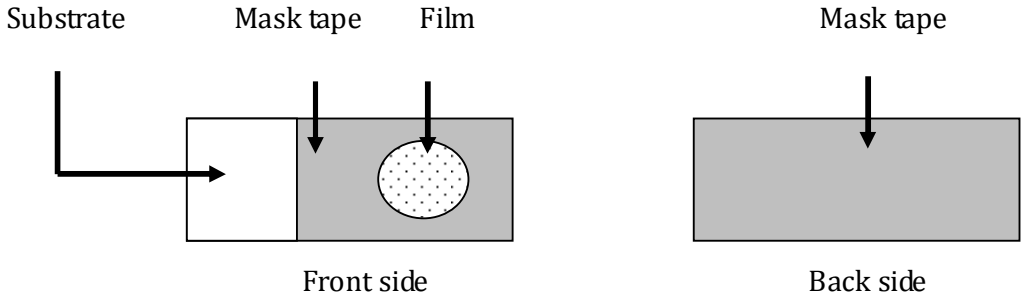

Fig.2.6 (b): The masking form for the sample to be ready for PEC measurement

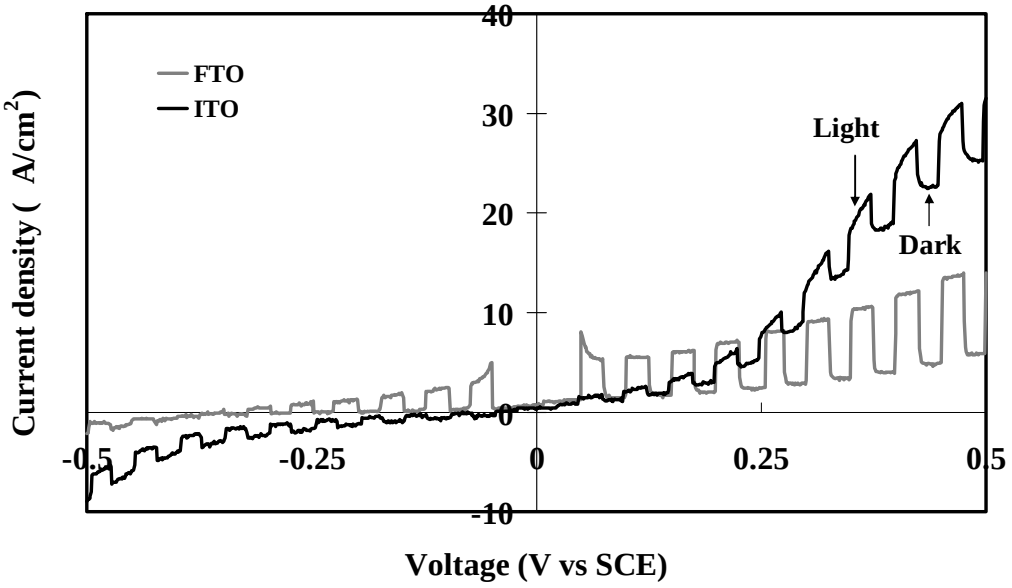

(a)

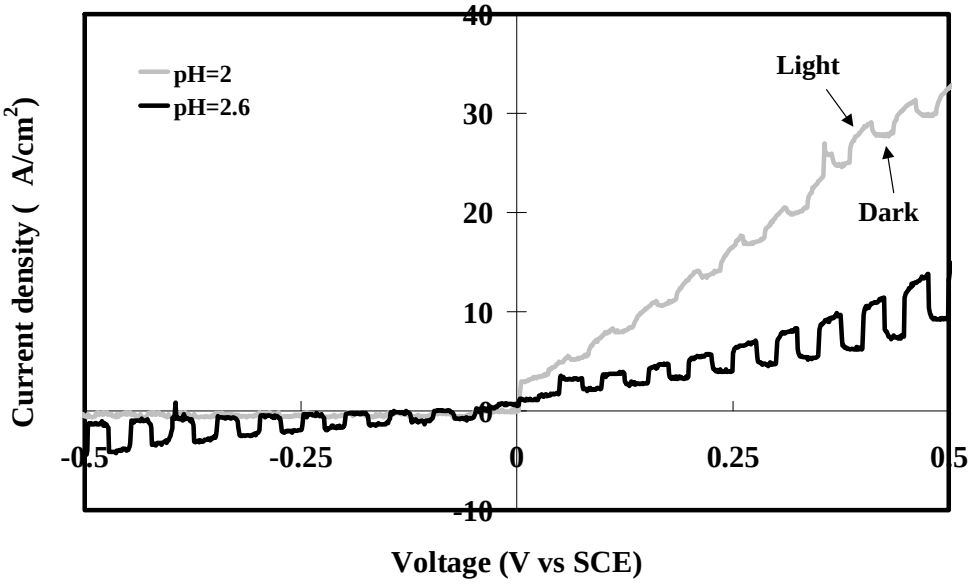

(b)

Fig.2.7. PEC measurements of the films deposited at (a) different values of pH on the ITO substrate and (b) unadjusted pH on different substrates

the film/electrolyte interface [14]. In the case of our GaS_xO_y thin film, this phenomenon was observed more clearly under anodic biasing than under cathodic biasing. This means that the oxidation reaction at the film surface is enhanced under illumination. This implies that the minority carriers generated here are holes. Thus, the deposited films are n-type semiconductors and exhibit photosensitive behavior. Figure 2.7(a) shows the PEC results for the films deposited on ITO at different values of pH. It is clear that the film deposited at the unadjusted pH exhibits stronger photosensitivity than that deposited at a low pH. Figure 2.7(b) shows the results for the films deposited on ITO and FTO at the unadjusted pH. A small negative photocurrent was observed during cathodic biasing for the film on the ITO substrate, whereas the photocurrent is always positive for the film deposited on the FTO substrate.

Considering all the above results, the solution with 10-20 mM $Ga_2(SO_4)_3$, 100 mM $Na_2S_2O_3$, and an unadjusted pH is optimum for GaS_xO_y thin-film deposition.

2.4. Conclusion

Using the ECD method, GaS_xO_y thin films were deposited from an aqueous solution of $Ga_2(SO_4)_3$ and $Na_2S_2O_3$. The as - deposited films are amorphous in nature and composition is oxygen-rich ($x<y$), even for a high $Na_2S_2O_3$ concentration (~200 mM), whereas almost no deposition was observed without $Na_2S_2O_3$ in the solution. The films deposited under the optimized conditions have a wide band gap of about 3.5 eV and exhibit n-type conduction and photosensitivity. These properties make the film suitable for use as a buffer layer in solar cells.

References

[1] A. Keys, S. G. Bott, A. R. Barron, Chem. Mater. 11 (1999) 3578.

[2] N. M. Gasanly, A. Aydinli, H. Ozkan, C. Kocabas, Solid State Commun. 116 (2000) 147.

[3] X. Chen, X. Hou, X. Cao, X. Ding, L. Chen, G. Zhao, X. Wang, J. Cryst. Growth,173 (1997) 51.

[4] C. H. Ho, Y. S. Huang, P. C. Liao, K. K. Tiong, J. Phys. Chem. Solids,60 (1999) 1797.

[5] S. Suh D. M. Hoffman, Chem. Mater. 12 (2000) 2794.

[6] Z. Ji, J. Du, J. Fan, W. Wang, Opt.Mater. 28 (2006) 415.

[7] T. Oshima, T. Okuno, S. Fujita, Jpn. J. Appl. Phys. 46 (2007) 7217.

[8] E. Fatos, R. Duo, P. Herrasti, F. Arjona, E. G. Camarero, J. Electrochem. Soc. 131 (1984) 2243.

[9] M. Senthilkumar, J. Mathiyarasu, J. Joseph, K. L. N. Phani, V. Yegnaraman, Mater. Chem. Phys. 108 (2008) 403.

[10] C. H. Ho S. L. Lin, J. Appl. Phys. 100 (2006) 083508.

[11] E. Aulich, J. L. Brebner, E. Mooser, Phys. Status Solidi,31 (1969) 129.

[12] M. Lazell, P. O'Brien, D. J. Otway, J.-H. Park, J. Chem. Soc., Dalton Trans.24 (2000) 4479.

[13] A. Ortiz, J. C. Alonso, E. Andrade, C. Urbiola, J. Electrochem. Soc. 148 (2001) 26.

[14] K. Mishra, K. Rajeshwar, A. Weiss, M. Murley, R. D. Engelken, M. Slayton, H. E. McCloud, J. Electrochem. Soc. 136 (1989) 7.

.

.

Chapter-3
Photochemical deposition of GaS_xO_y thin films

3.1. Introduction

Photochemical deposition (PCD) is a technique of film preparation from solutions by UV light illumination. In this chapter, GaS_xO_y thin films were deposited on fluorine-doped-tin-oxide-coated glass substrates by PCD from an aqueous solution of $Ga_2(SO_4)_3$ and $Na_2S_2O_3$. Using photochemical deposition technique, deposition of GaS_xO_y thin films is the first report so far as our knowledge is concerned. In chapter-2, we have deposited GaS_xO_y electrochemically onto indium-doped tin oxide (ITO) and fluorine-doped tin oxide (FTO) coated glass substrates from an aqueous bath containing 20 mM $Ga_2(SO_4)_3$,100 mM $Na_2S_2O_3$,at unadjusted pH by DC biasing [1].

In view of finding a more low-cost, simple experimental setup and better controllability, recently, a novel photochemical deposition (PCD) method has been found successful in depositing semiconductor thin films from an aqueous solution [2-5]. The deposition experiment was carried out under various amounts of gallium sulfate and sodium thiosulfate, different pH, deposition time to determine basic compositional, structural and optical characteristics of the as-deposited films.

3.2. Experimental details

An aqueous solution of 50 ml containing $Ga_2(SO_4)_3$ in the range of 2- 40 mM and $Na_2S_2O_3$ in the range of 0-100 mM was prepared. pH of the solution was varied from 1.0 to 12.0 by adding few drops of H_2SO_4 and NaOH. Lactic acid 100 - 270 mM was used to avoid precipitation for high pH. The apparatus for PCD is schematically shown in Fig.3.1. A degreased substrate was immersed in the solution and illuminated by a high-pressure mercury lamp through a spherical

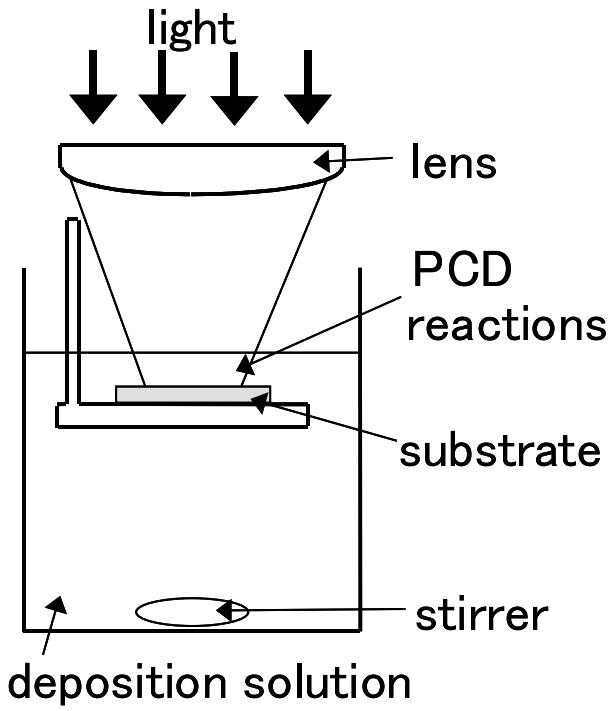

Fig.3.1. Schematic diagram of the PCD method

lens from above as shown in Fig.3.1. The distance from the solution surface to the substrate was maintained about 2-3 mm. It was observed that the substrate position affects the deposited film thickness, and we could not precisely control this position. The diameter of the illumination region was approximately 10 mm.The power density of the UV region is 100 mW/cm^2

Compositional analysis was carried out by Auger electron spectroscopy (AES) using a JEOL JAMP 7800 Auger microprobe at a probe voltage of 10 kV and a current of $2x10^{-8}$ A. Argon ion etching with an acceleration voltage of 3 kV and a current of 20 mA was used to sputter the film surface. The AES spectra were recorded after sputtering the surface for 6 to 10 s. The S/Ga and O/Ga atomic ratios were calculated using standard Ga_2S_3 and Ga_2O_3 compounds, respectively. The X-ray diffraction (XRD) measurement was carried out by the RIGAKU RINT-2000 diffractometer using Cu $K\alpha_1$ radiation at 40 kV/30 mA. The thickness of the films was measured by an Accretech Surfcom-1400D profile meter. The optical transmission measurement was performed using a JASCO U-570 UV/VIS/NIR spectrometer with the

substrate as the reference. The surface morphology of the film was analyzed using a Hitachi S-2000S scanning electron microscope (SEM) at a constant acceleration voltage of 10 kV and a magnification of 2000. The electrical properties were characterized by current-voltage (I-V) measurements along the thickness direction. After the film deposition, the In electrodes were evaporated, and then the resistance of GaS_xO_y/FTO was compared with the FTO resistance of the same piece of the substrate to calculate the resistivity of the GaS_xO_y film.

3.3. Results and discussion

3.3.1. Deposition at unadjusted pH

The experiment was carried out using 2-20 mM $Ga_2(SO_4)_3$, 0-100 mM $Na_2S_2O_3$ at unadjusted pH for 1 hour deposition period. The pH value was in a range from 2 to 3, depending on the solution composition. The solutions were slightly milky with no precipitation and stable in dark. We found that there was no deposition from the bath containing 20 mM $Ga_2(SO_4)_3$ and 0 mM $Na_2S_2O_3$. Thus $Na_2S_2O_3$ is essential for the deposition. On the other hand, when 100 mM $Na_2S_2O_3$ was added in the solution, yellow-white powder was formed without deposition of a continuous film on the substrate. By reducing the $Na_2S_2O_3$ concentration to 50 mM, a continuous film was formed but there was still some powder observed on the surface. When $Na_2S_2O_3$ concentration is 25 mM, a film was deposited without powder formation. Therefore, in the following, the amount of $Na_2S_2O_3$ is fixed at 25 mM.

Table - 3.1: Atomic composition and characteristics of the GaS_xO_y films deposited at unadjusted pH, different $Ga_2(SO_4)_3$ concentrations. The deposition time is one hour.

$Na_2S_2O_3$ (mM)	$Ga_2(SO_4)_3$ (mM)	pH	Thickness (μm)	S/Ga	O/Ga
25	2	3.0	0.05	0.16	1.61
25	5	2.8	0.2~ 0.3	0.26	1.53
25	10	2.6	0.1~0.15	0.27	1.56
25	20	2.4	0.075~ 0.2	0.16	2.32
25	40	2.2	0.01		

To optimize the $Ga_2(SO_4)_3$ concentration, the GaS_xO_y films were deposited at various $Ga_2(SO_4)_3$ concentrations as shown in Table 3.1. Figure 3.2 shows an example of an AES

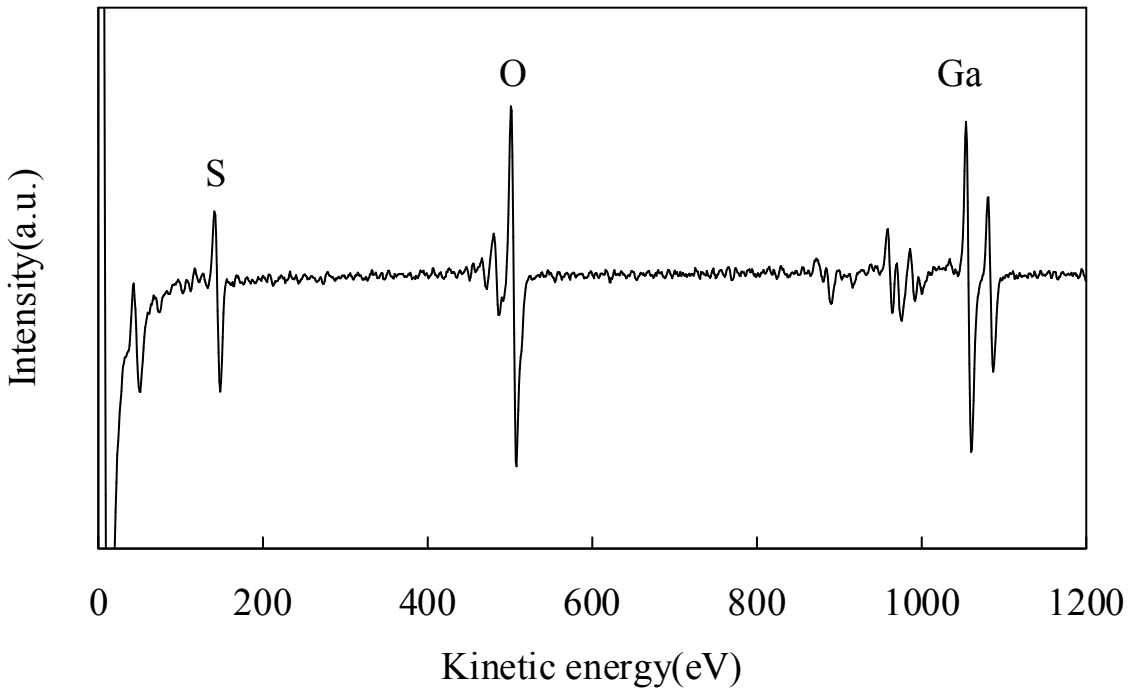

Fig.3.2. AES spectrum for the GaS_xO_y thin film deposited at $Ga_2(SO_4)_3$ = 5 mM , $Na_2S_2O_3$ = 25 mM, unadjusted pH

spectrum for the film deposited with a 25 mM $Na_2S_2O_3$ and 5 mM $Ga_2(SO_4)_3$ concentration at unadjusted pH. As shown in Table 3.1, the O/Ga ratio is close to the stoichiometric ratio (1.5) and slightly group-VI-rich, for $Ga_2(SO_4)_3$ concentrations up to 10 mM. However, the film deposited with 20 mM $Ga_2(SO_4)_3$ contains a large amount of excess oxygen. We may expect that beside Ga_2O_3 formation, $Ga(OH)_3$ may be formed in the solution, and the high O/Ga ratio would be due to $Ga(OH)_3$ formation. There is a variation in thickness values between deposition runs even under the same deposition condition, as shown in Table 3.1, which would be due to the fact that the substrate position was not controlled very precisely, as noted in the previous section. When $Ga_2(SO_4)_3$ concentration was increased to 40 mM, the film thickness became too small to accurately obtain the film composition. This will be because the reaction was so active that the homogeneous particle formation dominates over the heterogeneous film deposition. From these results, the optimum $Ga_2(SO_4)_3$ concentration will be 5-10 mM. We performed XRD measurements for the deposited films, but we observed only peaks due to FTO. Hence, our deposited films are amorphous in nature.

Figures 3.3 (a) and (b) show the film morphology for the films deposited at $Ga_2(SO_4)_3$ = 5 mM

and 10 mM. In both the cases, the entire substrate surfaces were covered with a continuous layer of small grains. The GaS_xO_y films deposited from different $Ga_2(SO_4)_3$ concentration show the optical transmission spectrum in Fig. 3.4. The transmission in the visible region is not so high, probably because of scattering by the surface roughness. It is observed that different amount of $Ga_2(SO_4)_3$ caused no significant difference in transmission. For this condition, the optical band gap energy was calculated from the classical relation for direct-band optical absorption, $\alpha=k(h\nu-E_g)^{1/2}/h\nu$, where k is a constant, E_g is the band gap and hν is the photon energy. From Fig.3.5 we can see that E_g is about 3.5 eV. The estimated value of E_g (3.5 eV) is close to the reported values for the direct band gap of GaS, 3.04 eV [6], 3.05 eV [7], and that reported for Ga_2S_3, 3.42 eV [7], whereas it is considerably lower than those reported for gallium oxide, 5.16 eV [8] and 4.94 eV [8], even though the composition is oxygen-rich. The lower value of E_g may be due to the effects of the random atom arrangement (i.e., the amorphous nature) and band-gap bowing in the gallium sulfide oxide alloy. Theoretically, for amorphous semiconductors, the lack of crystal structure, removes the possibility of phonon momentum; thus for direct transition, $\alpha = k(h\nu-Eg)^2/h\nu$.Considering this point, the plot of $(\alpha h\nu)^{1/2}$ versus hν, shown in fig.3.5 exists the lower value of Eg. Further studies are needed to explain this behavior which will be considered in future. We observed a similar value for GaS_xO_y films deposited by the electrochemical deposition [1]. The I-V measurement was performed for the film deposited from the solution containing 25 mM $Na_2S_2O_3$ and 5 mM $Ga_2(SO_4)_3$. The In contact had ohmic characteristics, and the resistivity of the deposited film is $6.6 \times 10^2\ \Omega - cm$.

GaS_xO_y is expected to be formed by the following mechanism. In the general process of sulfide PCD, the thiosulfate ions present in the solution absorb the UV light and are exited. These photo exited thiosulfate ions release solvated electrons and sulfur atoms [2].

$$S_2O_3^{2-} + h\nu \rightarrow S + SO_3^{2-} \quad (1)$$
$$2\,S_2O_3^{2-} + h\nu \rightarrow S_4O_6^{2-} + 2e^- \quad (2)$$

We can expect that GaS_x is formed with S and e^- generated by the above reactions. However, GaS_x is hydrolytically unstable: we confirmed that pure Ga_2S_3 is vigorously dissolved in water. Thus GaS_x once formed will react with water, and Ga_2O_3 and $Ga(OH)_3$ will be formed.

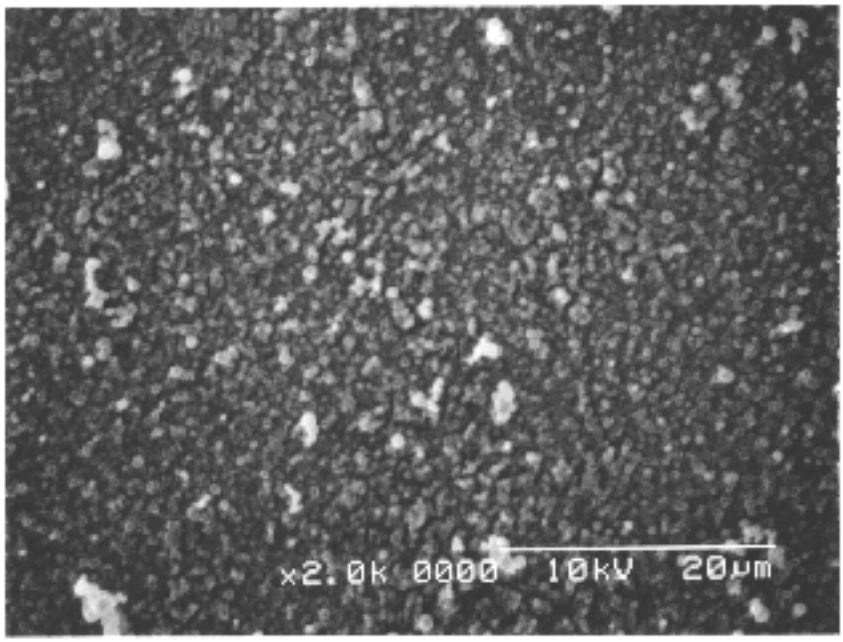

(a)

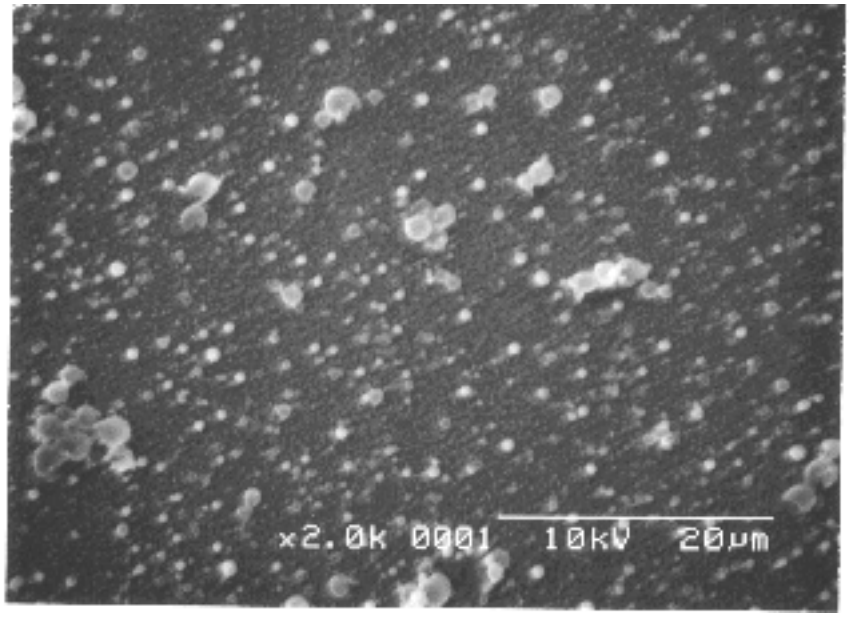

(b)

Fig.3.3. SEM image of the film deposited at unadjusted pH, $Na_2S_2O_3$ =25mM with (a) $Ga_2(SO_4)_3$ = 5mM and (b) 10 mM

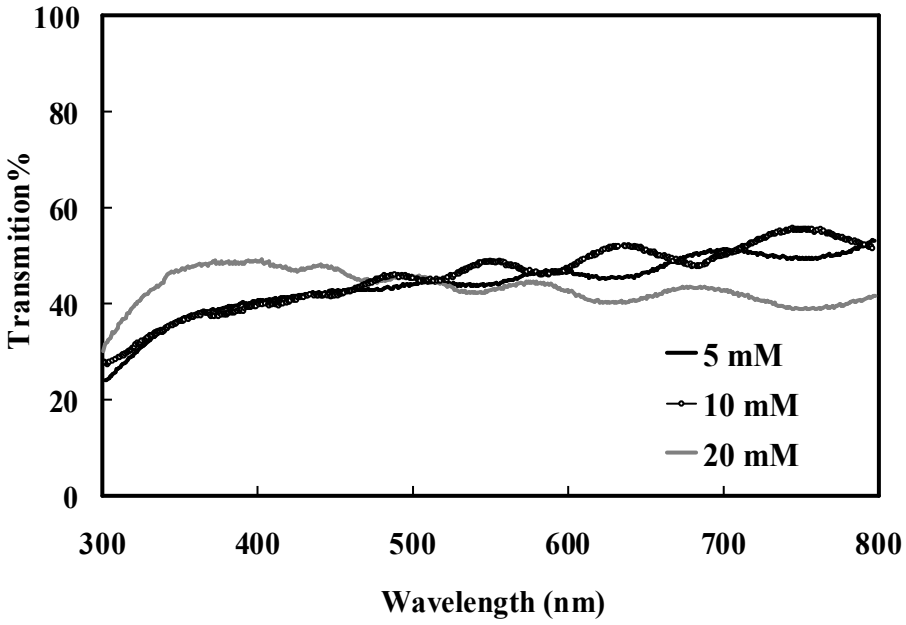

Fig.3.4. Optical transmission of the film deposited at unadjusted pH, $Na_2S_2O_3$ =25mM with $Ga_2(SO_4)_3$ = 5mM, 10mM, 20 mM.

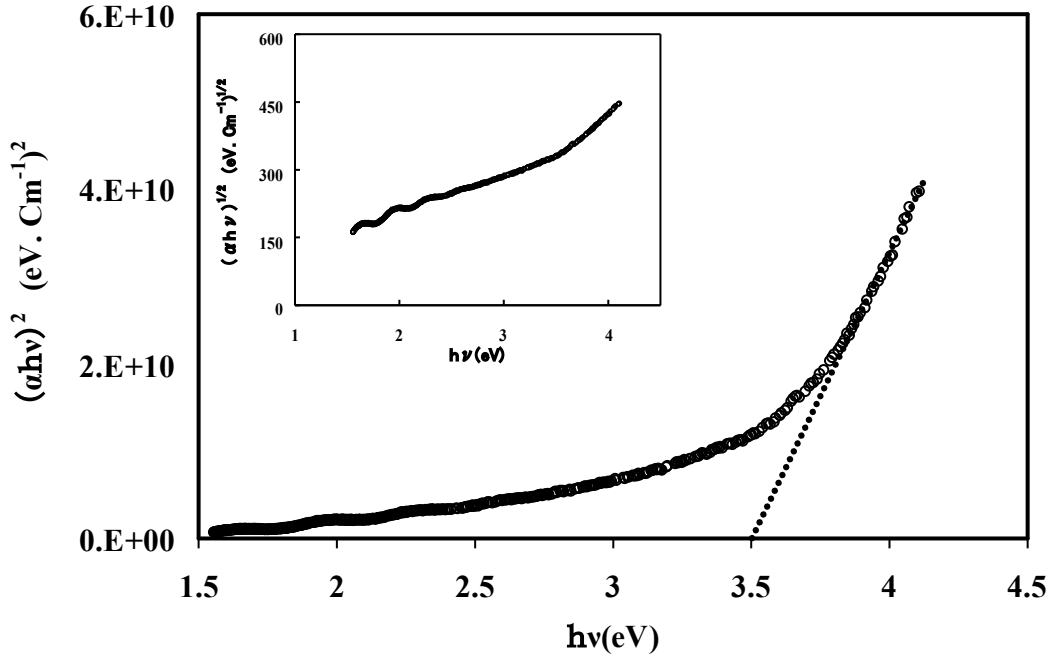

Fig.3.5. Estimated bandgap of the film deposited for $Na_2S_2O_3$ =25mM, $Ga_2(SO_4)_3$ = 5mM at unadjusted pH

3.3.2. Deposition bath at high pH

We studied the pH effects by varying pH from 4 to 12 for solutions containing 0 - 100 mM $Na_2S_2O_3$ and 20 mM $Ga_2(SO_4)_3$. A uniform GaS_xO_y film was deposited at pH = 9, but there was significant amount of white precipitates in the solution. We confirmed that without photo irradiation, no film was deposited on the substrate, and thus the deposition is photo-activated. However, spontaneous reactions also occurred, resulting in precipitation. Table 3.2 shows the compositional ratio and thickness of the films deposited at pH =9, $Ga_2(SO_4)_3$ = 20 mM and different $Na_2S_2O_3$ concentrations for a deposition time of 2 hours. The average thickness of the films was found in the range of 0.05 – 0.15 μm. It should be noted that the film was deposited even without $Na_2S_2O_3$ in the solution. Thus the deposition reaction is obviously different from that in the lower (unadjusted) pH, but we did not understand its details. Figure 3.6 shows the optical transmission of the films deposited from solution bath containing different $Na_2S_2O_3$ concentration at pH=9. It is observed that the deposited films have a gradual absorption edge near 360 nm, almost the same wavelength as that for the films deposited at unadjusted pH.

3.3.2.1. Optimize the Lactic acid concentration

Lactic acid ($C_3H_6O_3$) was added to the solution as a complexing agent to avoid precipitation at pH= 9. In order to obtain the suitable lactic acid concentration, first we select the deposition bath containing 25 mM $Na_2S_2O_3$, 20 mM $Ga_2(SO_4)_3$, and the films were deposited at different lactic acid concentration. As shown in Table 3.3, for 270 mM lactic acid, the deposited film is very thin, although the solution was clear. On the other hand, the precipitations were still observed in the solution bath containing 100 mM lactic acid. As shown in the table, we were unable to find a condition with reasonably large deposition rate and no precipitation formation for the bath containing lactic acid.

Considering the above results, the solution at high pH is not suitable for deposition because the precipitation is formed (without lactic acid) or the deposition rate is too low (with lactic acid).

Table - 3.2: Atomic composition and characteristics of the GaS_xO_y films deposited at different $Na_2S_2O_3$ concentration. The deposition time is two hour

$Na_2S_2O_3$ (mM)	$Ga_2(SO_4)_3$ (mM)	pH	Thickness (μm)	S/Ga	O/Ga
0	20	9	0.05	0	1.66
25	20	9	0.05	0	1.70
100	20	9	0.15	0.02	1.79

Table - 3.3: Deposition condition and film thickness of the GaS_xO_y films deposited at pH=9 for different amount of lactic acid concentration. The deposition time is two hour

$Ga_2(SO_4)_3$ (mM)	$Na_2S_2O_3$ (mM)	Lactic acid(mM)	Thickness (μm)
20	25	200	0.1
20	25	270	0.025
20	0	200	0.05
20	100	200	not continuous

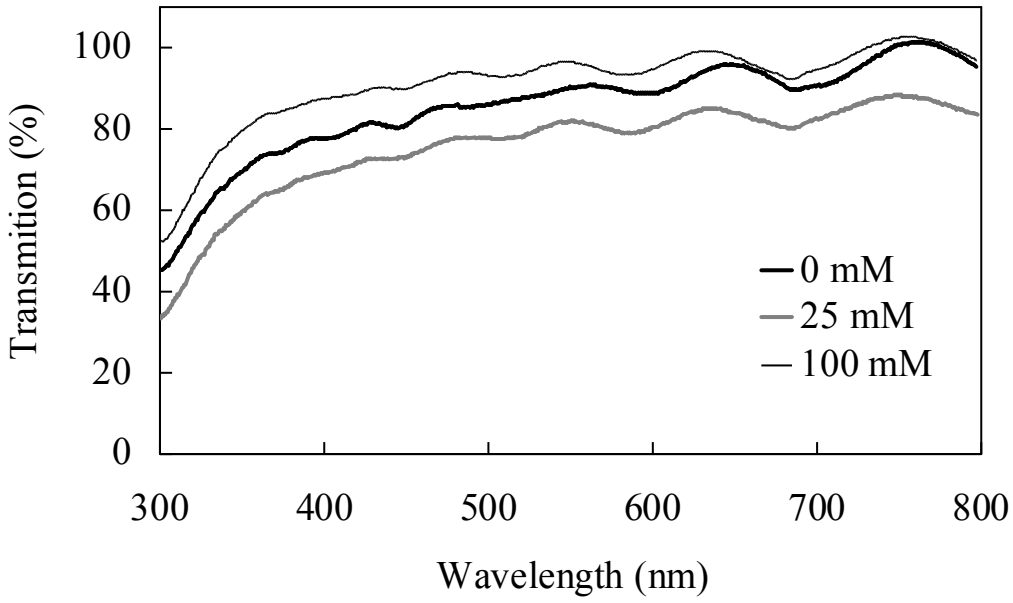

Fig.3.6. Optical transmission of the films deposited at $Ga_2(SO_4)_3$ = 20 mM and $Na_2S_2O_3$ =0 mM, 25 mM and 100 mM for pH =9

3.4. Conclusion

GaS_xO_y thin films were prepared by photochemical deposition. At unadjusted pH, an amorphous, uniform, oxygen rich film was deposited for 25 mM $Na_2S_2O_3$ and 5 mM $Ga_2(SO_4)_3$ with a growth rate of about 0.2~ 0.3 μm/hour. At unadjusted pH, the deposited films were very rough for a high $Na_2S_2O_3$ concentration (~100 mM), whereas no deposition was observed without $Na_2S_2O_3$ in the solution. At high pH = 9, relatively smooth films were obtained, but the solution bath contained precipitation. By adding lactic acid in the growth solutions, precipitation were avoided, but the deposition rate were low. The films deposited under the optimized conditions at unadjusted pH have a wide band gap of about 3.5 eV and the resistivity of 6.6×10^2 Ω – cm.

References

[1] S. Chowdhury, M. Ichimura, Jpn. J. Appl. Phys. 48 (2009) 061101.

[2] F. Goto, M. Ichimura, E. Arai, Jpn. J. Appl. Phys. 36 (1997) L1146.

[3] M. Ichimura, F. Goto, Y. Ono, E. Arai, J. Cryst. Growth 198/199(1999)308.

[4] M. Ichimura, K. Takeuchi, A. Nakamura, E. Arai, Thin Solid Films 384 (2001) 157.

[5] J. Podder, R. Kobayashi, M. Ichimura, Thin Solid Films 472(2005) 71.

[6] E. Aulich, J. L. Brebner, E. Mooser, Phys. Status Solidi 31 (1969) 129.

[7] M. Lazell, P. O'Brien, D. J. Otway, J.-H. Park: J. Chem. Soc., Dalton Trans.24 (2000) 4479.

[8] A. Ortiz, J. C. Alonso, E. Andrade, C. Urbiola, J. Electrochem. Soc. 148 (2001) 26.

Chapter-4

Potentiostatic and galvanostatic electrochemical deposition of $CuGa_xS_yO_z$ alloy thin films for photovoltaic applications

4.1. Introduction

In this chapter, we report the $CuGa_xS_yO_z$ (CGSO) alloy thin films fabrication onto fluorine-doped-tin-oxide-coated glass by potentiostatic (deposition at constant voltage) and galvanostatic (deposition at constant current) electrochemical deposition (ECD) from an aqueous solution. At the first stage, films were deposited by potentiostatic electrochemical deposition (P-stat ECD) at six different Cu to Ga ratios, i.e., Cu/Ga= 3/2, 1/1, 1/2, 1/4, 1/12 and 1/30. The impact of the Cu/Ga ratio on composition, surface morphology, photosensitivity and optical transmission of the films were investigated. We successfully deposited both the Cu-rich and Ga-rich thin films. At the second stage for galvanostatic electrochemical deposition (G-ECD) of CGSO alloy thin films, we choose 10 mM $CuSO_4$ and 10 mM $Ga_2(SO_4)_3$, i.e. Cu/Ga =1/2 bath so that the effect of $CuSO_4$ and $Ga_2(SO_4)_3$ molar ratio on the properties of deposited films are same. Moreover, potentiostatically deposited CGSO films from this ratio exhibit high photosensitivity with better surface morphology.

In chapter-2, we focused on a Ga based buffer or window layer GaS_xO_y electrochemically deposited on fluorine-doped-tin-oxide (FTO)-coated glass substrates from an aqueous solution containing 20mM of $Ga_2(SO_4)_3$ and 100 mM of $Na_2S_2O_3$ using DC biasing [1]. The deposited GaS_xO_y film had high optical transmission about 87% for 0.25 μm thickness and wide energy gap of ~3.5 eV. In chapter-3, we discussed about GaS_xO_y thin films depositing by the photochemical deposition technique [2].In the present study, we attempt to deposit Ga-based compounds which is suitable for the absorber layer also.

Ga-based chalcopyrite compound $CuGaS_2$ has a direct band gap of 2.5 eV at 293 K and thus has great potential for optical applications in the green part of the visible spectrum [3]. Many

deposition methods have been developed for the preparation of $CuGaS_2$, such as metal-organic chemical vapor deposition [4, 5], modulated flux deposition [6], vacuum evaporation [7, 8], and molecular beam epitaxy [9]. In the present study, we attempt to deposit $CuGa_xS_yO_z$ alloy in order to potentially have both absorber and window layers by tuning composition. The alloy $CuGa_xS_yO_z$ is expected to have properties between the related binary and ternary compounds, e.g., Cu_2O, Cu_xS, Ga_2O_3, Ga_2S_3, $CuGaS_2$. Therefore, the aim of this research are- firstly, to study the effect of Cu-to-Ga ratio on the properties of the deposited CGSO films. Secondly, to study the effect of deposition condition over film characteristics. Depending on our knowledge, this is the first report of thin film deposition of this alloy system.

In this study for P-stat ECD, we adopt electrochemical deposition (ECD) as in our previous study at chapter two and for G-stat ECD; we apply different current densities for films deposition. ECD is the most suitable for the commercial and large-scale application, and has widely been employed for the deposition of elemental, binary, ternary or even more complex compound and alloy thin films. The optimum condition for CGSO thin film formation from different baths and different current densities, and the effect of deposition condition over their compositional, structural, optical characteristics are investigated.

The P-stat ECD process is controlled by electric parameters which are easily adjusted to control thickness, microstructure and composition. The G-stat ECD process is easier to adapt in the industrial electroplating process because only a working electrode and a counter electrode are required and the current is produced by a simple generator [10].

4.2. Experimental details

A three-electrode cell was used for ECD with a saturated calomel electrode (SCE) as the reference electrode and connected to a Potentiostat/Galvanostat HA-301. A FTO-coated glass was used as the working electrode (substrate) and a platinum sheet was used as the counter electrode. Both the FTO substrate and the platinum sheet were washed ultrasonically in alkyl benzene and dried by nitrogen before the experiment. The deposition area was about 1x1 cm^2. After the experiment, the deposited films were washed softly in pure water and naturally dried

in air. The films were deposited at room temperature and an un-adjusted pH. In a 50 ml aqueous solution, $Ga_2(SO_4)_3$ (gallium source), $CuSO_4$ (copper source) and $Na_2S_2O_3$ (sulfur source) were contained.

For P-stat ECD, the $Na_2S_2O_3$ concentration was fixed at 100 mM, and the $Ga_2(SO_4)_3$ and $CuSO_4$ concentrations were varied at six different bath as shown in Table 4.1.On the other hand, for G-stat ECD as shown in Table-4.3, 100 mM $Na_2S_2O_3$,10 mM $Ga_2(SO_4)_3$ and 10 mM $CuSO_4$ were used in precursor bath

In the deposition process elemental sulfur is released from $S_2O_3^{2-}$ by the following chemical reaction:

$$2\ S_2O_3^{2-} + H^+ \rightarrow S + HSO_3^- \qquad (1)$$

At the cathode, the metal sulfides will be formed with the metal ions, S, and electrons. Besides, we can consider formation of the oxides through the following three routes. First, GaS_x is hydrolytically unstable, i.e, pure Ga_2S_3 is vigorously dissolved in water. Thus GaS_x once formed will react with water, and Ga_2O_3 and $Ga(OH)_3$ will be formed [2]. Second, pH is enhanced at the cathode, and the metal hydroxides will be formed and then decomposed to the oxides. Third, the reduced metal will react with dissolved oxygen in the solution.

The compositional, optical and structural properties of the electrochemically deposited films were characterized by various techniques. The compositional analysis was carried out by Auger electron spectroscopy (AES) using the model JEOL JAMP 7800 Auger microprobe at probe voltage 10 kV and current 2×10^{-8} A. An argon-ion sputtering with acceleration voltage 3 kV and current 20mA was used to sputter the film surface. Profile meter Accretech, Surfcom-1400D, was used to measure the thickness of the thin film. The X-ray diffraction (XRD) measurement was carried out by the RIGAKU RINT-2000 diffractometer using Cu $K\alpha_1$ radiation at 40 kV/30 mA. The optical transmission measurement was performed using the JASCO U-570 spectrometer with the FTO substrate as the reference. The surface morphology of the film was analyzed by scanning electron microscope (SEM; Hitachi S-3000H), keeping the acceleration voltage at 10 kV and magnification at 2000. The photoconductivity of the film was examined by means of the photoelectrochemical (PEC) measurements. The PEC

measurement was carried out using the same three electrode cell as used for the deposition. The deposited film was used as a working electrode and a 100mM $Na_2S_2O_3$ aqueous solution was used as an electrolyte. We used the $Na_2S_2O_3$ solution to avoid dissolution of sulfide during the PEC measurement. The backside of the sample was illuminated by pulsed light coming from a Xenon lamp (100mW/cm^2). The incident light is turned off and on mechanically every 5 s by putting and removing a barrier between the lamp and the sample, respectively. A ramp potential, with a potential step equal to 5mV/s, was applied between the working and the reference electrodes; first in the cathodic bias range (from 0 to -1V) and then the anodic bias range (from 0 to +1 V). At the same time the released current was monitored.

4.3. Results and discussion

4.3.1. Potentiostatic electrochemical deposition of $CuGa_xS_yO_z$ films

Cyclic voltammetry (CV) was used to determine the most suitable potential for the deposition. During the CV experiment a sweeping potential from +0.5 to −1.5V (reduction scan) and then back to +0.5V (oxidation scan) at a potential step equal to 20 mV/s was applied between the working and reference electrodes of the three-electrode cell, and the resulted current was monitored. Figure 4.1(a) shows the CV for the baths with Cu/Ga =3/2, 1/1, and 1/2, where Cu/Ga is the concentration ratio of Cu ion to Ga ion in the solution. For Cu/Ga=1/1, both the reduction and oxidation peaks shifted by about -0.1 V from the corresponding peaks for Cu/Ga=1/2. In case of Cu/Ga=3/2, two reduction peaks appeared around -0.98 and -0.74 V, and the second reduction peak and oxidation peak have similar values to the reduction and oxidation peaks for Cu/Ga=1/2. The CV results for the Ga-rich solution are shown in Fig.4.1 (b).

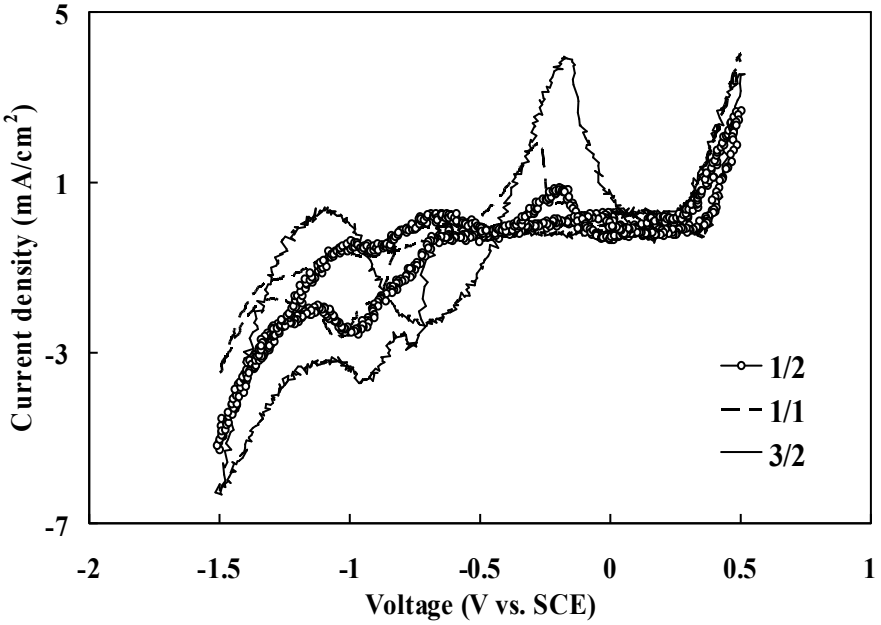

(a)

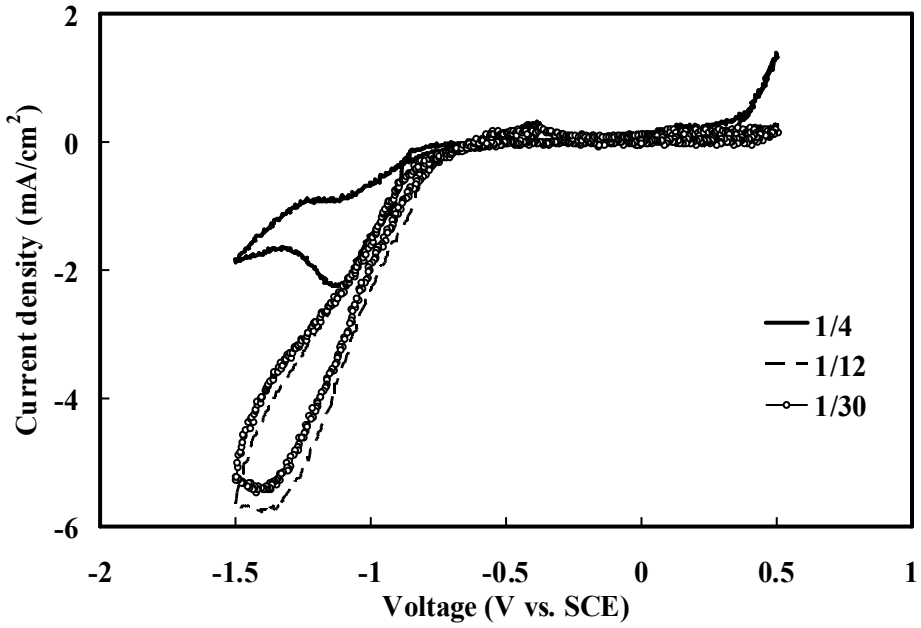

(b)

Fig.4.1. CV for different Cu/Ga ratios in the aqueous solution (a) Cu/Ga = 1/2, 1/1, and 3/2 (b) Cu/Ga = 1/4, 1/12 and 1/30

For bath Cu/Ga=1/4, the reduction and oxidation peaks appears around −1.15 V and -0.37 V respectively, whereas for Cu/Ga=1/12 and 1/30, no reduction and oxidation peaks appeared and the current increased monotonically in the negative scan. To determine a suitable potential at each bath, different samples were deposited under the application of different DC-biased potentials with -0.1 V intervals at and around the local reduction peaks (from -0.75 to -1.35V) appeared on the CV graph. The most suitable deposition voltage was selected so that the film has good adhesion to the substrate, relatively small surface roughness, and enough thickness (around 1~1.5μm for deposition time 10 to 30 minutes). It was observed that for each bath, voltage more negative than the optimum value tends to make the film thinner and deteriorate the adhesion. The deposition conditions are listed in Table 4.1. As shown in the table, the deposited Cu-rich films appeared as gray-black or black, and the color of the Ga rich films varies from yellow-gray to gray. Electrochemically deposited GaS_xO_y films are light golden [1] in colour. Therefore, change in colour of the deposited CGSO films is the clear effect of Cu/Ga ratio in the aqueous solution.

Table - 4.1: Atomic composition and characteristics of the $CuGa_xS_yO_z$ films deposited from the baths with six different Cu/Ga ratios.

$CuSO_4$: $Ga_2(SO_4)_3$ (mM)	Cu/Ga ratio	deposition voltage (V)	deposition time (min)	colour of the films	thickness (μm)
15:5	3/2	-0.85	30	Black	1
10:5	1/1	-1.05	25	Gray-black	1
10:10	1/2	-1.05	20	Gray-black	1
5:10	1/4	-1.05	20	Yellow-Gray	1
5:30	1/12	-1.05	10	Yellow-Gray	1
2:30	1/30	-1.15	20	Gray	1.5

The atomic compositions of the deposited films were calculated from the AES spectra. The obtained values of x, y and z are given in Table 4.2. To see the Cu to Ga ratio and the cation to anion ratio clearly, the atomic ratio of each element with respect to (Cu+Ga) was calculated: namely Cu/(Cu+Ga), Ga/(Cu+Ga), S/(Cu+Ga) and O/(Cu+Ga).

Table 4.2: Composition ratio x, y, z of the $CuGa_xS_yO_z$ films deposited from the baths with six different Cu/Ga ratios.

Cu/Ga ratio	x	y	Z
3/2	0.31	0.23	0.78
1/1	0.82	0.35	1.71
1/2	1.83	0.35	3.37
1/4	1.98	0.95	3.37
1/12	3.23	1.04	5.58
1/30	2.94	0.45	4.86

Figure 4.2 shows the atomic composition ratios for the films deposited from the different Cu/Ga bath. As expected, the Cu content in the film decreases and the Ga content increases with decreasing Cu/Ga ratio in the bath. The O content is higher for a lower Cu/Ga ratio, and thus there is a correlation between the Ga and O contents in the deposited films. However, further increase in the Cu/Ga ratio of the bath (i.e., Cu/Ga= 1/12, 1/30) does not lead to increase in Ga or O contents. The S content of the film does not show clear dependence on the Cu/Ga ratio in the bath.

We performed XRD measurements for the deposited films, but we observed only peaks due to FTO and did not find any phases of related binary and ternary compounds, e.g., Cu_2O, Cu_xS, Ga_2O_3, Ga_2S_3, $CuGaS_2$. To confirm the uniformity of composition, we measured AES signals with different sputtering time. An example is shown in Fig.4.3. The composition is more Cu-rich near the surface, but the body of the film has almost uniform composition. (The data in Fig.4.2 are taken in such uniform composition regions.) Thus we did not observe significant composition modulation in the film. Therefore, we may expect that the films do not include separate binary or ternary phases but are just the quaternary alloy $CuGa_xS_yO_z$.

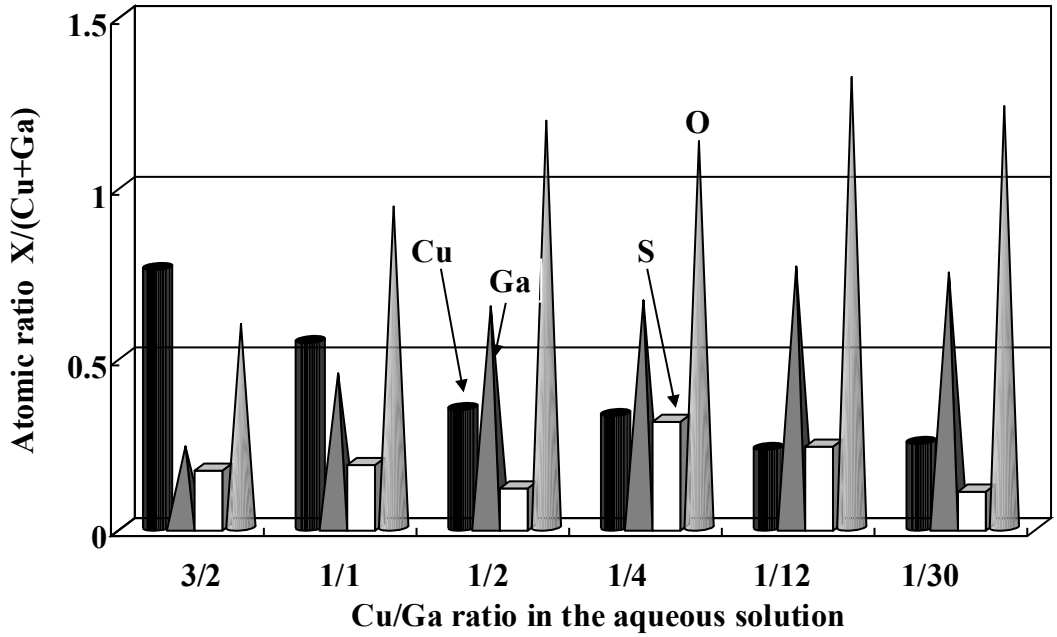

Fig.4.2. Atomic composition ratios Cu/(Cu+Ga), Ga/(Cu+Ga), S/(Cu+Ga) and O/(Cu+Ga) for the $CuGa_xS_yO_z$ films deposited from the baths with different Cu/Ga ratios.

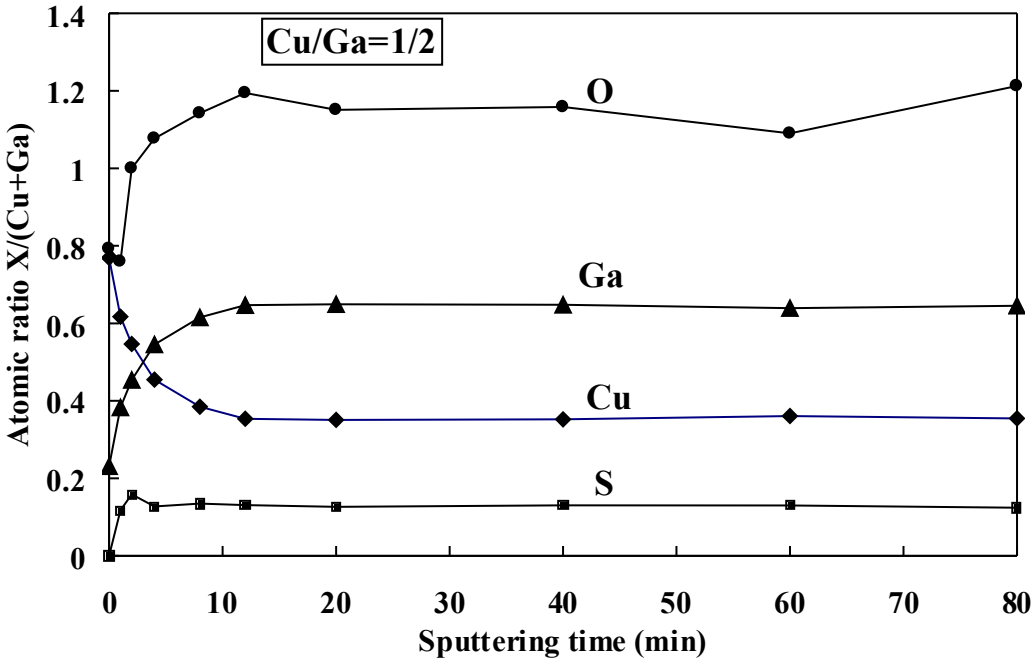

Fig.4.3. AES depth profile for the film deposited from the bath with Cu/Ga=1/2. The substrate (FTO) signal started to appear for >80min sputtering.

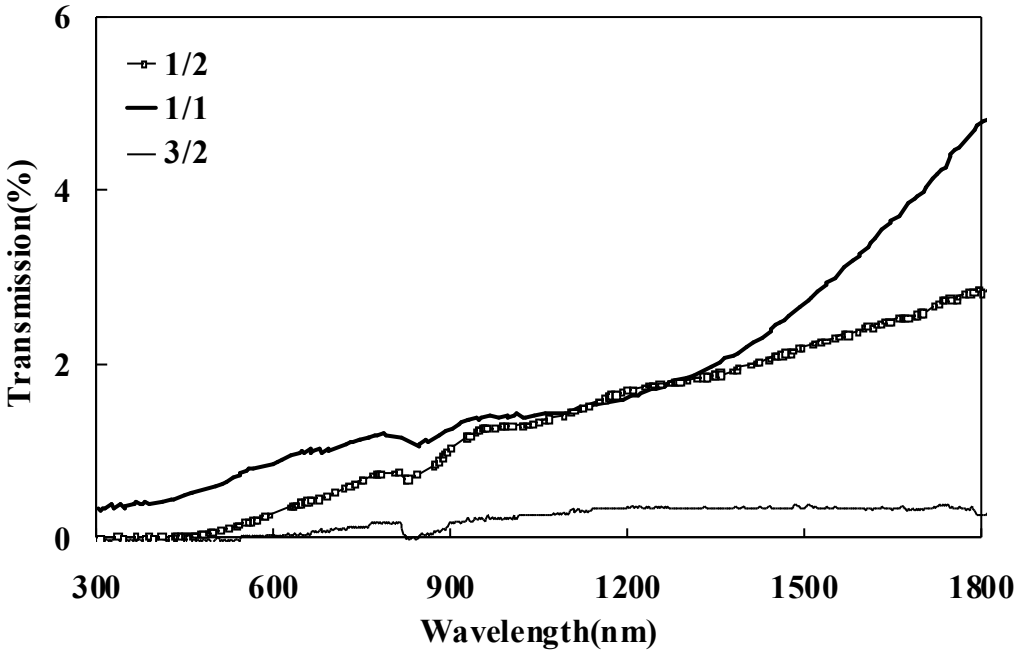

(a)

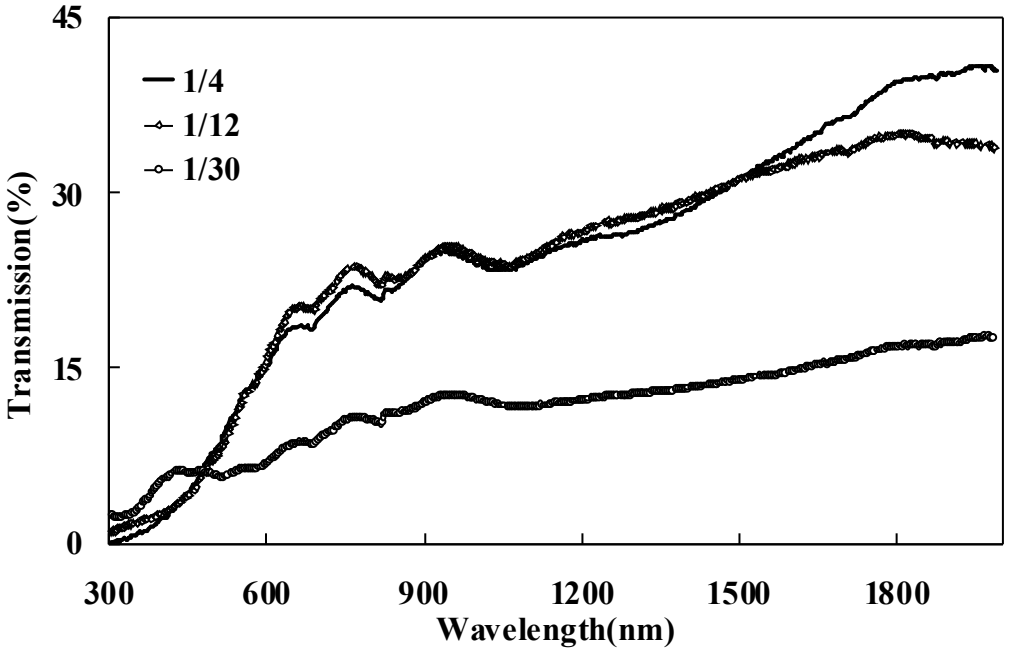

(b)

Fig.4.4. Optical transmission of the $CuGa_xS_yO_z$ thin films deposited from the baths with (a) Cu/Ga = 1/2, 1/1 and 3/2 and (b) Cu/Ga = 1/4, 1/12 and 1/30.

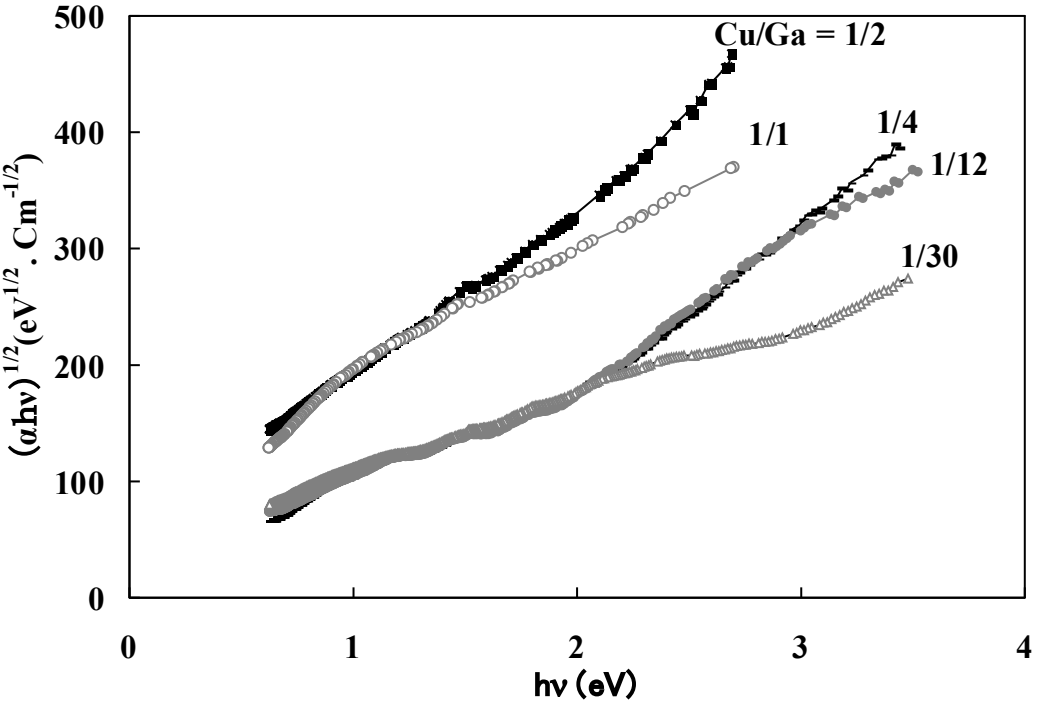

(a)

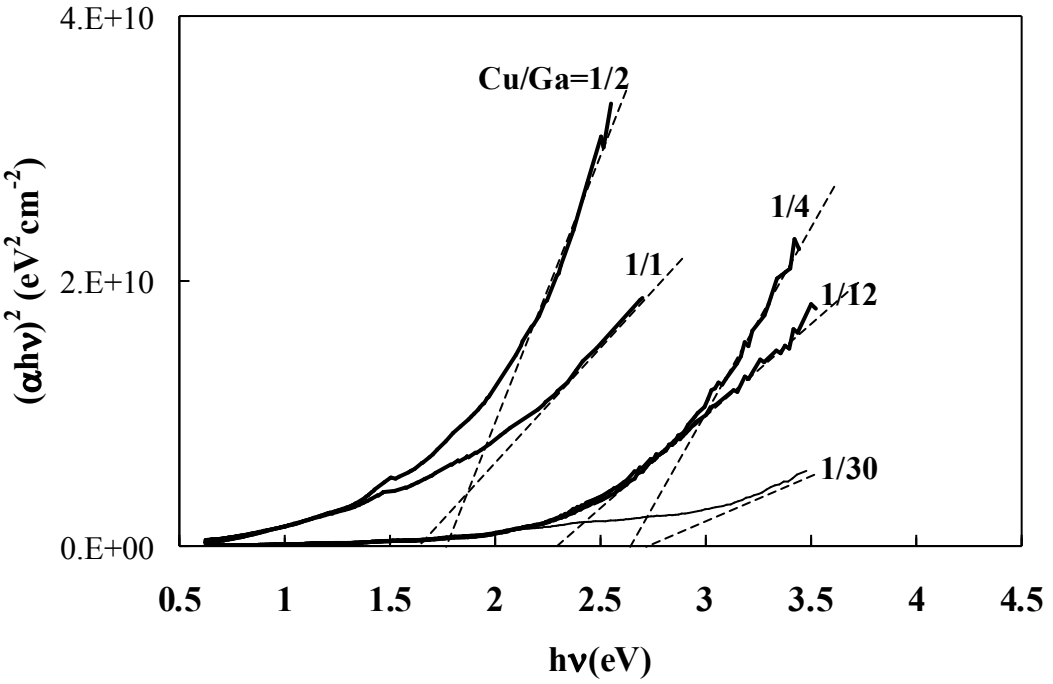

(b)

Fig.4.5. Bandgap estimation of the $CuGa_xS_yO_z$ films deposited from the baths with different Cu/Ga ratios.

Figure 4.4 shows the optical transmission measurements from the UV to near infra-red (300 to 1800 nm) region for the samples deposited from the different Cu/Ga ratio baths. The abrupt change of the transmission around 820 nm is due to error in sensitivity correction for the change of the detector in the machine. The figure revealed that the optical transmission of the Ga-rich films is higher than that of the Cu-rich films with equivalent film thickness (1~1.5 μm).In Fig.4.4 (a), the film deposited from Cu/Ga = 3/2 bath has very low transmission without clear absorption edge. On the other hand, the films deposited from Cu/Ga=1/4 and 1/12 baths show clear absorption edge around 600 nm. The films deposited from the Cu/Ga = 1/30 bath shows low transmission, probably because of its larger thickness, since there is no significant difference in compositional ratio between the film with Cu/Ga=1/12 and that with Cu/Ga=1/30.

For the direct-band optical absorption, $\alpha = k(h\nu - Eg)^n / h\nu$, where α is the absorption coefficient calculated from transmission data, $h\nu$ the photon energy, k is a constant, Eg the band gap and n is the refractive index. As we mentioned in previous chapter-2 and 3, theoretically, for amorphous semiconductors, the lack of crystal structure, removes the possibility of phonon momentum; thus for direct transition, n = 2 i.e. $\alpha = k(h\nu - Eg)^2 / h\nu$.Considering this point, the plot of $(\alpha h\nu)^{1/2}$ versus $h\nu$, shown in Fig.4.5(a) exists a negative and lower value of Eg. Further studies are needed to explain this behavior which will be considered in future. However, for n = 1/2 the plot of $(\alpha h\nu)^2$ versus $h\nu$, shown in Fig. 4.5(b), does not give a clear straight line, and therefore accurate determination of the band gap is not possible. In that case, we can not get an exact value of Eg but an approximate value only. As shown in the figure, the Cu-rich films (Cu/Ga=1/1, 1/2) seem to have a band gap in a range 1.5–2.0 eV, and the Ga-rich film (Cu/Ga=1/4, 1/12, 1/30) a band gap in a range 2.3–2.8 eV. (For Cu/Ga=3/2, we were not able to obtain reasonable value of α because the transmission is too low and much affected by the measurement error.) Thus, there is a tendency that more Cu-rich films have a smaller band gap. The estimated band gap energy of CGSO films are close to the values for Cu_xS (1.7~2.5 eV). Cu_2O (2.1eV) and $CuGaS_2$ (2.5eV) also have the band gap values in this range. On the other hand, the band gap of the films are smaller than those reported for GaS (3.05 eV [11]), Ga_2S_3 (3.42 eV [11]) and Ga_2O_3 (4.94 eV [12]). The Ga-rich films (Cu/Ga=1/12 and 1/30) have a composition close to Ga_2O_3 but a significantly smaller bandgap than Ga_2O_3. This will be due to effects of random atom arrangement (amorphous nature) and band-gap bowing in the alloy. We found similar tendency for GaS_xO_y alloy [1].

Figure 4.6 shows the SEM images of the films deposited for different Cu/Ga ratios in the bath. The films from the baths with Cu/Ga = 1/1, 1/2 and 1/4 are dense with small grains covering the entire substrate surface without voids or cracks. The films deposited from the high Cu content bath i.e. Cu/Ga = 3/2 and the high Ga content bath Cu/Ga = 1/12 and 1/30 consist of grains, but micro-cracks appeared at its surface. The grain size became larger and the micro-cracks became wider with higher Ga content in the solution. The cause of such micro-cracks is not exactly known. Micro-cracks have been observed in other electrochemically deposited Ga-based chalcogenide thin films [13-15]. From the optical transmission measurement shown in Fig.4.4, the micro-cracks do not adversely affect the absorption, and thus they seem to be superficial cracks: if the cracks reach the substrate, the light could go through the cracks and the transmission would not decrease as observed. More work is required to improve the surface morphology of the films deposited at higher Cu and Ga content.

Figure 4.7(a) shows the PEC measurements for the $CuGa_xS_yO_z$ deposited film at Cu/Ga = 1/2 in the aqueous bath. It is clear that the current was changed due to the light chopping. When a semiconductor is illuminated with photons that have energy greater than the band gap, photogenerated electrons/holes are separated in the space charge region. The photogenerated minority carriers arrive at the interface of the semiconductor–electrolyte during their lifetime to participate in the electrochemical reaction at the film/electrolyte interface. For the baths with Cu/Ga = 3/2 to 1/12, the current became more negative when the illumination is turned on during the cathodic scan, but in the anodic scan, the current value was not changed by illumination. This implies that the minority carriers generated here are electrons. Thus, the deposited films all are p-type semiconductors. The photocurrent is of the order of 100 $\mu A/cm^2$ for Cu/Ga=1/1 - 1/12, while it is of the order of 10 $\mu A/cm^2$ for Cu/Ga=3/2. On the other hand, film deposited from higher Ga content bath i.e., Cu/Ga = 1/30, there is a significant effects of light for both the anodic and cathodic scans as shown in Fig.4.7 (b). Under the light illumination, the current becomes more negative in the cathodic scan and the current become more positive during the anodic scan. This characteristic indicates that the film deposited with Cu/Ga = 1/30 is an intrinsic semiconductor. Those PEC results indicate that the Cu-rich films can be considered promising as an absorber layer material of heterojunction solar cells.

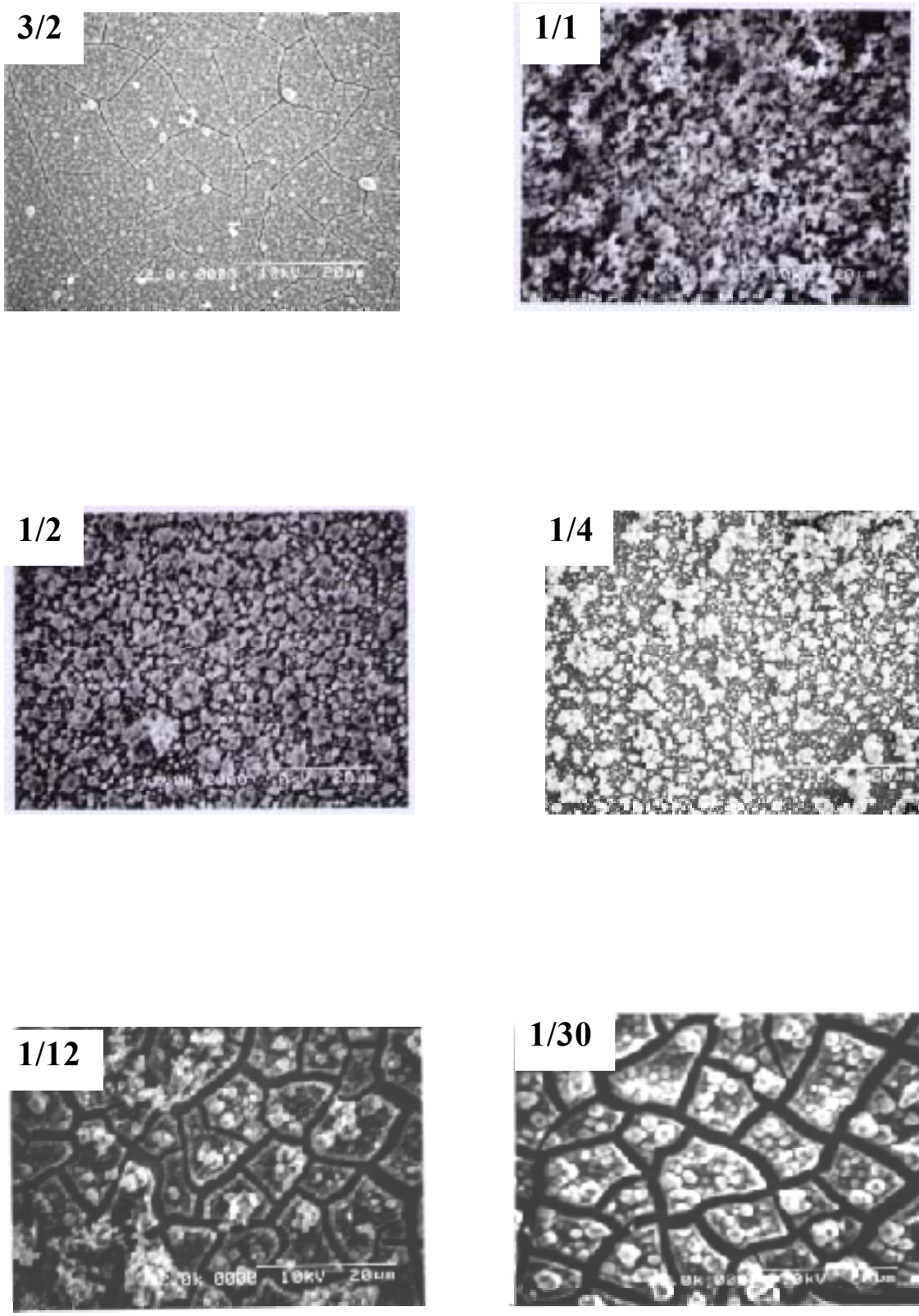

Fig.4.6. SEM of the $CuGa_xS_yO_z$ films deposited from the baths with different Cu/Ga ratios.

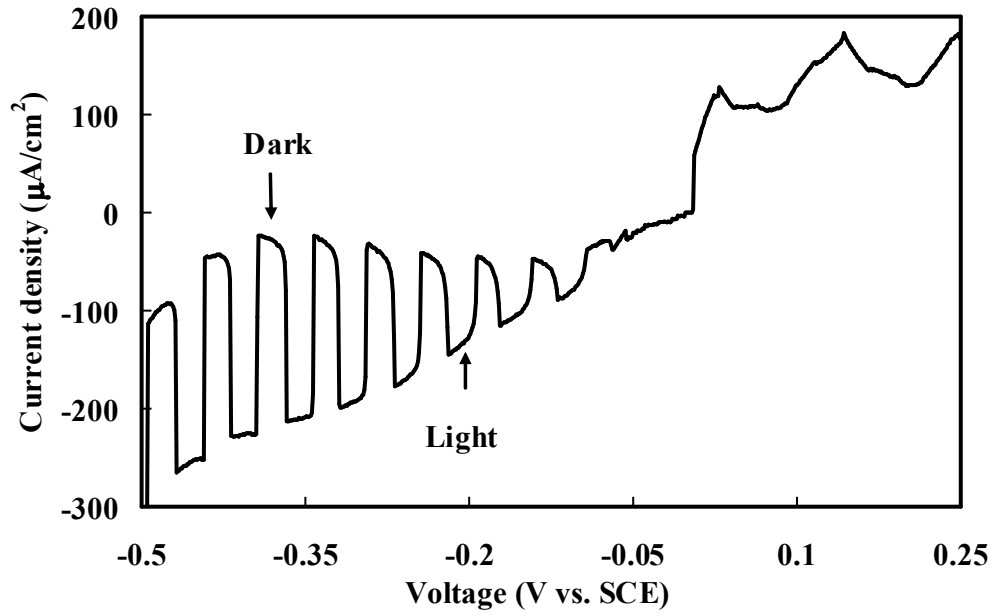

(a)

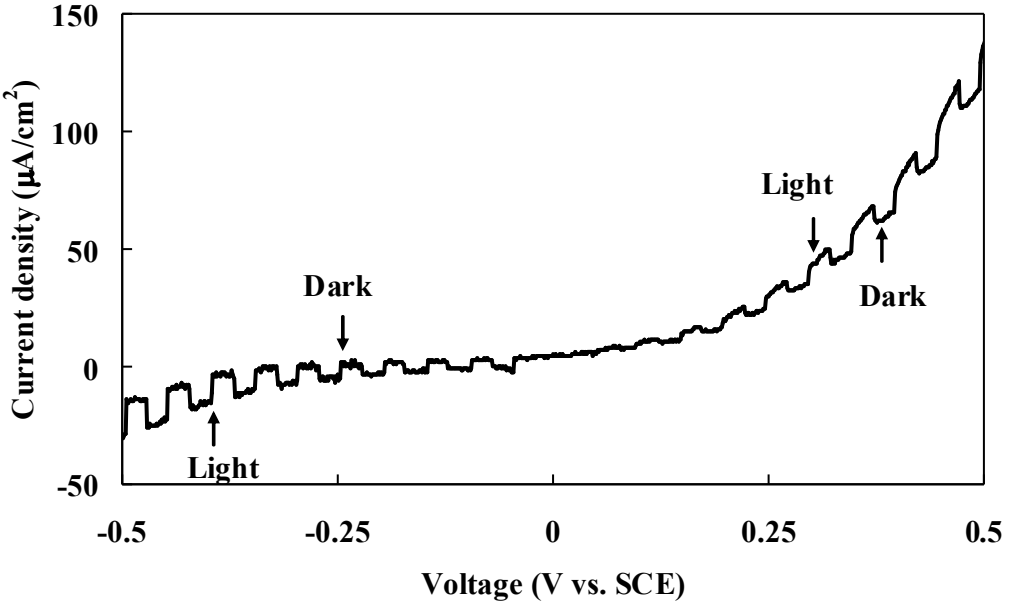

(b)

Fig.4.7. PEC results for the $CuGa_xS_yO_z$ thin films deposited from the baths with (a) Cu/Ga = 1/2 and (b) Cu/Ga = 1/30.

4.3.2. Galvanostatic electrochemical deposition of $CuGa_xS_yO_z$ films

Galvanostatic deposition carried out at cathodic current density selected from current profile for first 1200 sec of P-stat CGSO deposition at optimum deposition voltage-1.05 V is shown in Fig.4.8. G-stat CGSO films were deposited at current density ranging from -1.56 to -1.90 mA/cm^2. At -1.56 mA/cm^2, better quality homogeneous films were observed. The current density limits leading poor adherence films at more negative value. The deposition conditions for G- stat CGSO films are listed in Table 4.3. As shown in the table, the films deposited at -1.56 mA/cm^2 appeared as gray-black, which is a good agreement with P-stat CGSO film deposited at -1.05 V.

Table – 4.3 : Atomic composition and characteristics of G - stat $CuGaS_xO_y$ films

Deposition current density mA/cm^2	Thickness μm	Colour	Bandgap energy, Eg eV	Cu:Ga:S:O
-1.56	0.8	Gray-Black	1.85	0.70:0.29:0.15:0.77
-1.63	0.3	yellow	2.5	0.70:0.29:0.18:0.74
-1.90	0.04	yellow	2.8	0.86:0.14:0.13:0.69

The atomic compositions of the potentiostatically deposited films were calculated from the AES spectra. To see the Cu to Ga ratio and the cation to anion ratio clearly, the atomic ratio of each element with respect to (Cu+Ga) was calculated: namely Cu/(Cu+Ga), Ga/(Cu+Ga), S/(Cu+Ga) and O/(Cu+Ga). Fig. 4.9 shows the atomic AES spectra for the films deposited at -1.56 mA/cm^2. Based on our experience [16], we may expect that G-stat CGSO films also do not include separate binary or ternary phases but are just the quaternary alloy $CuGa_xS_yO_z$. Fig. 4.10 shows the SEM images of the G-stat CGSO films at different current densities. The films are dense with small grains covering the entire substrate surface without voids or cracks. Fig.4.11 shows the direct band gap of G-stat CGSO film deposited at -1.56 mA/cm^2 is about 2 eV. The inset of figure 4.11 shows the bandgap plot for refractive index, n = 2 (in case of amorphous semiconductor) as discussed before.

4.3.3. Effect of deposition process on $CuGa_xS_yO_z$ thin films

Considering the above film characteristics we selected that-1.05 V and -1.56 mA/cm^2 were the optimum deposition condition for P-stat CGSO and G-stat CGSO films respectively. We observed that, the colour of the films deposited at more negative current densities was yellow-gray. Electrochemically deposited GaS_xO_y films were light golden [1] in colour. Therefore, change in colour of the deposited CGSO films was the clear effect of ionic ratio [16] in the aqueous solution and deposition current densities and there was no role for deposition process.

Figure 4.12 shows the optical transmission measurements from the UV to near infra-red (300 to 1800 nm) region for the samples deposited from the different ECD process. This figure revealed that the optical transmission of the G-stat CGSO films is higher than that of the P-stat CGSO films, probably because of its lower thickness, since there is no significant difference in compositional ratio between the films of different deposition process. At optimum condition, the calculated band gap energy of G-stat CGSO films is about 2 eV which is slightly larger than that of P-stat films seems to have a band gap around 1.5 eV as shown in fig. 4.5 [16].

As shown in Fig. 4.10(a) and 4.6(SEM for Cu/Ga=1/2), the grain size became larger for P-stat CGSO film in contrast to the G-stat CGSO film. Since no significant change of composition is evident in the films then may be this change in surface morphology was directly influenced by deposition condition [10].

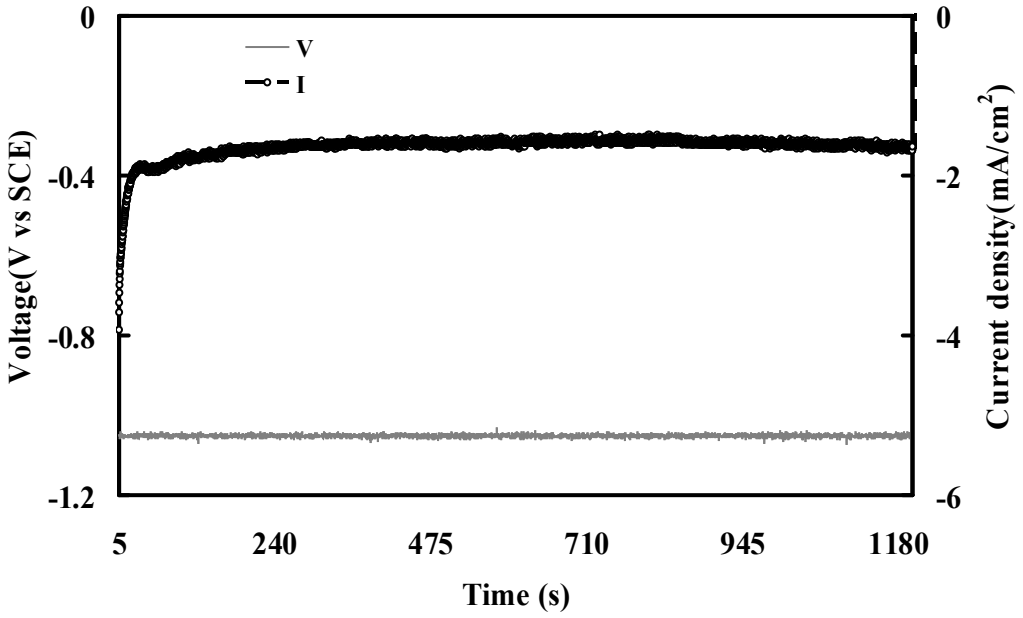

Fig.4.8. Current profile for G-stat CGSO deposition at -1.05 V

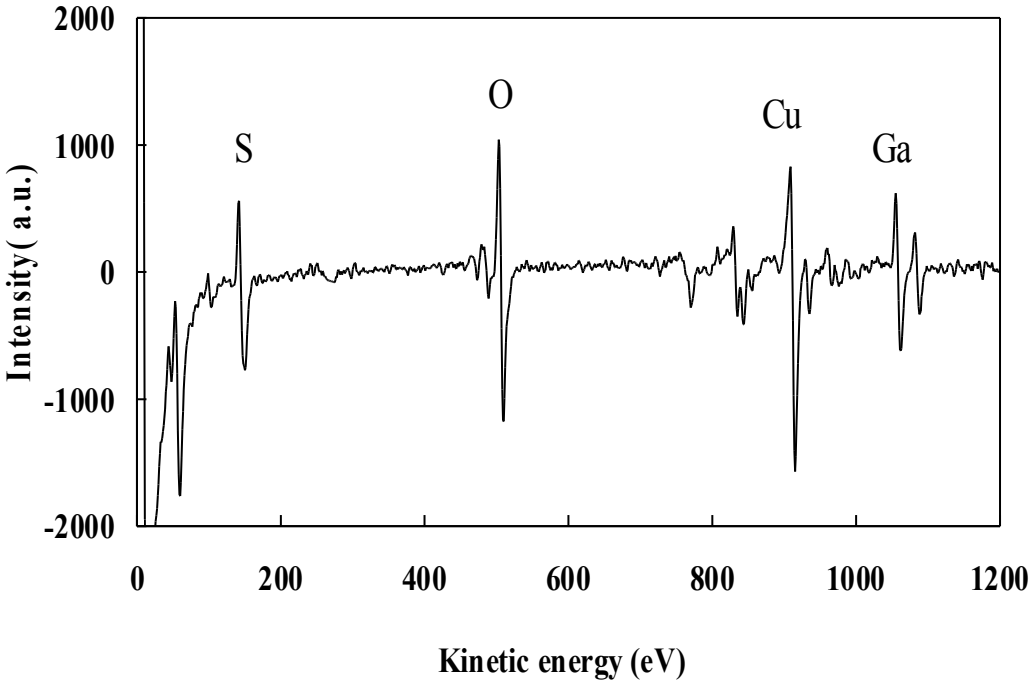

Fig.4.9. AES spectra for the CGSO films deposited at -1.56 mA/cm^2 by G-stat ECD process

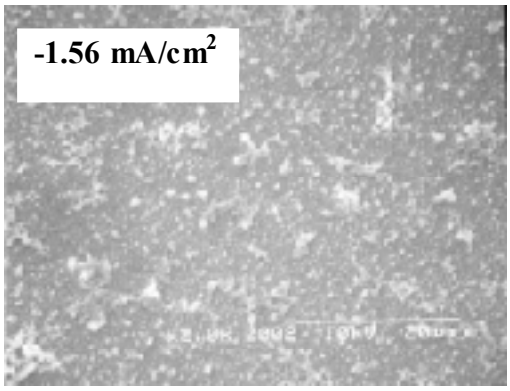

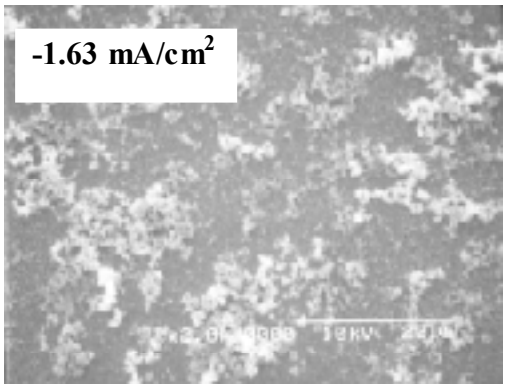

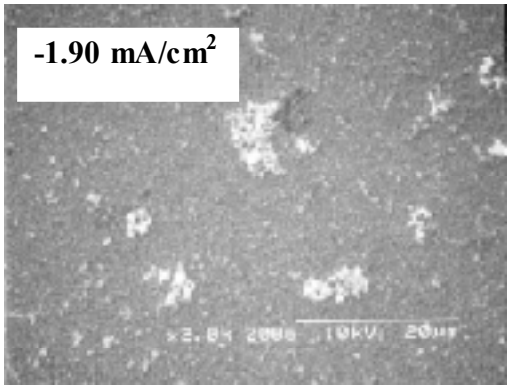

Fig. 4.10. SEM images of the CGSO films deposited at different current densities by G-stat ECD process

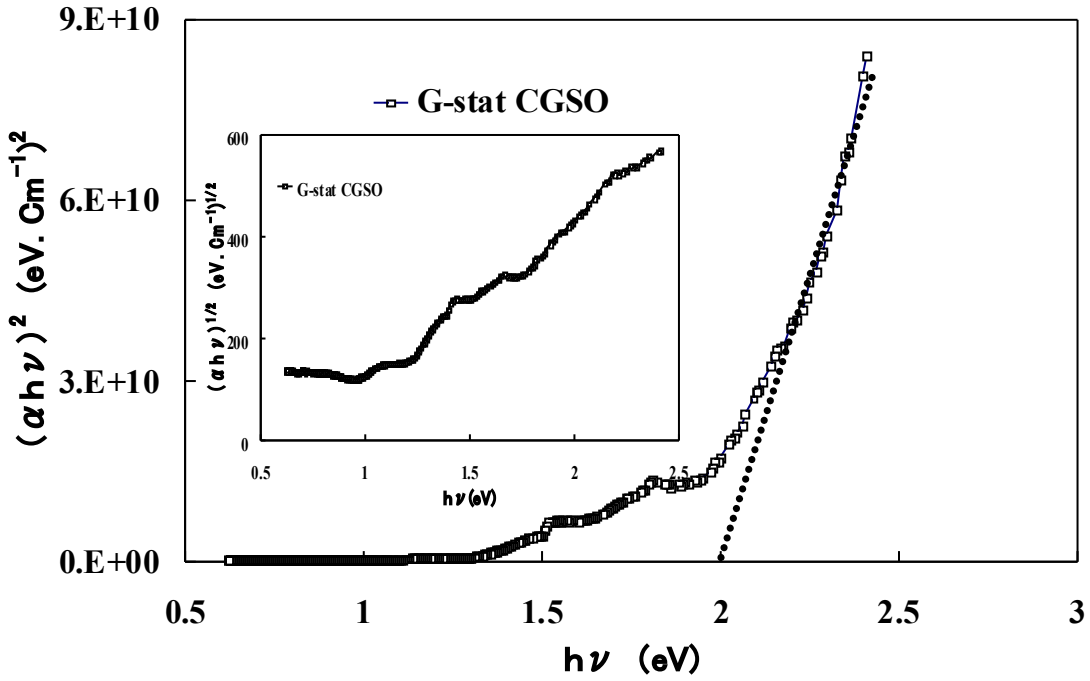

Fig.4.11. Optical band gap of G-stat CGSO film deposited at -1.56 mA/cm^2

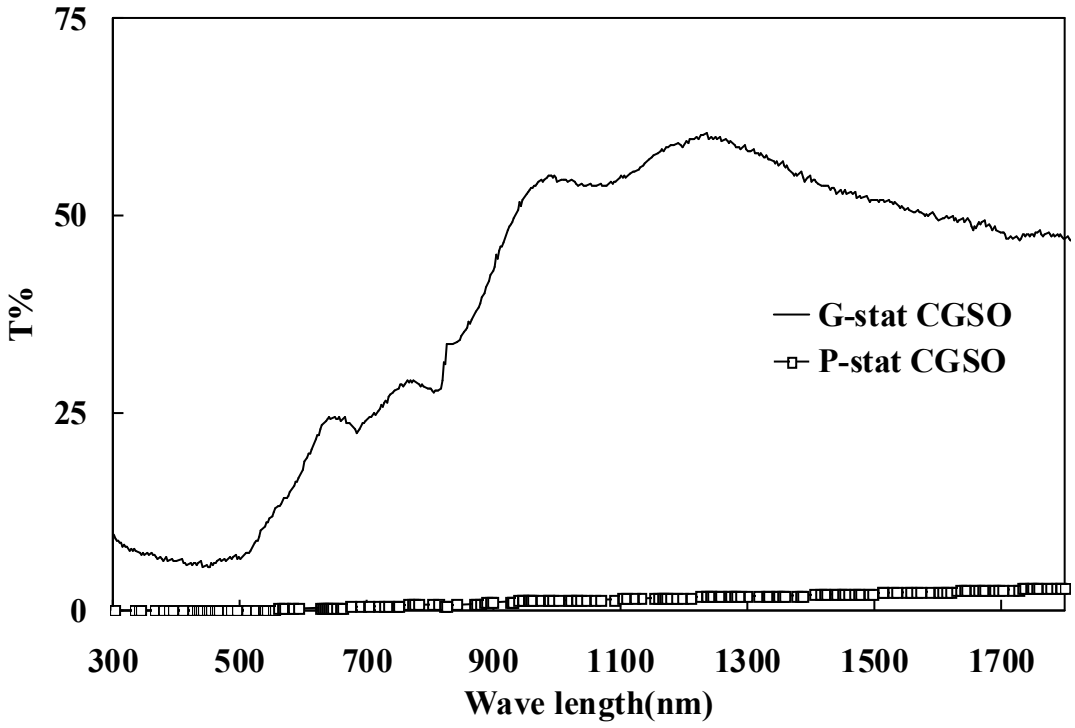

Fig.4.12. Optical transmissions of CGSO films deposited by different ECD process.

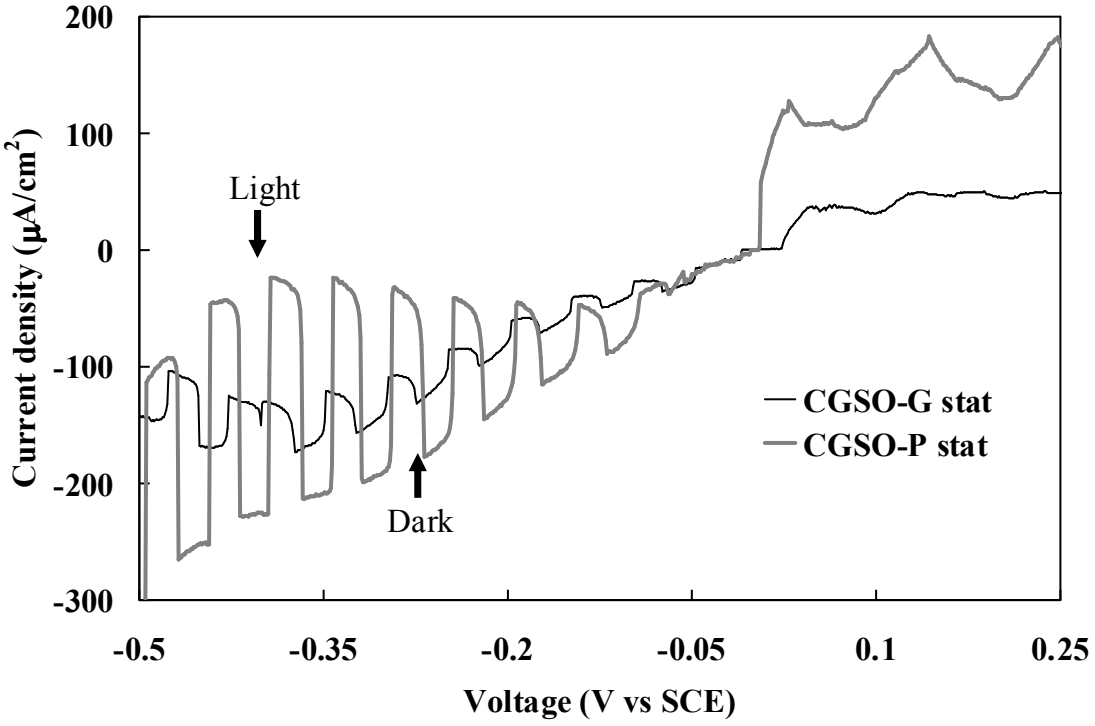

Fig.4.13. PEC measurements for the CGSO films deposited by different ECD process

Table – 4.4: Comparison between CGSO films characteristics deposited by different deposition process

Characteristics	P-stat CGSO films	G-stat CGSO films
Colour	Gray-Black	Gray-Black
Thickness, μm	1	0.8
Bandgap energy, Eg eV	~ 1.5	~ 2
Composition ratio Cu:Ga:S:O	0.76 : 0.24 : 0.17 : 0.59	0.70 : 0.29 : 0.15 : 0.77

Figure 4.13. shows the PEC measurement for the CGSO films deposited by different ECD process. It is clear that the current was changed due to the light chopping. When a semiconductor is illuminated with photons that have energy greater than the band gap, photogenerated electrons/holes are separated in the space charge region. The photogenerated minority carriers arrive at the interface of the semiconductor–electrolyte during their lifetime to participate in the electrochemical reaction at the film/electrolyte interface. For both films, the current became more negative when the illumination is turned on during the cathodic scan, but in the anodic scan, the current value was not changed by illumination. This implies that the minority carriers generated here are electrons. Thus, the deposited films are p-type semiconductors. It is clear that the P-stat CGSO film exhibits stronger photosensitivity than that of G-stat CGSO films. These PEC results indicate that deposited films can be considered promising as a absorber layer material of heterojunction solar cells.

The comparison result between CGSO film characteristics deposited by two different processes was included in Table-4.4, shows the clear effect on CGSO film Characteristics. It shows that under optimum condition, films deposited by galvanostatic process have larger energy band gap with lower film thickness. However, film colour and atomic composition were not affected by the deposition process.

4.4. Conclusion

$CuGa_xS_yO_z$ thin films were electrochemically deposited in potentiostatic process from different concentrations of Ga and Cu ions in the bath and in galvanostatic process at different current densities for the first time. The AES measurements revealed that there is a correlation between the Ga and O contents in the deposited films. The XRD measurement did not reveal binary or ternary compound phases in the films, and significant composition-modulation was not observed by the AES depth profiling. Thus, the films are considered to be alloys with fairly uniform composition. For P-stat CGSO, the optical transmission increased for the higher Ga concentration films compared with the higher Cu concentration film. The SEM study revealed that the films deposited at higher Cu content (Cu/Ga = 3/2) and higher Ga content (Cu/Ga = 1/12, 1/30) contained micro-cracks. The PEC measurements revealed that all the deposited films are p-type semiconductors except the film deposited with Cu/Ga = 1/30, which shows

intrinsic character. Under optimum condition, films deposited from Cu/Ga = 1/2 bath show high photosensitivity with better surface morphology. The optimum deposition current densities for G-stat CGSO films is -1.56 mA/cm^2.The potentiostatic and galvanostatic process of electrodeposition has clear effect on surface morphology, bandgap energy, thickness and photosensitivity of deposited CGSO films. In surface morphology, the grain size is larger for P-stat CGSO film comparing with G-stat CGSO films at optimum condition. At optimum condition, the optical transmission and bandgap energy, Eg were increase for G-stat CGSO films may be due to lower film thickness. The deposition process has no significant effect on atomic composition and film colour.

References

[1] S. Chowdhury, M. Ichimura, Jpn.J. Appl. Phys. 48(2009)061101.

[2] S. Chowdhury, M. Ichimura, Jpn.J. Appl. Phys. 49(2010)062302.

[3] S. Shirakata, K. Saiki, S. Isomura, J. Appl .Phys. 68(1990)291.

[4] S. Chichibu, S. Shirakata, M.Uchida, Y. Harada, T. Wakiyama, S. Matsumoto, H. Higuchi, S. Isomura, J. Appl. Phys. 34(1995)3991.

[5] MS. Branch, PR. Berndt, WL. Leitch, J. Weber, JR. Botha, Thin Solid Films 480-481(2005)188.

[6] C. Guillen, J. Herrero, Phys. Stat. Sol. (a) 203(2006)2438.

[7] WJ. Jeung, GC. Park, Sol. Energy Mater. Sol. Cells 75(2003)93.

[8] SK. Kim, JP. Park, MK. Kim, KM. Ok, IW. Shim, Sol. Energy Mater. Sol. Cells 92(2008) 1311.

[9] H. Metzner, Th. Hahn, J. Cieslak, U. Grossner, U. Reislohner, W. Witthuhn, R. Goldhahm, J. Eberhardt, G. Gobsch., J. Krau Blich, Appl. Phys. Lett. 81(2002)156.

[10] S.Michel, S.Diliberto, C.Boulanger, N.Stein, J.M.Lecuire, J.Crystal Growth, 277 (2005)274.

[11] M. Lazell, PO. Brien, DJ. Otway, JH. Park, J. Chem. Soc. Dalton Trans. (2000) 4479.

[12] A .Ortiz, JC. Alonso, E. Andrade, C. Urbiola, J. Electrochem. Soc. 148(2001)26.

[13] RN.Bhattacharya, AM. Fernandez, Sol. Energy Mater. Sol. Cells 76(2003)331.

[14] AM .Fernandeza, RN. Bhattacharya, Thin Solid Films 474 (2005)10.

[15] AMA.Hallem, M. Ichimura, Mat. Sci. Eng. B 164(2009)180.

[16] S.Chowdhury, M.Ichimura, Mater.Science and Semiconductor Processing, (Accepted on October 2010).

Chapter-5
Applications of GaO-based thin films on solar cells

5.1. Introduction

P-type semiconductor SnS are non toxic and having bandgap about 1.3 eV are widely used in CdS or ZnS based solar cells. It was reported that SnS based solar cell theoretically achieved more than 25% of conversion efficiency [1].In practical case, the highest efficiency achieved by SnS based solar cell is about 1.3% [2].Among the various techniques of SnS deposition [2-10], we follow the three step pulse electrochemical deposition of SnS [8] for GaO- based thin film soar cell.

ZnO is an n-type wide bandgap (3.3 eV) semiconductor with wurtzite crystal structure [11]. ZnO has attracted attention as a future thin film solar cell, due to a theoretical conversion efficiency of around 18% [12]. This is feasible owing to its good electrical, optical and piezoelectric properties [13-17] and has many different applications such as: anti-reflecting coatings in solar cells, gas sensors, ultrasonic oscillators and transducers among others. ZnO thin films have been fabricated by various methods such as: electrochemical deposition [18-20] chemical vapor deposition [21, 22], sputtering [23, 24], molecular beam epitaxy [25], chemical bath deposition [26, 27] and photochemical deposition [28]. Among them electrochemical deposition (ECD) is a very simple and cost effective techniques for large area deposition, thus we deposit window layer ZnO film using both DC and two step pulse potential for $CuGa_xS_yO_z$/ZnO heterostructure fabrication.

In this chapter we present the fabrication and characterization of the SnS/ GaS_xO_y , $CuGa_xS_yO_z$ / GaS_xO_y and $CuGa_xS_yO_z$ /ZnO heterojunction solar cells.

5.2. Experimental details

We fabricated and characterized SnS/GaS_xO_y, $CuGa_xS_yO_z$ /GaS_xO_y and $CuGa_xS_yO_z$ /ZnO heterojunction solar cells. Indium metal electrodes (metallic contacts) were deposited by thermal evaporation. The electrode size is 1x1 mm^2 and the distance between two adjacent electrodes is 1 mm. The light source was a Xenon lamp with intensity 100 mW/cm^2. Sometimes, the substrate ITO was replaced by FTO and both as-deposited and annealed GaS_xO_y were used for heterostructure formation. Here, SnS and ZnO films were electrochemically deposited by ECD technique according to the following deposition conditions:

(a) Electrochemically deposited SnS (ECD-SnS):

SnS thin film was deposited from an aqueous solution contained $SnSO_4$ (25 mM) and $Na_2S_2O_3$ (100 mM). The SnS layers were deposited using a three-step pulse ECD for two bias condition.Therefore, potential shifted to - 0.2 V i.e. V_1 =-0.2, V_2 = -0.8, and V_3 = -1.2V vs. SCE than Komoto et al.[8] and the other condition is potential V_1 = -1, V_2 = -0.6, and V_3 = 0V vs. SCE [20]. The applied time for each potential was $t_1 = t_2 = t_3$ =10 sec and film deposition time was 10 min.

(b) Electrochemically deposited ZnO (ECD- ZnO):

ZnO films were deposited by ECD techniques, from aqueous solution of 100 mM $Zn(NO_3)_2$ at 60°C and an unadjusted pH. The ZnO were deposited using both two step pulse potential V_1= -1.3 V and V_2 = -0.6 V vs SCE, where V_1 and V_2 are applied for $t_1 = t_2$ = 10 sec [20] and DC potential = -1.3 V vs SCE. ZnO deposition time was 1-3 min. According to our experience [29, 30], the DC potential was selected from reduction peak of CV which possess same value as reduction (deposition) voltage, V_1 of two step deposition. On the other hand, both P-stat ECD and G-stat ECD were applied to fabricate the $CuGa_xS_yO_z$ film for $CuGa_xS_yO_z$ /ZnO heterostructure.

For the current voltage measurement, an indium electrode was fabricated by vacuum evaporation. The light source used for the photovoltaic characterization was a Xe lamp with an

AM 1.5 radiation filter, and its radiation power was about 100mW/cm^2.Light was illuminated on the glass side of the sample.

5.3. Results and discussion

5.3.1. Solar cells based on SnS/ GaS_xO_y

5.3.1.1. SnS/ECD GaS_xO_y solar cells

A novel heterojunction of SnS / GaS_xO_y in the form of superstrate and substrate configuration were fabricated and shown in Fig.5.1.The I-V characteristics were measured based on 2-electrode techniques, as shown schematically in Fig 5.1.

For SnS/GaS_xO_y heterostructure, the window layer was ECD GaS_xO_y and absorber layer SnS deposition potential was V_1 =-0.2, V_2 = -0.8 and V_3 = -1.2V vs. SCE. Fig.5.2 shows a very small rectification property for superstrate heterojunction ITO/ GaS_xO_y /SnS/In solar cells. To improve the rectification property, we also fabricate SnS/ annealed GaS_xO_y heterostructure. ECD GaS_xO_y films were annealed at 100-300°C for 60 min at nitrogen atmosphere and characterized. It was observed that photosensitivity increased for sample annealed at 200°C though optical transmission, atomic composition ratios and SEM (cracks were exist for annealed samples) did not show any significant difference. Hence we selected the annealing temperature at 200°C and varied annealing time for 30 to 90 min. As shown in Fig.5.3, film annealed at 200°C for 90 min improves the photosensitivity. Therefore, 200°C for 90 min was the optimum annealing condition for ECD GaS_xO_y. But, Fig 5.4 shows that rectification property of FTO/annealed GaS_xO_y /SnS/In solar cell did not improve.

5.3.1.2. SnS/PCD GaS_xO_y solar cells

As shown in Fig.5.5 and 5.6 SnS / PCD GaS_xO_y /SnS heterojunction were fabricated in the form of superstrate and substrate respectively. Here SnS deposition potential were V_1 = -1, V_2 = -0.6, and V_3 = 0V vs. SCE. In such case also, rectification property did not improve noticeably.

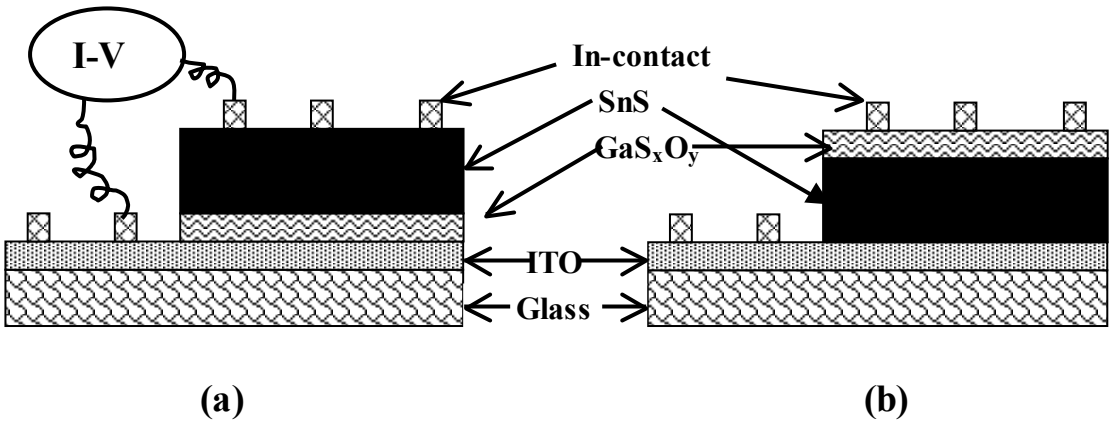

Fig. 5.1. The fabricated solar cells based on SnS/GaS_xO_y heterojunction in their (a) superstrate and (b) substrate configurations.

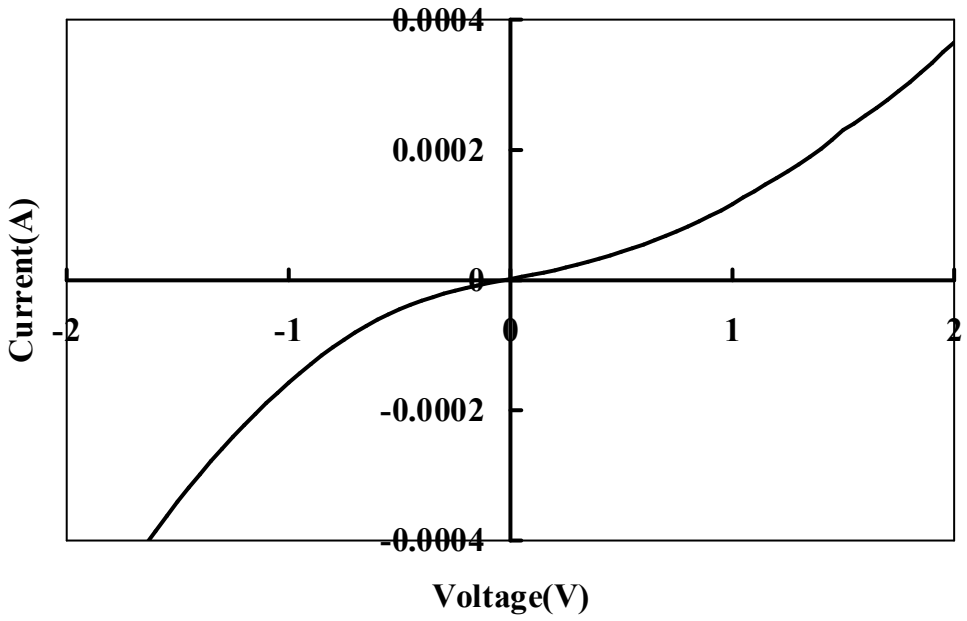

Fig.5.2. **Rectification property FTO/GaS_xO_y/SnS heterojunction solar cell**

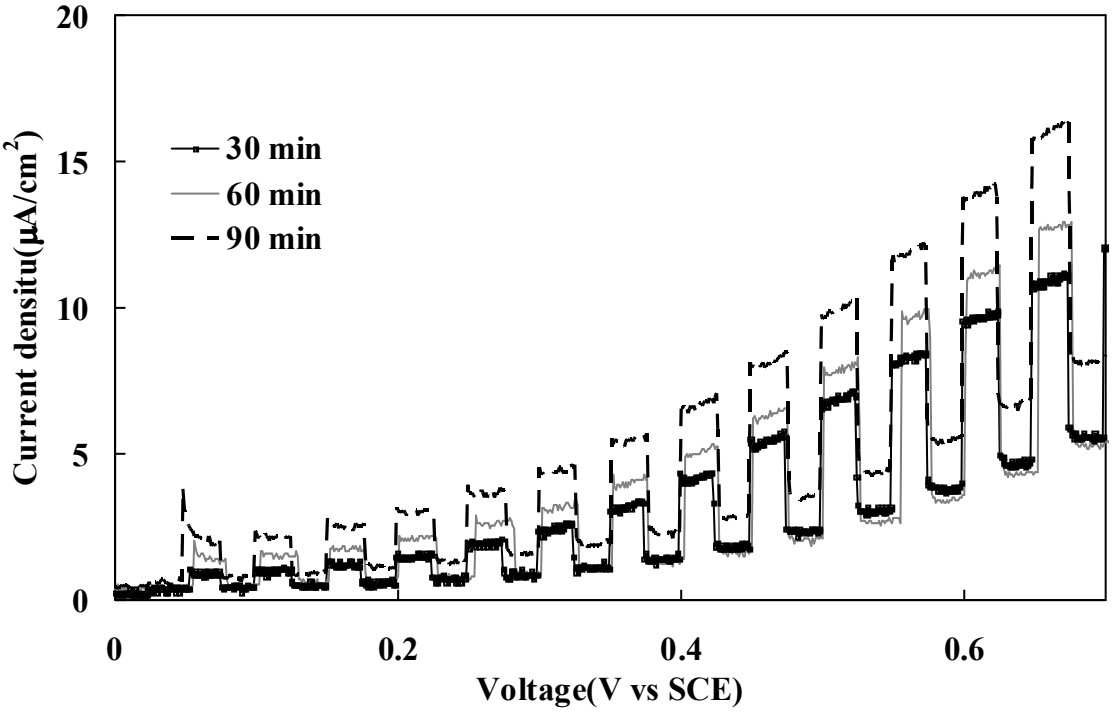

Fig.5.3. **PEC measurements of GaS_xO_y films annealed at 200°C for different time**

5.3.2. Solar cells based on $CuGa_xS_yO_z$ / ECD GaS_xO_y

5.3.2.1. Potentiostatic $CuGa_xS_yO_z$ / ECD GaS_xO_y solar cells

In FTO/ GaS_xO_y / $CuGa_xS_yO_z$ superstrate heterostructure, the absorber layer ($CuGa_xS_yO_z$) was fabricated by P-stat ECD. The ECD GaS_xO_y in as deposited and annealed form was used for window layer. As shown in Fig 5.7, ohmic like I-V characteristics was observed for FTO/ annealed GaS_xO_y / P stat - $CuGa_xS_yO_z$ configuration.

5.3.2.2. Galvanostatic $CuGa_xS_yO_z$ / ECD GaS_xO_y solar cells

Fabricated heterojunction $CuGa_xS_yO_z$ /GaS_xO_y in the form of superstrate and substrate configuration are shown in Fig.5.8 and 5.9 respectively. In this case, absorber layer ($CuGa_xS_yO_z$) was fabricated by G-stat ECD and figures show the ohmic like I-V characteristics.

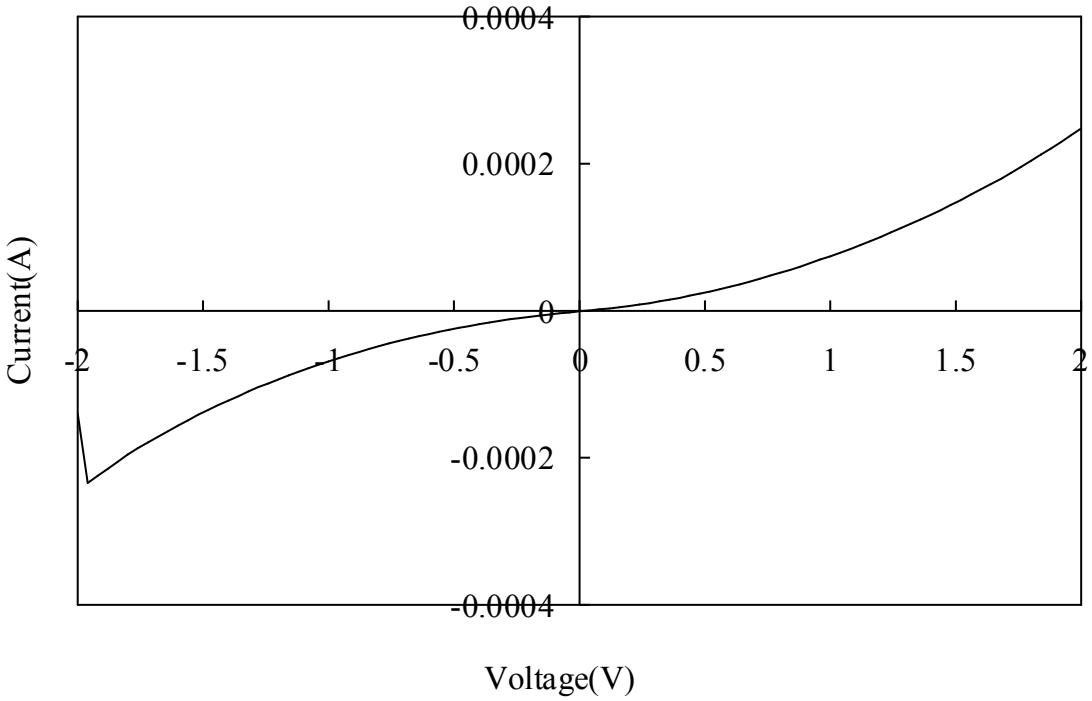

Fig. 5.4. Rectification property FTO/Annealed GaS_xO_y /SnS heterojunction solar cell

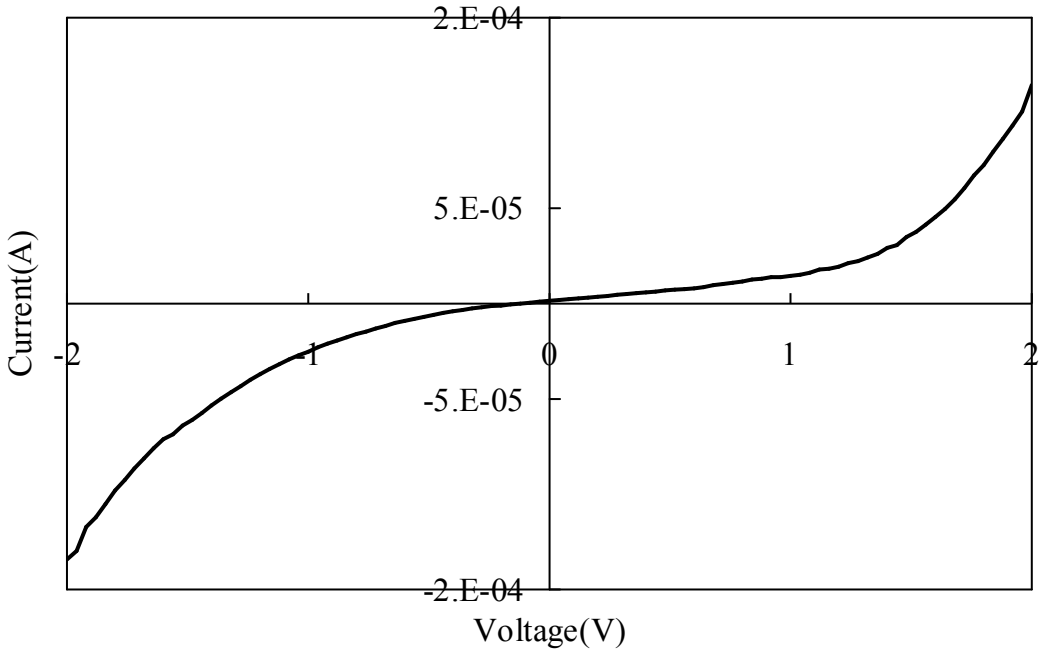

Fig. 5.5. Rectification property FTO/PCD GaS_xO_y /SnS heterojunction solar cell

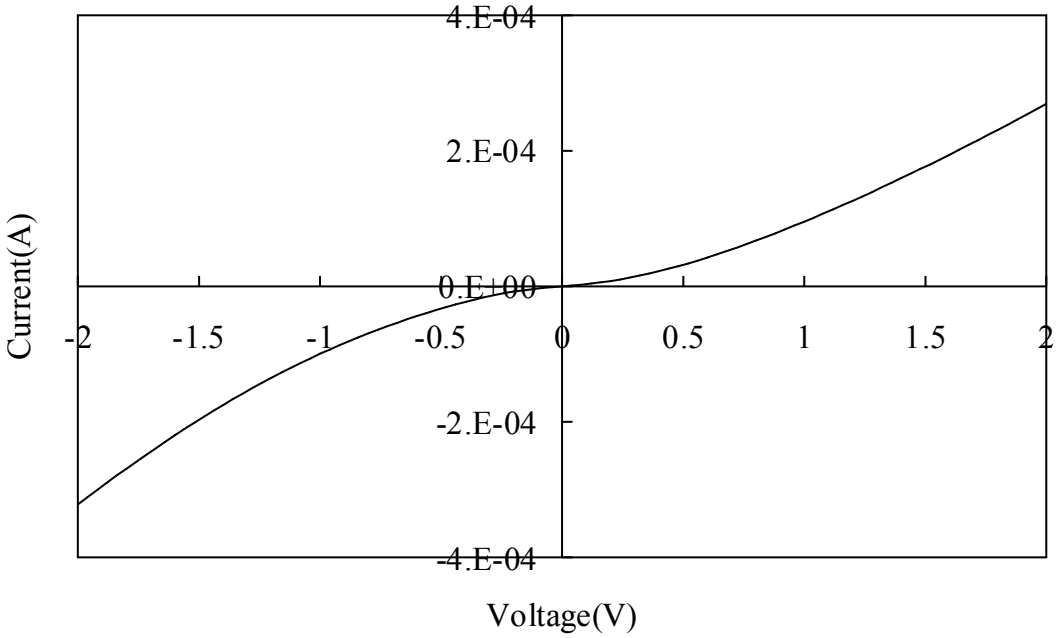

Fig. 5.6. Rectification property FTO/SnS /PCD GaS_xO_y heterojunction solar cell

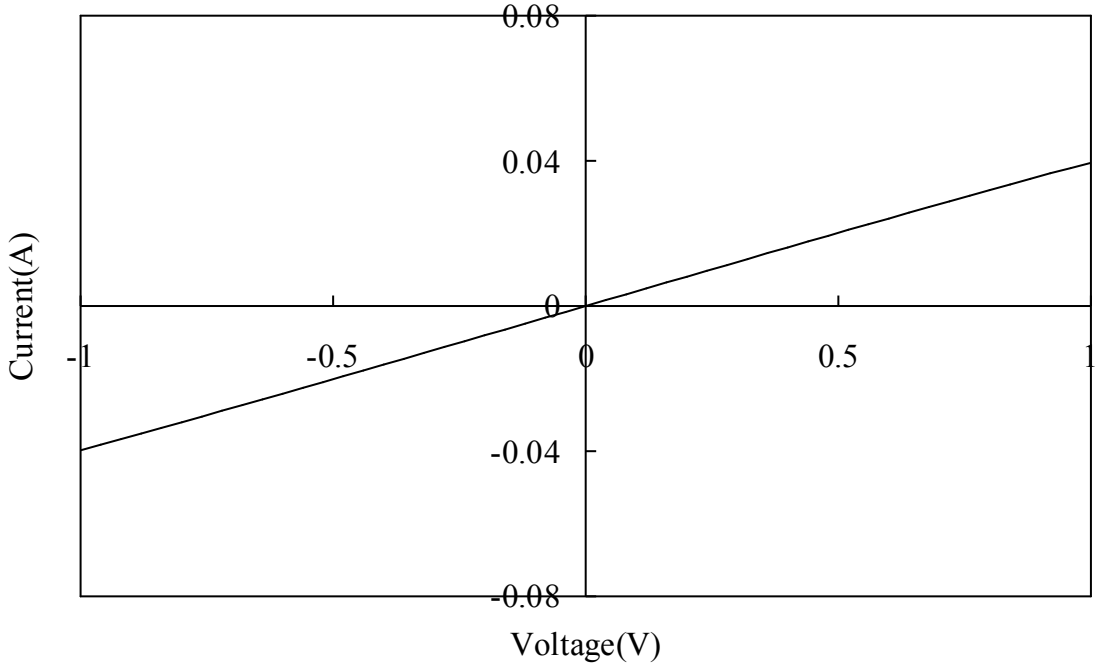

Fig. 5.7. I-V graph under dark condition of the FTO/ Annealed GaS_xO_y / $CuGa_xS_yO_z$ - P stat superstrate heterojunction

5.3.3. Solar cells based on $CuGa_xS_yO_z$ /ZnO

5.3.3.1. Potentiostatic $CuGa_xS_yO_z$ / ZnO solar cells

A novel heterojunction of $CuGa_xS_yO_z$ / ZnO in the form of superstrate and substrate configuration were fabricated. Here, the window layer (ZnO) was deposited by ECD applying both DC and two step potential and the absorber layer ($CuGa_xS_yO_z$) was fabricated by P-stat ECD. In superstrate cases, substrate ITO was replaced by FTO.

Fig.5.10 (a) shows small rectification property of the substrate heterojunction FTO /P-stat $CuGa_xS_yO_z$ / ZnO/ In solar cells, where ZnO film (bottom layer) was deposited by DC potential. As shown in Fig. 5.10 (b), the small photovoltaic effect was mainly because the light was incident on the absorption layer ($CuGa_xS_yO_z$) side [20].Whereas; substrate heterostructure cell P-stat $CuGa_xS_yO_z$ / ZnO (ZnO deposited by two-step potential) has no rectification property. On the other hand, no rectification property was observed for superstrate heterostructure fabricated by ZnO (DC and two step potential) with P-stat $CuGa_xS_yO_z$ films.

5.3.3.2. Galvanostatic $CuGa_xS_yO$ / ZnO solar cells

Figures 5.11(a) and (b) showed the rectification property and photovoltaic effect of the superstrate heterojunction solar cell ITO/ZnO/G-stat $CuGa_xS_yO$ respectively. In this case, ZnO film (bottom layer) deposited by two step potential [20]. These figures revealed that fabricated heterojunction showed a good rectification property and a noticeable PV current. Fig.5.12 (a) and (b) showed the rectification property and photovoltaic effect of the ITO/ZnO/G-stat $CuGa_xS_yO$ heterojunction solar cell respectively. In this case, ZnO film (bottom layer) was deposited by DC potential. It is noticeable that the dark I-V curve shown in fig.5.12 (a, b), does not cross the origin in the narrow voltage range. The I-V characteristic under illumination condition showed a photovoltaic response, but it is very low. In particular, the open circuit voltage is very low because of the large dark reverse saturation current density [31]. But substrate heterostructure fabricated by ZnO (DC biasing and two step) film with G-stat $CuGa_xS_yO$ has no rectification property. This may be due to photocorrosion, which occurs at the electrolyte–semiconductor interface. Photocorrosion damages the semiconductor electrode during the operation of the solar cell [32].

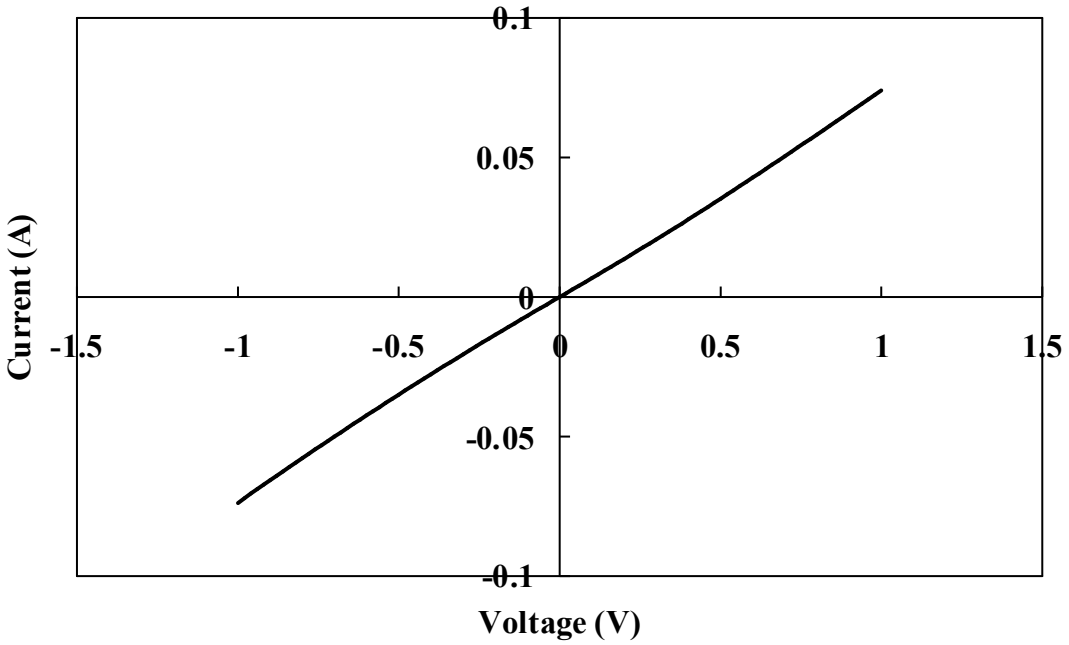

Fig.5.8. I-V graph under dark condition of the FTO/GaS_xO_y/G stat-$CuGa_xS_yO_z$ superstrate heterojunction solar cell

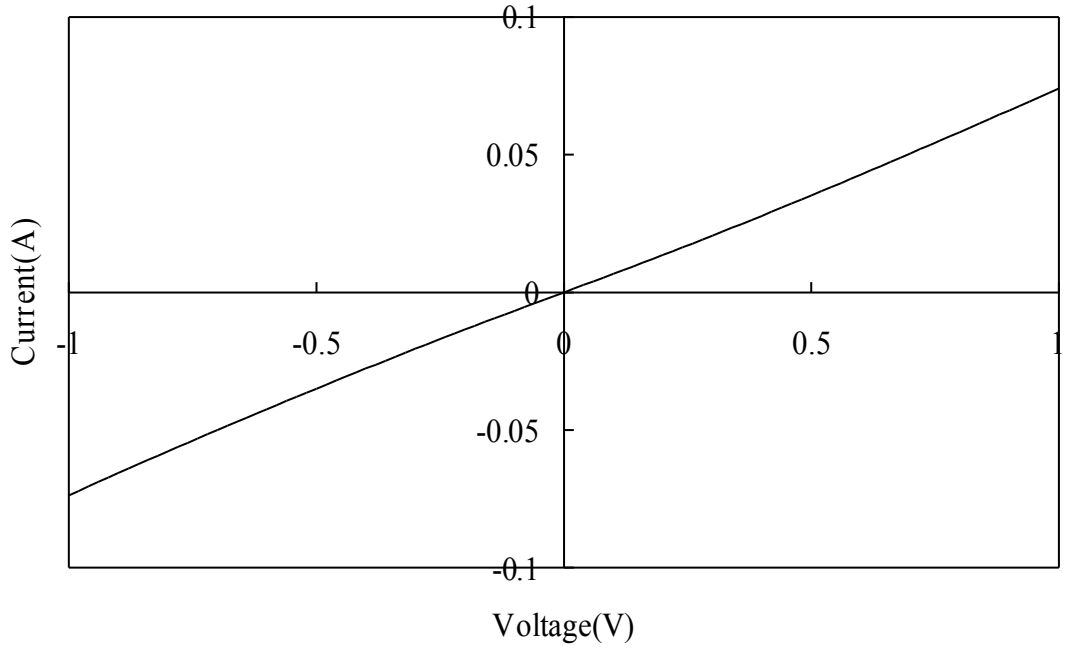

Fig.5.9. I-V graph under dark condition of the FTO/ G stat-$CuGa_xS_yO_z$ /GaS_xO_y substrate heterojunction solar cell

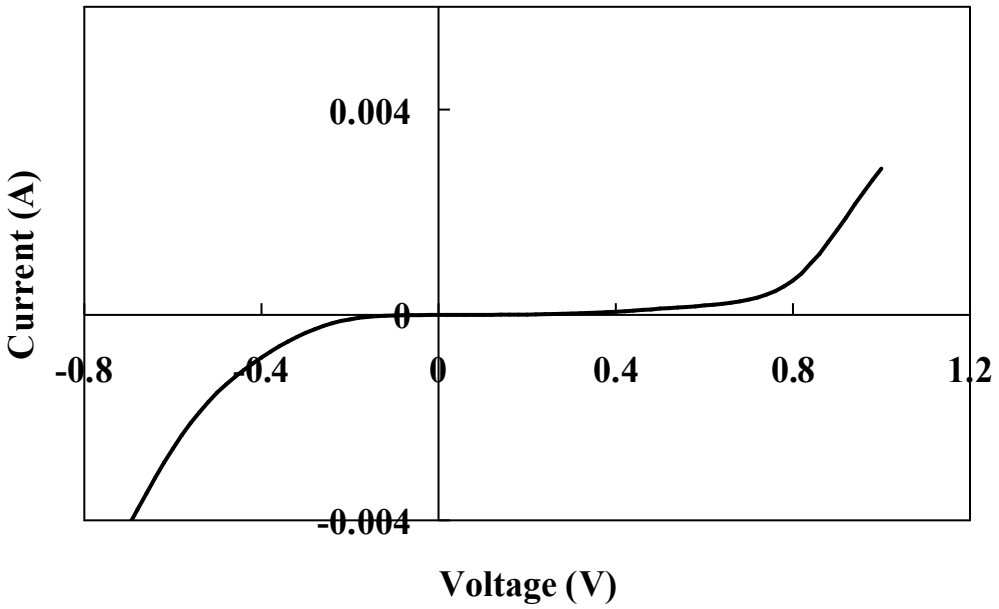

(a)

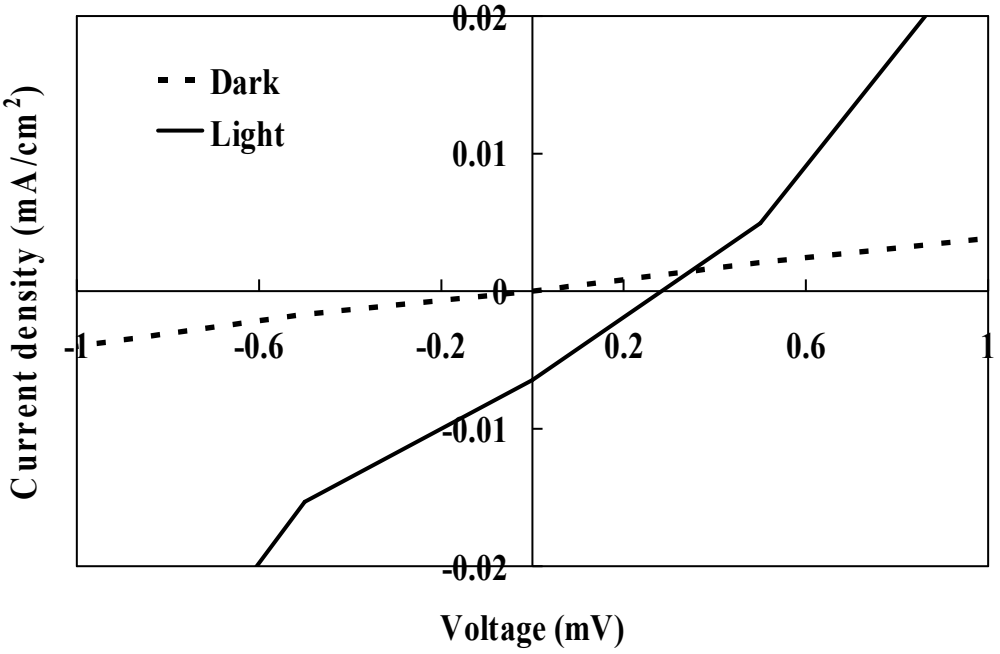

(b)

Fig.5.10. (a)Rectification property and (b) photovoltaic effect of the FTO/ P-stat $CuGa_xS_yO_z$ /ZnO heterojunction solar cell (ZnO film deposited by DC potential).

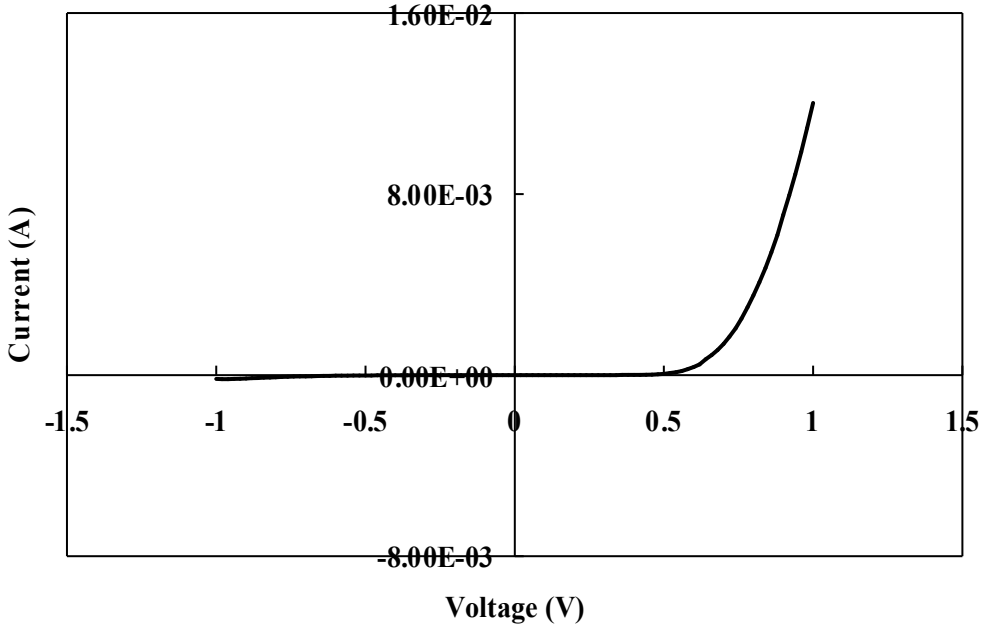

(a)

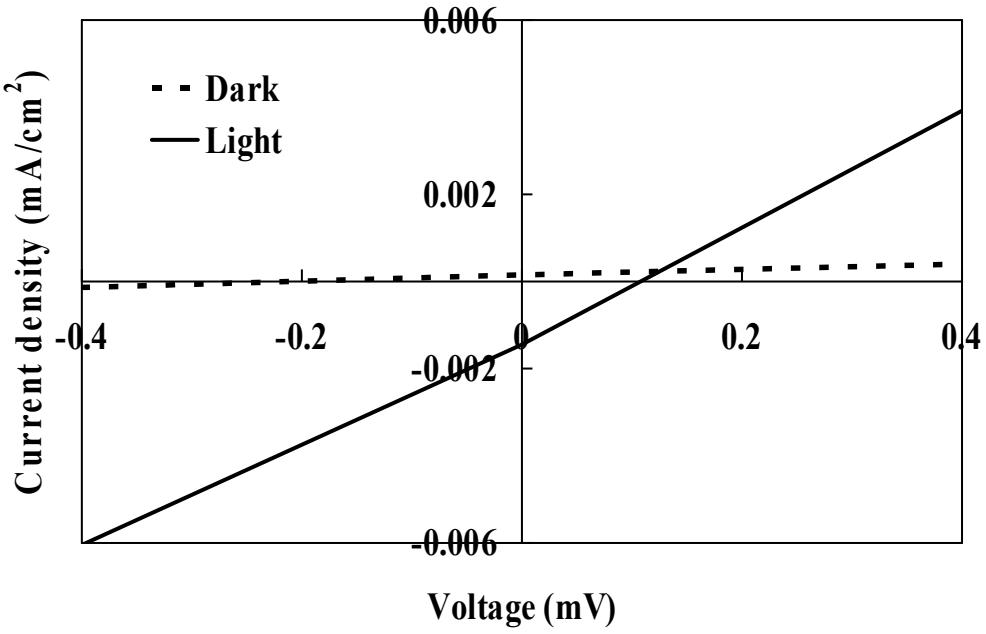

(b)

Fig.5.11. (a) Rectification property and (b) photovoltaic effect of the ITO/ZnO/G-stat $CuGa_xS_yO_z$ heterojunction solar cell (ZnO film deposited by two step potential).

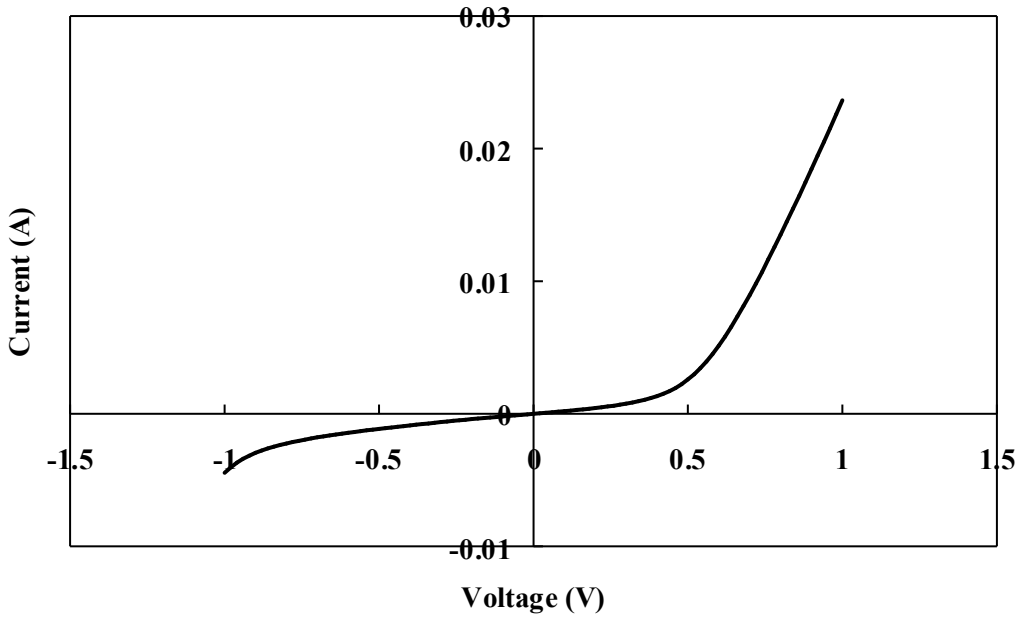

(a)

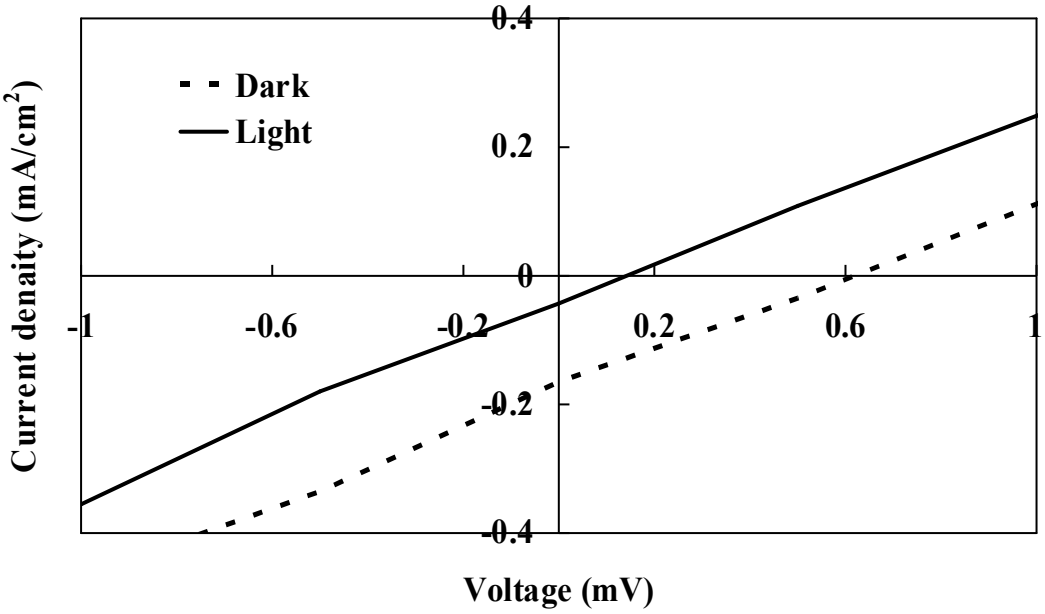

(b)

Fig.5.12. (a) Rectification property and (b) photovoltaic effect of the ITO/ZnO/G-stat $CuGa_xS_yO_z$ heterojunction solar cell (ZnO film deposited by DC potential).

Table-5.1: Solar cell parameter of $CuGa_xS_yO_z$ /ZnO based heterostructure showing photovoltaic effect for light intensity 100 mW/cm^2

Figure no.	Solar cell structure	Short circuit current, Isc mA/cm^2	Open circuit voltage,Voc mV	Fill factor, FF	Calculated efficiency, η
5.10	**FTO/P-stat $CuGa_xS_yO_z$ /Dc-ZnO**	0.0064	0.29	0.25	4.8×10^{-09}
5.11	**ITO/2-step-ZnO/G-stat $CuGa_xS_yO_z$**	0.0014	0.12	0.20	3.5×10^{-10}
5.12	**ITO/DC-ZnO/G-stat $CuGa_xS_yO_z$**	0.043	0.15	0.15	1.0×10^{-08}

Therefore, $CuGa_xS_yO_z$ /ZnO based heterostructure; those showing better photovoltaic effects are summarized in Table-5.1.

It was concluded that the superstrate structure ITO/DC-ZnO/G-stat $CuGa_xS_yO_z$ solar cell has better rectification property and higher photocurrent than others structures, though, the photo response and thus the conversion efficiency are still very low.

5.4. Conclusion

GaO-based heterostructure of SnS/ GaS_xO_y, $CuGa_xS_yO_z$ / GaS_xO_y and $CuGa_xS_yO_z$ /ZnO were fabricated as superstrate and substrate structure and characterized. It was noted that annealed GaS_xO_y could not improve the rectification property and $CuGa_xS_yO_z$ / GaS_xO_y heterostructure show ohmic-like I-V characteristics. However, some of the configuration showed rectification properties with very low conversion efficiencies. But, the overall performance of the heterojunctions was not improved.

References

[1] J.P. Singh and R.K. Bedi, Thin Solid Films 199 (1991) 9.

[2] K.T.R. Reddy, N.K. reddy, and R.W. Miles, Sol. Energy Mater. Sol. Cells 90 (2006) 3041.

[3] M. Parenteau, and C. Carlone, Phys. Rev.B. 41 (1990) 5227.

[4] G. Valiukonis, D.A. Guseinova, G. Krivaite, and A. Sileika, Phys. Stat. Sol. B. 135 (1986) 299.

[5] K. Mishra, K. Rajeshwar, Alex Weiss, M. Murley, Robert D. Engelken, Mike Slayton, and Hal E. McCloud, J. Electrochem. Soc. 136 (1989) 1915.

[6] M.T.S. Nair, and P.K. Nair, Semicond. Sci. Technol. 6 (1991) 132.

[7] H. Noguchi, A. Setiyadi, H. Tanamura, T. Nagatomo, and O. Omoto, Sol. Energy Mater. Sol. Cells 35 (1994) 325.

[8] K. Omoto, N. Fathy, and M. Ichimura, Jpn. J. Appl. Phys. 45 (2006) 1500.

[9] M. Ichimura, K. Takeuchi, Y. Ono, and E. Arai, Thin Solid Films 361-362 (2000) 98.

[10] D. Avellaneda, G. Delgado, M.T.S. Nair, and P.K. Nair, Thin Solid Films 515 (2007) 5771.

[11] E, M.A.Martinez, J.Herrero, M.T.Gutierrez, Solar energy mater. Solar cells 45 (1997)75-86.

[12] J.J.Lofeski, J.Appl.Phys 27(1956)777.

[13] J.B. yoo, A.L. Fahrenbruch, R.H.Bube, J.Appl.Phys.68 (1990)4694.

[14] S.Matsushima, D.Ikeda, K.Kobayashi, G.Okada, Chem Lett.2 (1992)323.

[15] S.Takata,T.Minami,H.Nanto,Thin Solid Films 135(1986)183.

[16] T.Mianmi,H.Nanto,S.Takata, Thin Solid Films 124(1985)43.

[17] Z.C.Jin,J.Hamberg,C.G.Granqvist,J.Appl.Phys.64(1988)5117.

[18] M.Izaki, J.Electrochem.Soc.144 (1997)1949

[19] S.Peulon, D.Lincot, J. Electrochem.Soc.145 (1998)864.

[20] M.Ichimura,H.Takagi, J. Appl .Phys. 47(2008)7845-7847

[21] S.Y. Myong, K.S. Lim, Solar Energy Mater. Solar Cells 86 (2005) 105.

[22] S. Fay¨, U. Kroll, C. Bucher, E. Vallat-Sauvain, A. Shah, Solar Energy Mater. Solar Cells 86 (2005) 385.

[23] J.C. Lee, K.H. Kang, S.K. Kim, K.H. Yoon, I.J. Park, J. Song, Solar Energy Mater. Solar Cells 64 (2000) 185.

[24] S. Tüzemen, G. Xiong, J. Wilkinson, B. Mischuck, K.B. Ucer, R.T. Williams, Physica B

308–310 (2001) 1197.

[25] H. Tampo, P. Fons, A. Yamada, K.-K. Kim, H. Shibata, K. Matsubara, S. Niki, H. Yoshikawa, H. Kanie, Appl. Phys. Lett. 87 (2005) 141904.

[26] T. Saeed, P. O'Brien, Thin Solid Films 271 (1995) 35.

[27] A. Ennaoui, M. Weber, R. Scheer, H.J. Lewerenz, Solar Energy Mater. Solar Cells 54 (1998) 277.

[28] M.Azuma, M.Ichimura, Materials research Bulletin43 (2008)3537-3542.

[29] A.M.A.Haleem, M.Ichimura, Thin Solid Films 516(2008)7783.

[30] N.Fathy, R.Kobayashi, M.Ichimura, Material Sci. and Engineering B 17(2004)271-276.

[31] A.M.A. Haleem, M.Ichimura, Jpn.J.Appl.Phys.48 (2009)035506.

[32] P.Turmezei, Acta Polytechnica Hungarica 1(2004) No. 2.

Chapter 6
Conclusion and future work

6.1. Main conclusion of this work

GaS_xO_y thin films were deposited from an aqueous solution of $Ga_2(SO_4)_3$ and $Na_2S_2O_3$by electrochemical deposition(ECD) method using DC biasing. Films were deposited onto two different substrate; ITO and FTO. For a high $Na_2S_2O_3$ concentration (~200 mM), deposited GaS_xO_y films were oxygen-rich (x<y), whereas no deposition was observed without $Na_2S_2O_3$ in the solution. The deposited films have bandgap energy of about 3.5 eV for both the substrates. Under the optimized conditions, films exhibit n-type conduction and photosensitivity.

GaS_xO_y thin films also prepared by photochemical deposition (PCD) methods from aqueous solution at different pH. At unadjusted pH, a uniform, oxygen rich film were deposited for 25 mM $Na_2S_2O_3$ and 5 mM $Ga_2(SO_4)_3$ with a growth rate of about 0.2~ 0.3 μm/hour. The deposited films were very rough for a high $Na_2S_2O_3$ concentration (~100 mM), whereas no deposition was observed without $Na_2S_2O_3$ in the solution of unadjusted pH. At high pH = 9, relatively smooth films were obtained, but the solution bath contained precipitation. Deposition rate were low when lactic acid was added in the growth solutions to avoid precipitation. Under the optimized conditions at unadjusted pH, deposited films show wide band gap energy of 3.5 eV and the resistivity of 6.6×10^2 Ω - cm.

$CuGa_xS_yO_z$ thin films were deposited from different concentrations of Ga and Cu ions in the solution bath by potentiostatic electrochemical deposition (P-stat ECD) method. The XRD measurement reveals that the films are amorphous in nature and significant composition-modulation was not observed by the AES depth profiling. Thus, the films are considered to be alloys with fairly uniform composition. The AES measurements revealed that there is a correlation between the Ga and O contents in the deposited films. The optical transmission increased for the higher Ga concentration films compared with the higher Cu concentration film. The band gap values of the deposited films were estimated to be about 1.5–2.0 eV for the Cu-rich films (Cu/Ga=1/1, 1/2) and 2.3–2.8 eV for the Ga-rich films (Cu/Ga=1/4, 1/12,

1/30).In SEM study it was observed that the film deposited from the baths with Cu/Ga = 1/1, 1/2 and 1/4 consisted of fine grains with good surface coverage. However the films deposited at higher Cu content (Cu/Ga = 3/2) and higher Ga content (Cu/Ga = 1/12, 1/30) contained micro-cracks. Under optimized condition, deposited films show p-type semiconductors except the film deposited with Cu/Ga = 1/30, which shows intrinsic character.

$CuGa_xS_yO_z$ (CGSO) films also deposited from the Cu/Ga = 1/2 bath by galvanostatic electrodeposition (G-stat ECD) process. The effect of deposition process on P- stat ECD and G-stat ECD CGSO film characteristics was studied. It was noted that, deposition process has clear effect on surface morphology, bandgap energy, thickness and photosensitivity of deposited CGSO films. At optimum condition, in surface morphology, P-stat CGSO film contains large grain comparing with G-stat CGSO films and the optical transmission, bandgap energy, Eg were increase for G-stat CGSO films may be due to lower film thickness. AES measurement revealed that deposition process has no significant effect on atomic composition.

Novel heterostructure of SnS/ GaS_xO_y, $CuGa_xS_yO_z$ / GaS_xO_y and $CuGa_xS_yO_z$ /ZnO were fabricated in superstrate and substrate structure and characterized. We observed that rectification was not improved even for annealed GaS_xO_y. The $CuGa_xS_yO_z$ /GaS_xO_y heterostructure configurations show ohmic like I-V characteristics. However, some of the heterostructure showed rectification properties with very low conversion efficiencies but the overall performance of the solar cell was not improved.

6.2. Suggestions for future work

In this work, we deposit GaO-based thin films from aqueous solution by ECD and PCD techniques for solar cell applications. Since, GaS_x is vigorously dissolved in the water hence deposited films are oxygen rich. Therefore, excess amount of oxygen could engage some defects with the film properties. This excess amount of oxygen could be avoided by choosing non aqueous solution bath for deposition.

In this work, films were deposited in room temperature. Applying various higher temperatures in growth solution, crystalline films could be achieved.

Chapter-6: Conclusion and future work

Deposition and characterization of Zn doped GaO- based films i.e. Ga-Zn-O or Cu-Ga-Zn-O could achieve the better efficiency of GaO-based thin film solar cells.

Now a day, metal oxide nanoparticles and nanorods are of great scientific interest as they are effectively a bridge between bulk materials and atomic or molecular structures. Thus, formation of GaO- nanoparticles and nanorods is the matter of high interest that could be able to modify the band gap, enhance the absorption co-efficient and carrier flow can be restricted to the desired direction. As a result, GaO- based nanoroparticles and nanorods would be the smart candidate for future technology with a wide variety of potential applications in biomedical, optical and electronic fields.

Journals

1. S.Chowdhury, M.Ichimura, "Electrochemical deposition and characterization of $CuGa_xS_yO_z$ thin films", Materials Science in Semiconductor Processing (Accepted on October 2010).

2. S.Chowdhury, M.Ichimura,"Photochemical Deposition of GaS_xO_y Thin Films from Aqueous Solution", Japanese Journal of Applied Physics, 49 (2010) 062302.

3. S.Chowdhury, M.Ichimura, "Electrochemical Deposition of GaS_xO_y Thin Films", Japanese Journal of Applied Physics, 48(2009) 061101.

Presentations

1. S. Chowdhury and M.Ichimura, "Photochemical Deposition of GaS_xO_y Thin Films", 19th International Photovoltaic Science and Engineering Conference (PVSEC 19), November 2009, Jeju, Korea.

2. S. Chowdhury and M.Ichimura, "Electrochemical deposition of gallium sulfide oxide thin films", 69th Autumn Meeting, The Japan Society of Applied Physics, September 2008, Kasugai, Japan.